

Distribution Agreement

In presenting this thesis or dissertation as a partial fulfillment of the requirements for an advanced degree from Emory University, I hereby grant to Emory University and its agents the non-exclusive license to archive, make accessible, and display my thesis or dissertation in whole or in part in all forms of media, now or hereafter known, including display on the world wide web. I understand that I may select some access restrictions as part of the online submission of this thesis or dissertation. I retain all ownership rights to the copyright of the thesis or dissertation. I also retain the right to use in future works (such as articles or books) all or part of this thesis or dissertation.

Signature:

Raven J. Peterson

Date

ALL THE SMALL THINGS: UTILIZING A NANOPARTICLE PLATFORM TO EXAMINE
APICAL INTEGRIN REGULATION OF THE EPITHELIAL BARRIER

By

Raven J. Peterson
Doctor of Philosophy

Graduate Division of Biological and Biomedical Science
Biochemistry, Cell, and Developmental Biology

Dr. Michael Koval, Advisor

Dr. Paul Dawson, Committee Member

Dr. Andrew Kowalczyk, Committee Member

Dr. Renhao Li, Committee Member

Dr. Khalid Salaita, Committee Member

Accepted:

Lisa A. Tedesco, Ph.D.
Dean of the James T. Laney School of Graduate Studies

Date

ALL THE SMALL THINGS: UTILIZING A NANOPARTICLE PLATFORM TO EXAMINE
APICAL INTEGRIN REGULATION OF THE EPITHELIAL BARRIER

By

Raven J. Peterson
B.S., Florida State University, 2016

Advisor: Dr. Michael Koval, Ph.D.

An abstract of
A dissertation submitted to the Faculty of the
James T. Laney School of Graduate Studies of Emory University
in partial fulfillment of the requirements for the degree of
Doctor of Philosophy
in Graduate Division of Biological and Biomedical Science
Biochemistry, Cell, and Developmental Biology
2021

Abstract

ALL THE SMALL THINGS: UTILIZING A NANOPARTICLE PLATFORM TO EXAMINE APICAL INTEGRIN REGULATION OF THE EPITHELIAL BARRIER

By: Raven J. Peterson

Epithelial cells form selectively permeable barriers that compartmentalize internal and external microenvironments and regulate the movement of water, ions, and other solutes critical for maintaining homeostasis. Tight junctions, comprised of transmembrane domain containing proteins (Ig superfamily, MarvelD, and claudins), and scaffold proteins (including the Zonula Occludens (ZO) family) are the major regulators of permeability forming the apical/basolateral barrier. Evidence has emerged that integrins, particularly those localized to the apical surface, play a role in regulating epithelial barrier morphology and function. In order to determine integrin specific contributions to the regulation of the epithelial barrier, we utilized a derivatized polymeric nanoparticle platform conjugated with anti-integrin antibodies to target apically localized integrins in human intestinal epithelial cells. We used immunofluorescence imaging of tight junction proteins and assessed barrier function by measuring flux of ions and small tracer molecules. We found that low aspect ratio nanowires conjugated with anti-integrin antibodies recognizing a closed conformation induced disparate effects on tight junction proteins, where these nanowires stimulated claudin-2, claudin-4, and ZO-1 to assume a ruffled morphology while claudin-1 and claudin-7 remained linear. These anti-closed integrin nanowires also increased permeability to ions and whole IgG, but not calcein. It is possible that these changes were driven by the actin cytoskeleton, as anti-closed integrin nanowires stimulated cortical F-actin localization and increased talin localization to cell/cell contacts. When low aspect ratio nanowires were conjugated with activating anti-integrin antibodies recognizing an extended conformation, they increased the linearity of ZO-1, had no effect on claudin morphology, and decreased permeability to ions. Particle geometry was also critical, since we found that anti-closed integrin antibody conjugated microspheres had little impact on tight junction morphology and ion permeability but activating anti-integrin antibody conjugated microspheres induced ZO-1 ruffling and caused biphasic changes in ion permeability. These observations support a role for integrins in regulating epithelial barrier function and suggests that anti-integrin nanoparticles may provide a tunable platform for regulating tight junction permeability.

ALL THE SMALL THINGS: UTILIZING A NANOPARTICLE PLATFORM TO EXAMINE
APICAL INTEGRIN REGULATION OF THE EPITHELIAL BARRIER

By

Raven J. Peterson
B.S., Florida State University, 2016

Advisor: Dr. Michael Koval, Ph.D.

A dissertation submitted to the Faculty of the
James T. Laney School of Graduate Studies of Emory University
in partial fulfillment of the requirements for the degree of
Doctor of Philosophy
in Graduate Division of Biological and Biomedical Science
Biochemistry, Cell, and Developmental Biology
2021

Acknowledgments

I want to start my dissertation by acknowledging that my entire life and education has taken place on land belonging to Indigenous tribes, and I have benefitted from the forced removal of these tribes from the lands belonging to their ancestors. My early education took place on land belonging to the Seminole and Tocobaga tribes, my secondary education took place on land belonging to the Myaamia, Kaskaskia, and Kiikaapoi tribes, and my entire post-secondary and graduate education took place on land belonging to the Muscogee Creek tribe. Beyond the personal privilege afforded to me as a settler, the fields of science and medicine have benefitted enormously from the exploitation of Indigenous bodies [1]. Though this is a personal acknowledgement, and it lacks the power of programmatic and institutional land acknowledgements, it is my hope that anyone reading this will reflect on the ways in which they have benefitted from living and working on land that is not their own, use that reflection to take action, and use the power they have to create systemic change and support Indigenous communities.

To my advisor, Dr. Michael Koval, thank you. For a PI who was not planning on taking students during my first year, I sure am glad you took a chance on me. You gave me the opportunity to drive an (at times) frustratingly complex project while still providing support. I would not be the scientist, thinker, or writer that I am were it not for the opportunities I had as a student in your lab. I would also like to thank my committee, Drs. Paul Dawson, Andrew Kowalczyk, Renhao Li, Brian Petrich, and Khalid Salaita for their continued support and guidance of my academic and professional development. The value of having a committee that was willing to listen to and problem solve both experimental woes and career concerns cannot be understated.

I am also immensely grateful to the insight and encouragement provided through collaboration with Dr. Tejal Desai's lab. Dr. Desai along with Colin Zamecnik and Joel Finbloom were always willing to provide feedback on my work and their ideas helped the progress of my project and proved to be invaluable to my own learning. They were incredibly patient and always willing to answer the vast number of questions I had related to engineering, using, and optimizing nanoscale materials.

I have been fortunate to be part of a large lab with the opportunity to work with a wide range of colleagues. Samuel Molina, Tarianna Stewart, and Rachel Morgan were instrumental in my adjustment to the Koval lab both during my rotation and during my start as a new member of the lab following my first year and beyond. Working with Prestina Smith and Skye Comstra was incredible, they are role models both in the lab and in the classroom, and they significantly contributed to my development as a scientist, an educator, and a person. Sharing lab space and lab meetings with Josh Levy was a joy because he was always willing to entertain my (sometimes) absurd questions about medicine and I always learned something new about the nose from him. I treasure the time spent working with Caro Schlipp and Aek Moonwiryakit, not only because it was an opportunity to work with great scientists, but also because it was interesting to learn about both life and graduate school for students in Germany and Thailand respectively.

The Koval lab has also had a string of wonderful research specialists that helped keep the lab running and have brought so many good times to the lab. I'll never forget talking about college football and Jeopardy! with Lionel Watkins, trying to find the most ridiculous plot lines in modern literature with Sarah Mashburn, Ram Gowrishankar always informing me when the Biebs had a new song that would get stuck in my head, or trying to assure Ryan Reed that I was a real person

and not an elaborate catfishing scheme before we had the chance to meet in real life ~8 months after he started.

Working in the Koval lab also gave me the opportunity to mentor students, which was one of the most fulfilling experiences in graduate school. To my surprise, there's no one-size fits all guide on how to be a good research mentor because each student that you work with is a little different. I'm glad that I had the opportunity to work with students with all different experience levels, it taught me a lot about how to help students find their path to independence in the lab. To Howard Wood, Chi Ohanu, Sarah Strassler, and Carly Lancaster—thank you for the opportunity to work with you, to learn from you, and for the hard work you did in the lab. To Emily Legan, my first mentee in graduate school, thank you for allowing me the opportunity to figure out how to be a good mentor...mostly by trial and error. And for your friendship, it has meant the world to me.

Lastly, to my fellow graduate students in the Koval lab, Sabrina Lynn, Lauren Jeffers, and Kristen Easley, thank you. I don't know words with a big enough magnitude to describe how much your presence in my life and alongside me in the lab meant. You are a group of incredible scientists that constantly pushed me to be better and a group of escape room masters that constantly reminded me to stop touching things. Thank you for letting me bounce ideas off you, for engaging in the eternal pursuit of finding free food on campus with me, and for not making me delete the embarrassing photos and videos of our shenanigans I've amassed over the years.

The BCDB program introduced me to incredible people. I am grateful to Emma D'Agostino, Skylar Dewees, Zane Laughlin, Raven Shah, and Stephanie Zimmer for being such a supportive cohort—from foundations to stats class to life's challenges—thank you for the opportunity to grow with you and learn from you. To Courtney Christian, Kelsey Maher, Tyler

Moser-Katz, Samantha Schwartz, and Rachel Turn—thank you for being part of the heart and soul of the program that created an accepting and welcoming environment. Graduate school was a tremendous opportunity for personal and professional growth, and you all helped me make the most of it. I wouldn't be the person I am today without all of you.

I have had the privilege of having fantastic educators at nearly every stage of my education. I am forever grateful to the teachers that had the biggest impact on my education: Susan Salerno, Patricia Stuart, Janet Mahowski, Jen Davis, Kristi LeVeque, Maureen Borto, Matt Dillon, Tom Maxam, Carleen Sabusap, Brian Chadwick, Emily Darrow, Tom Keller, Ronderrick Mitchell, Antron Mahoney, and Deanna Rohlinger. These educators shaped who I am, from the way I think to the way I move. They gave me an enduring love of learning, creativity, problem solving, and public speaking. More importantly, they encouraged me to ask questions and be curious, which has served me well as a graduate student and a student of life.

To my mom, a simple thank you is not enough, but it's all I have. Ever since I was little you looked for ways to challenge me and never discouraged me from asking questions. You pushed me into taking chances on things that I thought I wouldn't like, and you were right more often than I care to admit. Thank you for supporting me and always believing in me.

To Spotify, thank you for allowing me access to whatever songs I needed to focus throughout the entirety of my graduate school career. Not only could I listen to the relaxing vibes of early 2000s pop punk music to my heart's content, but you also provided a much-needed refuge from Weezer's cover of "Africa" when I needed it the most. I'm not sure I would've made it through this degree without the constant encouragement of Paramore, Eminem, Bastille, Missy Elliot, Neon Trees, MGK, Fall Out Boy, AC/DC, Green Day, Blink-182, Yungblud, and (begrudgingly) Justin Bieber.

And finally, to you dear Raven. Take pride in this accomplishment and know that your ideas are worth hearing and that there is value in showing up as yourself—those that cannot recognize this are not your problem. I hope that you take *everything* you learned during graduate school and use it to be the best you can be. You finished a Ph.D. during what felt like the apocalypse, which means you can accomplish just about anything. There's a whole future waiting, and it's pretty bright. Take it from Dr. Charles Xavier who summed it up nicely, "everything that happens now is in your hands. I have faith in you Raven" [2].

References

1. Hodges FS. No meaningful apology for American Indian unethical research abuses. *Ethics and Behavior* **22**, 431-444. (2012).
2. Singer B, Simon K, Goldman J, Vaughn M, Shuler-Donner L, Parker H, Lee S, Hallowell T, McLaglen J, Jackman H, McAvoy J, Fassbender M, Lawrence J, Berry H, Hoult N, Paquin A, Page E, Dinklage P, Ashmore S, Sy O, Peters E, Helman J, Cudmore D, Fan B, Canto A, Stewart BB, McKellen I, Stewart P, Sigel NT, Myhre J, Ottoman J, Mingenbach L. X-men: Days of future past. (2014).

Table of Contents

Abstract	1
Acknowledgments	vi
References.....	xi
List of figures	xv
List of tables	xvii
Abbreviations	xviii
Chapter 1: Introduction	1
1.1 The epithelial barrier.....	1
1.2 Scope of the dissertation.....	2
References.....	5
Chapter 2. Ruffles and spikes: Control of tight junction morphology and permeability by claudins	7
2.1 Abstract.....	7
2.2 Introduction.....	8
2.3 Ruffled junctions.....	10
2.3.1 Roles for claudin/ZO-1 interactions in tight junction ruffling.....	12
2.3.2 Hypoxia induced tight junction ruffles.....	15
2.3.3 Integrin stimulation by nanostructured surfaces.....	17
2.3.4 Ruffles formed by mechanical stimulation.....	18
2.4 Tight junction spikes and discontinuities.....	19
2.4.1 Tight junction spikes as organizers of vesicular traffic.....	21
2.4.2 Spikes formed in response to chronic alcohol exposure are due to impaired claudin/ZO-1 interactions.....	23
2.4.3 Roles for claudins in regulating tight junction ultrastructure.....	24
2.5 Summary and future directions.....	26
References:.....	37
Chapter 3: Above the matrix: functional roles for apically localized integrins	57
3.1 Abstract.....	57
3.2 Introduction.....	57
3.2.1 Integrin structure.....	58
3.2.2 Sensing and manipulating integrin activation using monoclonal antibodies.....	59
3.2.3 Roles for divalent ions and disulfide bonds in integrin conformation.....	60
3.3 Function of apical integrins.....	62
3.3.1 Reproduction and control of cell phenotype.....	62
3.3.2 Apical integrins as bacterial receptors.....	64
3.3.3 Regulation of epithelial barrier function.....	66
3.3.4 Regulation of Cell Migration.....	67
3.3.5 Mechanosensing.....	68

3.4 Summary and future directions	70
References.....	76
Chapter 4: Apical integrins as a switchable target to regulate the epithelial barrier.....	89
Abstract.....	89
4.1 Introduction.....	89
4.2 Materials and Methods.....	92
4.2.1 Fabrication and conjugation of nanowires.....	92
4.2.2 Cell culture	93
4.2.3 Immunofluorescence	93
4.2.4 Barrier function assays.....	95
4.3 Results.....	96
4.3.1 Multimeric engagement of apical integrin β 1 by A1B2 induces tight junction ruffling	96
4.3.2 The effect of targeting apical integrin β 1 subunits on barrier function depends on epitope and valency	99
4.3.3 Effect of targeting apical integrin β 1 subunits on actin depend on valency	100
4.4 Discussion.....	102
References.....	115
Chapter 5. Impact of anti-integrin particle geometry on tight junctions	122
Abstract.....	122
5.1 Introduction.....	123
5.2 Materials and Methods.....	124
5.2.1 Fabrication and conjugation of nanoparticles	124
5.2.2 Cell culture	125
5.2.3 Immunofluorescence	125
5.2.4 Barrier function.....	126
5.3 Results.....	127
5.3.1 Effects of targeting apical integrins on junction morphology is dependent on nanoparticle aspect ratio	127
5.3.2 Role of aspect ratio on the effects of anti-integrin particles on epithelial barrier structure.....	128
5.3.3 Apical integrin conformation state and interaction with nanoparticles.....	128
5.3.4 Aspect ratio and integrin conformation state control how apical integrins regulate epithelial barrier function.....	130
5.4 Discussion.....	131
References.....	141
Chapter 6: Practical issues related to applications of anti-integrin nanowires	144
Abstract.....	144
6.1 Introduction.....	145
6.2 Materials and Methods.....	147
6.2.1 Fabrication and conjugation of nanoparticles	147
6.2.2 Caco-2 cell culture.....	147
6.2.3 NhBE cell culture	147

6.2.4 Glutathione competition.....	148
6.2.5 Immunofluorescence	148
6.2.6 Barrier function	149
6.3 Results	149
6.3.1 Duration of nanowire mediated changes of epithelial barriers	149
6.3.2 Reversibility of anti-integrin nanowire/cell interactions	151
6.3.3 The effects of AIB2 nanowires are abrogated by MMP-2 inhibitors.....	152
6.3.4 Targeting apical integrins in upper airway epithelial cells	153
6.4 Discussion	154
References.....	165
<i>Chapter 7. Conclusions and future directions</i>	<i>170</i>
7.1 Overview of findings and significance.....	170
7.2 Future directions	172
7.2.1 Integrins	172
7.2.2 The nanoparticle platform itself.....	174
7.2.3 Tension.....	176
References.....	179

List of figures

- Figure 2.1. Graphical abstract
- Figure 2.2. Protein composition of tight junctions and adherens junctions
- Figure 2.3. Roles for actin in control of tight junction morphology
- Figure 2.4. Quantitation of tight junction ruffles
- Figure 2.5. Model for claudin-directed changes in ZO-1 conformation
- Figure 2.6. Tight junction spikes induced in lung epithelial cells
- Figure 2.7. Model for claudin-claudin interactions affecting scaffold protein binding
- Figure 3.1. Overview of integrin conformation and domain composition.
- Figure 4.1 Targeting apical integrins with AIIB2 nanowires produce a ruffled ZO-1 morphology
- Figure 4.2 AIIB2 nanowires cause differential changes in claudin morphology
- Figure 4.3 AIIB2 nanowires cause changes in adherens junction proteins localization
- Figure 4.4 Differential effects of targeting apical integrins on ion and small molecule permeability
- Figure 4.5 Actin reorganization and recruitment of talin in response to AIIB2 nanowires
- Supplemental Figure 4.1 Cell viability
- Supplemental Figure 4.2 Targeting apical integrins with AIIB2 nanowires and claudin morphology
- Figure 5.1 Aspect ratio of AIIB2 nanoparticles is important in triggering ruffled ZO-1 morphology
- Figure 5.2 Actin reorganization depends on the geometry of AIIB2 nanoparticles

- Figure 5.3 9EG7 microspheres and 5 μ m nanowires induce ruffled ZO-1 morphology
- Figure 5.4 9EG7 nanoparticles and junctional localization of proteins in the apical junctional complex
- Figure 5.5 Anti-integrin nanoparticle geometry and the effect on barrier function
- Figure 6.1 Effects of AIIB2 nanowires influence cells for at least 24hr
- Figure 6.2 Glutathione competition can reverse AIIB2 blocking nanowire effects on tight junction morphology
- Figure 6.3 Inhibiting MMP-2 in AIIB2 nanowire treated cells prevents changes in barrier morphology and function
- Figure 6.4 Apical integrin targeting in NhBE cells causes changes in barrier structure and function

List of tables

Table 2.1.	Stimuli inducing ruffled tight junctions
Table 3.1.	Cells and tissues with apically oriented integrins
Supplemental Table 4.1	Primary antibodies and fixation conditions
Table 5.1	Nanoparticle surface area and aspect ratio

Abbreviations

AIIB2	Blocking monoclonal antibody to integrin β 1
AJC	Apical Junctional Complex
BAR	Bin/Amphiphysin/Rvs
BAEC	Bovine Aortic Endothelial Cells
BSA	Bovine Serum Albumin
CF	Cystic Fibrosis
CFTR	Cystic Fibrosis Transmembrane Regulator
Cx	Connexin
DMPA	2,3-dimercapto-1-propanesulfonic Acid
DTT	Dithiothreitol
ECM	Extracellular Matrix
EDTA	Ethylenediaminetetraacetic acid
EGF	Epidermal Growth Factor
EGFR	Epidermal Growth Factor Receptor
eNOS	endothelial Nitric Oxide Synthase
FcRn	Neonatal Fc Receptor
FLIM	Fluorescence Lifetime Microscopy
FRAP	Fluorescence Recovery After Photobleaching
GSH	Glutathione
GUK	Guanylate Kinase
HEK	Human Embryonic Kidney

HIF	Hypoxia Induced Factor
HUVEC	Human Umbilical Vein Endothelial Cells
IGF	Insulin-like Growth Factor
kDa	Kilodalton
LABS	Ligand Attenuated Binding Sites
LIBS	Ligand Induced Binding Sites
mAb	monoclonal Antibody
mAChR	muscarinic Acetyl Choline Receptor
MDCK	Madin Darby Canine Kidney
MEM	Minimum Essential Medium
MLCK	Myosin Light Chain Kinase
MMP	Matrix Metalloprotease
MP-PCL	Malemidophenyl-Polycaprolactone
NhBE	Normal human Bronchial Epithelial
NSF	Nanostructured Film
PBS	Phosphate Buffered Saline
PCL	Polycaprolactone
PDZ	Postsynaptic density protein (PSD95), Drosophila disc large tumor suppressor (DlgA), and Zonula Occludens-1 protein (ZO-1)
PEG	Polyethylene glycol
PFA	Paraformaldehyde
PSI	Plexin/Semaphorin/Integrin
PVA	Poly(vinyl alcohol)

RGD	Arginylglycylaspartic Acid
RPE	Retinal Pigment Epithelial Cells
STORM	Stochastic Optical Reconstruction Microscopy
TER	Transepithelial Electrical Resistance
TOCA	Transducer of Cdc42 dependent Actin assembly
WASP	Wiskott–Aldrich Syndrome Protein
XperT	eXpress micromolecule Permeability Testing
ZnUMBA	Zinc-based Ultrasensitive Microscopic Barrier Assay
ZO	Zonula Occludens
9EG7	Activating monoclonal antibody to integrin β 1

Chapter 1: Introduction

1.1 The epithelial barrier

The polarization and subsequent formation of protective and selective barriers by epithelial cells allows for compartmentalization of organs that protects them from their external environments and is a critical requirement for maintaining homeostasis. Together tight junctions and adherens junctions work in concert to form the apical junctional complex (AJC) which both regulates adhesion between neighboring cells and coordinates proteins that mediate the polarization process that defines the barrier separating the apical and basolateral domains of the cell [1-3]. Once formed, the epithelial barrier is selectively permeable to ions and solutes. Movement from the apical to basolateral sides of the cell can only occur through one of two paths: the transcellular pathway that involves transcytosis or ion channels and movement through the cell, and the paracellular pathway that involves movement of molecules through the pericellular space between adjacent cells [4]. Of the proteins that comprise tight junctions—the transmembrane domain containing Ig superfamily, MarvelD family, and claudin family of proteins, as well as cytosolic zonula occludens (ZO) family proteins—the claudin family plays a central role in determining barrier selectivity [5].

Though there is considerable research defining roles for these specific tight junction proteins in regulating the paracellular barrier, tight junctions are not an isolated structure either within individual cells or through the population of cells in a tissue. As part of the AJC tight junctions and adherens junctions are coordinately regulated and also interact with the actin cytoskeleton [5]. The actin cytoskeleton is regulated by a family of transmembrane proteins known as integrins, which have classically been considered as receptors that induce signaling and actin rearrangement in response to binding to extracellular matrix or by cell-cell interactions [6]. The vast majority of

work linking integrins to epithelial barrier function and phenotype has focused on integrins localized to the basal surface of the cell, where they form focal adhesions that act as signaling hubs and actin organizing centers [7]. Recently, lines of evidence have emerged suggesting that there are also integrins present on the apical surface of epithelial cells [8-10]. Further studies examining different stimuli targeting the apical surface that alter epithelial barrier function have suggested that integrins are involved in their mechanism of action [11-14]. However, there is a knowledge gap in understanding their roles in cell function and whether they are regulated differently than the basal pool of integrins binding to the extracellular matrix. As a result, precise roles for integrins have not been specifically interrogated.

1.2 Scope of the dissertation

The previous work that has identified apical integrins as regulators of the epithelial barrier were indirect. Techniques involving substrates that directly contact large heterogenous patches of the apical membrane to alter barrier function were subsequently found to involve apical integrins, based on analysis using blocking agents and other methods [11-14]. While this has helped define roles of apical integrins, to date these techniques have been unable to elucidate the specific roles integrins have in regulating tight junction structure and function. This dissertation project describes a novel platform developed to more precisely stimulate specific apically localized integrins and then measure the effects on tight junction morphology, composition and barrier function. Therefore, in this dissertation we examine three main questions: 1) what happens to the epithelial barrier if we specifically target apical integrins? 2) if we modify the nanoparticle platform we use to target apical integrins, does this change the barrier response? 3) is the phenomenon observable in other cell types, and what should be taken into consideration for therapeutic applications?

Chapter 2 provides an introduction to and background on two different types of changes to tight junction morphology that we have observed, ruffles and spikes. This chapter reviews the literature that reports different occurrences of these structures, how claudins and ZO proteins may regulate ruffle and spike formation, and how these non-linear tight junctions effect barrier function. The chapter establishes hypotheses about ZO-1 and claudin interactions that are tested in this dissertation.

Chapter 3 provides an introduction to and background on integrins and their apical localization. This chapter reviews the literature that reports the occurrence of apical integrins and organizes them by the functions they regulate. The chapter establishes what is known about apical integrins and identifies knowledge gaps that the work in this dissertation seeks to fill.

Chapter 4 presents work that aims to answer our first question, what happens to the epithelial barrier if we specifically target apical integrins? To do this, we leverage an antibody conjugated nanowire platform to target and cluster apical integrins. We find that consistent with other literature, targeting and clustering apical integrins with nanowires is sufficient to regulate barrier structure and function. Interestingly, we see a difference in cell response depending on the type of anti-integrin antibody we conjugate with the nanowires. The use of a ligand blocking antibody that detects integrins in their closed conformation induces ruffling of ZO-1 and a specific subset of claudins as well as increase permeability to ions and large molecules. However, the use of a stimulating antibody that detects and binds to integrins in their open conformation linearizes tight junctions and decreases permeability to ions but not large molecules.

Knowing that we have a platform that targets apical integrins and can tune the barrier response based on the functionality of the integrin targeting antibodies used, **Chapter 5** presents work that aims to answer our second question, how does the geometry of the platform itself impact

our ability to induce integrin mediated changes in barrier function? To do this, we generated spherically shaped nanoparticles and shorter nanowires that can be conjugated with anti-integrin antibodies. We find that anti-integrin conjugated nanospheres and short nanowires more strongly induce tight junction ruffling than long anti-integrin nanowires, confirming that platform geometry is an important parameter in the cell response to integrin engagement.

Chapter 6 presents findings related to the practical application of anti-integrin nanowires in different contexts, including their use on airway epithelial cells, how they are impacted by reducing agents and influenced by membrane metalloproteases.

Chapter 7 provides a summary of our findings and their significance. This chapter also expands on the future directions of this work. Experiments are proposed that would help further define mechanisms for how apical integrins with different conformations regulate tight junction morphology, composition, and function.

References

1. Vogelmann R, Amieva MR, Falkow S, Nelson WJ. Breaking into the epithelial apical-junctional complex--news from pathogen hackers, *Current Opinions in Cell Bioogyl.* 16, 86-93 (2004).
2. Knust E, Bossinger O. Composition and formation of intercellular junctions in epithelial cells. *Science* 298, 1955-1959 (2002).
3. Matter K, Balda MS. Signalling to and from tight junctions. *Nature Reviews Molecular and Cell Biology* 4, 225-36 (2003).
4. Koval M. Structure and Function of Epithelial and Endothelial Barriers. *Drug Delivery Across Physiological Barriers.* 3-40 (2016).
5. Anderson JM, Van Itallie CM. Physiology and Function of the Tight Junction. *Cold Spring Harbor Perspectives in Biology* 1, a002584 (2009).
6. Schwartz MA. Integrins and Extracellular Matrix in Mechanotransduction. *Cold Spring Harbor Perspectives in Biology* 2: a005066. (2010).
7. Hynes RO. Integrins: Bidirectional, Allosteric Signaling Machines. *Cell* 110, 673-687. (2002).
8. Beaulieu JF. Differential expression of the VLA family of integrins along the crypt-villus axis in the human small intestine. *Journal of Cell Science* 102, 427-463. (1992).
9. Gut A, Balda MS, Matter K. The cytoplasmic domains of a β 1 integrin mediate polarization in Madin-Darby canine kidney cells by selective basolateral stabilization. *The Journal of Biological Chemistry* 273, 29381-29388. (1998).
10. McCormick BA, Nusrat A, Parkos CA, D'Andrea L, Hofman PM, Carnes D, Liang TW, Madara JL. Unmasking of intestinal epithelial lateral membrane β 1 integrin consequent to

- transepithelial neutrophil migration in vitro facilitates *inv*-mediated invasion by *yersinia pseudotuberculosis*. *Infection and Immunity* 65, 1414-1421. (1997).
11. Kam KR, Walsh LA, Bock SM, Koval M, Fischer KE, Ross RF, Desai TA.
Nanostructure-mediated transport of biologics across epithelial tissue: Enhancing permeability via nanotopography. *Nano Letters* 13, 164-171. (2013).
 12. Walsh L, Ryu J, Bock S, Koval M, Mauro T, Ross R, Desai T. Nanotopography facilitates *in vivo* transdermal delivery of high molecular weight therapeutics through and integrin-dependent mechanism. *Nano Letters* 15, 2434-2441. (2015).
 13. Stewart T, Koval WT, Molina SA, Bock SM, Lillard JW, Ross RF, Desai TA, Koval M.
Calibrated flux measurements reveal a nanostructure-stimulated transcytotic pathway. *Experimental Cell Research* 2, 153-161. (2017).
 14. Garbi, C., Negri, R., Cali, G., and Nitsch, L. Collagen interaction with apically expressed beta 1 integrins: loss of transepithelial resistance and reorganization of cultured thyroid cell monolayer. *European Journal of Cell Biology* 69, 64-75. (1996).

Chapter 2. Ruffles and spikes: Control of tight junction morphology and permeability by claudins

This chapter is a modified version of a work authored by K.S. Lynn*, R.J. Peterson*, and M. Koval, where * denotes co-first authorship. The original article, of the same name, was published in: *BBA-Biomembranes* 1862, 183339. 2020. Copyright Elsevier, reproduced with permission.

2.1 Abstract

Epithelial barrier function is regulated by a family of transmembrane proteins known as claudins. Functional tight junctions are formed when claudins interact with other transmembrane proteins, cytosolic scaffold proteins and the actin cytoskeleton. The predominant scaffold protein, zonula occludens-1 (ZO-1), directly binds to most claudin C-terminal domains, crosslinking them to the actin cytoskeleton. When imaged by immunofluorescence microscopy, tight junctions most frequently are linear structures that form between tricellular junctions. However, tight junctions also adapt non-linear architectures exhibiting either a ruffled or spiked morphology, which both are responses to changes in claudin engagement of actin filaments. Other terms for ruffled tight junctions include wavy, tortuous, undulating, serpentine or zig-zag junctions. Ruffling is under the control of hypoxia induced factor (HIF) and integrin-mediated signaling, as well as direct mechanical stimulation. Tight junction ruffling is specifically enhanced by claudin-2, antagonized by claudin-1 and requires claudin binding to ZO-1. Tight junction spikes are sites of active vesicle budding and fusion that appear as perpendicular projections oriented towards the nucleus. Spikes

share molecular features with focal adherens junctions and tubulobulbar complexes found in Sertoli cells. Lung epithelial cells under stress form spikes due to an increase in claudin-5 expression that directly disrupts claudin-18/ZO-1 interactions. Together this suggests that claudins are not simply passive cargoes controlled by scaffold proteins. We propose a model where claudins specifically influence tight junction scaffold proteins to control interactions with the cytoskeleton as a mechanism that regulates tight junction assembly and function (Fig. 2.1).

2.2 Introduction

A major epithelial function is to provide a barrier that separates two distinct microenvironments, the apical and basolateral compartments of a wide range of organs. To support a physiologically functional barrier, epithelial cells must be selectively permeable to ions and solutes. Selective permeability requires cells to regulate two different pathways across the epithelial barrier: the transcellular and the paracellular routes that occur through and between cells, respectively.

Paracellular transport is regulated by specialized intercellular points of contact that form the apical junctional complex (AJC), which separates polarized cells into distinct apical and basolateral domains. The AJC encircles each cell, pairing with neighboring cells to create an adhesive network formed by several classes of intercellular junctions, including adherens junctions, tight junctions, gap junctions and desmosomes [1,2]. The AJC also establishes the apical/basolateral polarity axis by organizing the Crumbs and Partitioning defective complexes [3]. The multifunctional nature of the AJC enables intercellular communication (gap junctions), provides mechanical integrity to epithelial monolayers (adherens junctions and desmosomes) and acts as a signaling hub that is sensitive to cell contact through differential interactions between

transmembrane and cytosolic junction proteins [4]. In addition, the AJC also serves as a site for recruitment and organization of the actin cytoskeleton [1,5].

Tight junctions are the AJC component that regulates paracellular barrier permeability to water, small molecules, and ions (Fig. 2.2). The main determinants of tight junction-regulated paracellular permeability are claudin-family transmembrane proteins. Claudins form paracellular ion channels of varying specificity and permeability (reviewed in [6–8]). Tissue-specific claudin composition allows for organ-specific paracellular permeability. Claudin composition and assembly into tight junctions is also sensitive to environmental stressors, such as inflammation. Moreover, claudins do not act in isolation. In concert with other transmembrane proteins, including other claudins, MarvelD proteins (e.g. occludin, tricellulin) and Ig-superfamily proteins (e.g. JAM-A), claudins form complexes with cytoplasmic scaffold proteins that regulate interactions with the actin cytoskeleton. In addition to their role as paracellular channels, there is increasing evidence that claudins can also serve as part of a signaling hub through their specific interactions with different classes of scaffold proteins [9,10].

In addition to the regulation of ion and water permeability, tight junctions also regulate the paracellular flux of soluble molecules, including large macromolecules [11]. Soluble molecules do not move through stable, claudin-based pores. Instead, their diffusion across tight junctions is due to transient discontinuities that create a path of diffusion [12,13]. Tricellular junctions also form a path for paracellular diffusion of soluble molecules that is regulated independently from bicellular tight junctions [14,15]. Here, we consider changes to the morphology of bicellular tight junctions that correlate with increases in paracellular permeability.

One implication of the ability of claudins to differentially recruit tight junction scaffold proteins is that changes in claudin composition can impact scaffold/cytoskeletal interactions,

thereby affecting the overall organization of tight junctions. This can be recognized by two characteristic non-linear tight junction morphologies that we refer to here as “tight junction ruffles” and “tight junction spikes”. Tight junction ruffles (Fig. 2.3B) are largely parallel to the site of cell-cell contact but they differ from linear tight junctions (Fig. 2.3A) in that they deviate from the most direct path interconnecting tricellular contact sites. By contrast, tight junction spikes are structures that are perpendicular to tight junctions along sites of cell-cell contact (Fig. 2.3C). As indicated in Fig. 2.3 and described in detail below, linear tight junctions, ruffles and spikes are associated with characteristic differences in the organization of junction associated actin filaments. In addition to tight junction ruffles and spikes, non-continuous distributions of claudins (e.g. strand breaks and puncta) at cell-cell contact sites also can influence paracellular permeability. Ruffles, spikes and strand breaks all correlate with impaired paracellular barrier function and thus provide valuable indicators of altered assembly of tight junction proteins.

In this review, we describe signal transduction events that induce changes in claudin composition driving changes in tight junction morphology to regulate barrier function. We propose a model where interactions between claudins, scaffold proteins, and the actin cytoskeleton alter tight junction morphology and function by influencing the balance of tension at intercellular junctions.

2.3 Ruffled junctions

When imaged by immunofluorescence microscopy, tight junctions typically appear as a relatively straight, continuous line that connects tricellular contact points (Fig. 2.4), however, there are several conditions where tight junctions exhibit a ruffled morphology [11,16,17]. Ruffled tight

junctions have been observed for several years (e.g. [18,19]). More recently they were systematically quantified by Tokuda et al. [20] in a study correlating changes in claudin expression by MDCK cells with differences in the extent of tight junction ruffling.

Other terms used to describe ruffled tight junctions include: wavy [21–23], tortuous [20,24–26], undulating [18,27], serpentine [11,26] or zig-zag [20,28]. Referring to these structures as tight junction ruffles parallels the term plasma membrane ruffles, formed by the leading edge of migrating cells [29]. In addition to comparable morphology, the mechanisms that drive plasma membrane ruffles at the leading edge and tight junction ruffles are likely to be comparable, (e.g. actin reorganization and branching by factors such as WASP) [30].

To date there have not been any examples of other junction proteins showing a ruffled morphology. Although there are no a priori reasons why other classes of junctions (e.g. adherens junctions) could not assume a ruffled conformation, junctional ruffles are likely unique to tight junctions. For instance, E-cadherin localization is not ruffled in intestinal epithelial cells that have tight junction ruffles [31].

Ruffled junctions have a distinct appearance (Fig. 2.4) and can be quantified by a measure sometimes referred to as the “zig zag index” [20]. The zig zag index is the actual path length of a tight junction between two tricellular junctions (A) divided by the minimum path length (B). A junction is considered ruffled if A/B is significantly larger than 1, where 1 is a completely unruffled (or linear) tight junction.

Tight junction ruffling frequently correlates with increased paracellular permeability (or leak) [27,32], although that is not always the case [20]. One intriguing hypothesis is that ruffling increases permeability by increasing tight junction circumference, thus enabling more functional

claudin channels per cell [24]. In addition, ruffled and linear tight junctions are differentially associated with actin which is also likely to have an impact on their barrier function [23].

Many stimuli have been shown to induce ruffling, including molecular manipulation of tight junction proteins, impaired oxygen signaling, integrin-mediated signaling and direct mechanical stimulation. Examples of each of these stimuli and the impact they have on claudin composition and tight junction morphology are described below and in Table 2.1.

2.3.1 Roles for claudin/ZO-1 interactions in tight junction ruffling

Claudins interact with each other both across tight junctions (trans-interactions) and within tight junctions (cis-interactions) [33–35]. In addition, the claudin C-terminal cytoplasmic domain interacts with cytosolic scaffold proteins, which crosslink these proteins to the cytoskeleton and can also act as a signaling hub [34,36,37]. Foremost among these is the tight junction scaffold protein zonula occludens-1 (ZO-1), which has a PDZ1 domain that binds to the “YV” motif found at the extreme C-terminus of most, but not all claudins [38]. Other proteins that interact with the claudin YV motif include ZO-2 and ZO-3 [39], as well as other non-ZO related proteins such as the E3 ubiquitin ligase LINXp80 and COPII cargo sorting protein Sec24C, both of which have been shown to play a role in regulating incorporation of claudin-1 into tight junctions via vesicular trafficking [40,41].

ZO-1 helps crosslink claudins to the actin cytoskeleton [19] and is uniquely implicated in the control of junction ruffling. This was demonstrated in MDCK II cells where ZO-1 depletion or low levels of ZO-1 resulted in tight junctions that were highly linear, whereas high levels of ZO-1 expression were associated with significant tight junction ruffling [20].

MDCK II cells engineered to be deficient in five claudins (MDCK quinKO) show non-ruffled, linear ZO-1 labeling under the control of JAM-A, underscoring a need for claudins in the formation of ruffled junctions [42]. Tight junction ruffling is unique to ZO-1/claudin interactions, since knocking out or overexpressing ZO-2 or ZO-3 has little effect on tight junction morphology [20]. Moreover, in order for ZO-1 to induce tight junction ruffles, it needs to have both the actin binding motif as well as the U6 region of the GUK domain [43]. Interestingly, the ZO-1 U6 domain plays a key role in conformational shifts in ZO-1 that limit occludin binding [43,44]. This further supports a model where ZO-1 binding to claudins, but not occludin, form more ruffled junctions in contrast to the linear tight junctions produced with ZO-1 binding concurrently to claudins and occludin.

When MDCK II cells are transduced to overexpress ZO-1, the increase in tight junction ruffling is also associated with an increase in tight junction-associated claudin-2 [20]. Consistent with a role for claudin-2 in regulating tight junction ruffling, MDCK I cells, which express low levels of claudin-2, tend to have less ruffled tight junctions than MDCK II cells that express high levels of claudin-2 [20,45]. Claudin-2 is a pore forming claudin that increases tight junction ion and water permeability [46,47]. Ruffled junctions have a higher capacity for claudin-2, which likely further enhances this effect [24].

Claudin-2 competes with other claudins for the ability to integrate into tight junctions, including claudin-1, claudin-4 and claudin-7 [20,48,49]. Although claudin-2 is less efficiently assembled into tight junction strands than claudin-1 and claudin-4 [50], claudin-2 has a longer half-life [51] and thus remains more effectively associated with tight junctions as compared with claudins having a shorter half-life. Control of claudin-2 turnover is a function of the C-terminal

domain and does not require ZO-1 binding, suggesting that other, as yet unknown, factors uniquely regulate claudin-2 integration into tight junctions [51].

Although high levels of claudin-2 correlated with tight junction ruffling, MDCK II cells deficient in claudin-2 expression did not have fully linear tight junctions [49]. Instead, increased expression of other claudins is also required to fully linearize tight junctions. For instance, claudin-2 deficient MDCK II cells transduced with exogenous claudin-4 have more linear tight junctions than claudin-2 deficient cells alone [50]. The ability of other claudins to influence formation of ruffled or linear tight junctions will require screening them for their effect on tight junction morphology and permeability.

How claudin-2 influences tight junction ruffling remains to be determined, although evidence is emerging that different claudins can influence downstream interactions between ZO-1 and other scaffold proteins. For instance, ZO-1 enhances assembly of claudin-1 into tight junction strands through interactions with the PDZ1 and PDZ3 motifs of ZO-1, whereas, claudin-2 assembly requires the PDZ1 and PDZ2 motifs [52]. Potential roles for the ZO-1 PDZ2 motif in claudin-2 recruitment into tight junctions include the PDZ2 motif mediating ZO-1 dimerization [53] or binding to other scaffold proteins. As one possibility, claudin-2 may promote folding of ZO-1 into a conformation that promotes binding of the F-BAR protein TOCA-1 complexed to WASP, leading to termination of branched actin filaments at junctions [54] (Fig. 2.5).

Claudin-dependent switching of ZO-1/scaffold protein complexes also provides a potential mechanism where the orientation of actin filaments interacting with tight junctions can switch between cortical (parallel to the plane of the plasma membrane) and filamentous (roughly perpendicular to the plasma membrane) (Fig. 2.3). In this model, the tension exerted on ruffled tight junctions is higher than linear junctions, yet still symmetrical across the plane of the junction.

It is well established that myosin light chain kinase (MLCK) and rho family kinases regulate barrier function by altering the magnitude of tension on tight junctions [1,55,56]. Differential tension can also lead to changes in ZO-1 conformation that affect its function and ability to interact with other proteins, including claudins [57]. In addition to tension, flow can also impact barrier function. For instance, blood flow through veins is much slower than through arteries, and veins are considerably more permeable than arteries [58,59]. Consistent with this difference in permeability, venous endothelial cells have more ruffled junctions and are associated with actin stress fibers as opposed to arterial endothelial cells that form high resistance barriers and have linear junctions associated with cortical actin [60].

Taken together, this suggests a model where claudin-directed reorientation of the actin cytoskeleton coordinated with changes in actomyosin-mediated tension regulates tight junction morphology and barrier function. Consistent with this model, tight junction ruffling was reversed by treatment with the myosin inhibitor blebbistatin, further underscoring a role for actin-associated tension in ruffle formation [20].

2.3.2 Hypoxia induced tight junction ruffles

Epithelial barrier function is highly sensitive to changes in oxygen tension, where each epithelial tissue has a particular oxygen set point ranging from hyperoxia (high oxygen tension) to hypoxia. The lung is an example of a hyperoxic tissue whereas the intestine and, counterintuitively, skin are hypoxic [61–63].

Oxygen tension is sensed by the Hypoxia Inducible Factor (HIF)-1 α and HIF-2 α (Endothelial PAS Domain Protein 1; EPAS1) transcription factors that act in concert with HIF-1 β [64,65]. At normoxia, prolines on HIF transcription factors become hydroxylated targeting them

to the proteasome to be degraded. However, in hypoxia, the non-hydroxylated forms of HIF-1 α and HIF-2 α translocate to the nucleus where they activate gene transcription.

Although HIF-1 α and HIF-2 α activate different subsets of the genome (e.g. [31]) both influence epithelial tight junctions, since depletion of either of these proteins experimentally or due to chronic inflammation impairs barrier function [66,67]. Specifically, it has been demonstrated in human intestinal epithelial cell lines that knockdown of either HIF-1 α [27] or HIF-2 α [31] induces a ruffled tight junction morphology as determined by immunofluorescence as well as decreased barrier function.

Despite the comparable effects of shRNA knockdown on tight junction morphology and permeability, HIF-1 α and HIF-2 α have different mechanisms of action. HIF-1 α is directly linked to claudin-1 expression, since HIF-1 α knockdown in intestinal and esophageal epithelial cells decreases claudin-1 and reporter assays demonstrate that HIF-1 α interacts with the CLDN1 promoter [27,68]. HIF-1 β depleted cells show reduced claudin-1 expression (because of the impact on HIF-1 α) and increased tight junction ruffling. Critically, transducing HIF-1 β depleted cells to overexpress claudin-1 reverses the ruffled tight junctions into a linear morphology and restores barrier function, indicating a direct role of claudin-1 in regulating paracellular permeability that corresponds with tight junction assembly [27].

In contrast to HIF-1 α , HIF-2 α does not directly regulate claudin-1 transcription [68], despite the observation that HIF-2 α knockdown also induces tight junction ruffling. Instead, HIF-2 α depletion decreases expression of several key enzymes involved in creatine metabolism, including creatine kinase M (CKM) and creatine kinase B (CKB), enzymes that otherwise co-localize with E-cadherin and ZO-1 [31]. Critically, creatine supplementation rescues intestinal epithelial barrier function of HIF-2 α deficient cells in vitro and in a dextran sodium sulfate

inflammatory bowel disease model in vivo, underscoring a role for localized energy metabolism in regulating tight junction morphology and function. It remains to be determined whether CK and claudin-1 overlap or represent parallel pathways that regulate the extent of tight junction ruffling.

While increasing claudin-1 expression leading to increased barrier function is due in part to the barrier forming properties of claudin-1 [69], the precise mechanisms whereby claudin-1 changes tight junction morphology have not been fully elucidated. As described above, the influence of claudin-1 on ZO-1 function can affect the recruitment of other proteins that can then affect tight junction morphology. However, with the exception of ZO-1, specific claudin-1 interacting proteins that determine whether tight junctions are ruffled or linear have not yet been identified.

2.3.3 Integrin stimulation by nanostructured surfaces

Contact of the basal surface of cells with the extracellular matrix has a considerable impact on cell phenotype and function, which is a key element in the ability to produce organoid cultures that faithfully mimic differentiated cell behavior in native tissues [70]. Specifically, receptors known as integrins bind to extracellular matrix components regulating the organization of the actin cytoskeleton that, in turn, have several downstream consequences impacting cell function [71]. In addition to the native biological substrates for integrins, recent work has determined that integrin contact with synthetic, nanostructured surfaces alters epithelial barrier function in a geometry-dependent manner [16,32]. The effects of nanostructured surfaces on cells depend on several parameters, including feature aspect ratio, density, pattern and substrate chemistry [32].

Several classes of nanostructured surfaces imprinted on inert polymers have been shown to increase paracellular permeability through direct contact with $\beta 1$ integrin [16,17]. This has

utility for design of devices for transdermal delivery of macromolecular therapeutics (e.g. Etanercept), since coating microneedles with a nanostructured surface significantly enhances macromolecule delivery as compared with bare stainless steel microneedles by increasing keratinocyte transepithelial permeability [17]. Agents delivered transdermally via nanostructure coated microneedles also are more effectively delivered to the cardiovascular and lymphatic systems by an as yet unknown mechanism [17,72,73]. One possibility that remains to be tested is that dermal cells stimulated by nanostructure contact secrete factors promoting downstream vessel permeability.

Epithelial cell contact with specific nanostructured surfaces increases paracellular leak and causes junctions to become ruffled [11,16,17]. This is accompanied by decreased expression of claudin-1 [17], consistent with the effect of HIF-1 α knockdown described above. Claudin-4 expression is also reduced by nanostructure contact, which may be directly associated with an effect of nanostructures on integrins, since claudin-4 is closely associated with β 1 and α 2 integrin [74].

In addition to the effects on claudin expression, nanostructure contact also stimulates focal adhesion kinase (FAK) and MLCK activity, both of which were required for the increase in paracellular permeability [16,17]. Whether the changes in claudin expression and kinase activation have an additive or redundant effect on tight junction morphology is not yet known.

2.3.4 Ruffles formed by mechanical stimulation

Mechanical stimulation of cells can also lead to tight junction ruffling and changes in paracellular permeability. A particularly dramatic example of this is cyclic stretch of Caco-2 cells [23]. Cyclic stretch activates MLCK, suggesting a potential mechanism comparable to the effect

of nanostructured surfaces on cells. Cyclic stretch also activates JNK and Src, which phosphorylate ZO-1 and occludin [23] and are likely to influence their ability to interact with each other (e.g. [75–77]) and potentially other proteins. Consistent with the effects of mechanical stress on tight junction assembly, precision cut lung slices subjected to stretch caused dissociation of claudins from ZO-1 in lung epithelial cells [78]. Moreover, cells transduced with constitutively activated MLCK show regions of localized ruffling that are deficient in claudin-1, further underscoring a role for claudin-1 in maintaining linear tight junctions [18].

2.4 Tight junction spikes and discontinuities

In contrast to tight junction ruffles, tight junction spikes are an asymmetric deviation from linear tight junction morphology. Tight junction spikes appear as projections at cell-cell interfaces that orient in a perpendicular direction from junctions towards the nucleus (Fig. 2.6). The asymmetry of tight junction spikes is shared by a comparable adherens junction structure, focal adherens junctions, that also can be asymmetric and have been studied in considerable detail (reviewed in [79,80]). Several other terms have been used to describe focal adherens junctions [81], including: perpendicular junctions [82,83], spot junctions [84], discontinuous junctions [83,85], punctate junctions [83], junction-associated intermittent lamellipodia [86] and buttons [87]. A comparable structure formed by desmosomes has been referred to as linear arrays [88] and another formed by gap junctions has been referred to as filadendrites [89].

Here we distinguish tight junction spikes from clearly discontinuous tight junctions [83,87,90–92], in that spikes typically project from intact regions of intercellular tight junctions.

While visually distinct, tight junction discontinuities and spikes also are quantifiable by image analysis of the relative amount of continuous, punctate and perpendicular junctions [83,93], using segmentation image analysis [94] or by neural network analysis of patterns of junctional disruption based on differential labeling intensity [92].

Tight junction spikes differ from focal adherens junctions which are usually punctate. Also, tight junction spikes formed by alveolar epithelial cells are clearly distinct from adherens junctions, since they are deficient in the cadherin-binding protein β -catenin, which instead is localized to areas that are adjacent to areas where tight spikes are formed [95]. The punctate nature of focal adherens junctions may reflect dissolution of lateral cadherin interactions that are weaker than trans cadherin interactions and thus more easily disrupted by increased tension [96,97]. Another key difference is that tight junction spikes more likely form from mature tight junctions as opposed to focal adherens junctions that tend to be precursors to fully mature adherens junctions [79,82].

Tight junction discontinuities generally correlate with gross disruption of the actin cytoskeleton [55,98] leading to paracellular leak. By contrast, tight junction spikes align with actin filaments perpendicular to intercellular tight junctions [95,99,100]. Actin also has a comparable role in organizing spikes formed by desmosomes [88] and gap junctions [89].

Although tight junction ruffles and spikes are both organized by actin filaments that are perpendicular to the plane of the plasma membrane, they differ in that ruffles are organized by comparable, symmetric actin filaments on both sides of the AJC, however the arrangement of actin in spikes is asymmetric (Fig. 2.3). Also, spikes are organized along the actin filaments (much as linear junctions are aligned along cortical actin) whereas ruffles are tethered to them. Otherwise, the molecular mechanisms that underlie tension generation and induce ruffles and spikes are

comparable (e.g. MLCK, Rho kinase activation) [55,56]. Several other molecular features are conserved between ruffles and spikes, including recruitment of vinculin [17,82] and F-BAR proteins [54,81] as regulators of cytoskeletal tension and membrane curvature, respectively.

2.4.1 Tight junction spikes as organizers of vesicular traffic

It has long been appreciated that formation of adherens junctions precedes tight junction formation [101]. This has previously been associated with the relative strength of trans interactions between cadherins as opposed to claudins. A more subtle role for adherens junctions in stabilizing tight junctions was revealed by an examination of α -catenin-deficient Eph4 epithelial cells, which were subject to constitutive delivery and endocytosis of claudin-3 to the plasma membrane [102]. The inability of α -catenin-deficient cells to form tight junctions was not due to a loss of mechanical junction stability, but instead was linked to an imbalance in plasma membrane cholesterol content. Replenishing cell cholesterol re-established the assembly of claudin-3 into tight junctions and stimulated the formation of claudin-3 containing spikes that also contained cholesterol [102]. These findings are consistent with previous studies demonstrating that tight junction proteins preferentially partition into cholesterol enriched microdomains [103] but extend this observation to include spikes as well as established tight junctions.

Although tight junctions appear to be relatively stable structures, in fact they are highly dynamic and are readily endocytosed [104–107]. In cells subjected to oxidative stress, tight junction spikes serve as active “hot spots” for vesicle budding and fusion [108]. Moreover, Eph4 epithelial cells plated at low density form tight junction spikes at cell-cell interfaces between two cells migrating in opposite directions; these spikes show double membrane structures by electron microscopy, indicating that one cell endocytoses both halves of a tight junction [104]. These data

suggest that tight junction spikes are associated with responses to cell stress and/or tension. Whether spikes reflect unique vs. constitutive processes that regulate tight junction turnover is an open question at present.

Tight junction spikes are reminiscent of a structure found in seminiferous tubule junctions, the basal tubulobulbar complex [109]. Tubulobulbar complexes are enriched in claudin-11, which has a limited pattern of expression and may be uniquely required for their formation [110]. Tubulobulbar complexes are enriched for actin, actin-binding proteins, dynamin and are active sites of vesicle budding and fusion, all of which are associated with tight junction spikes in other epithelial cells.

Interestingly, tubulobulbar complexes are also associated with endoplasmic reticulum-plasma membrane (ER-PM) contact sites, which form a calcium signaling-complex that controls junction remodeling [111]. A comparable ER-PM contact site is also involved in epidermal growth factor receptor (EGFR) endocytosis and signaling [112]. It also has been shown that in MDCK II cells, EGFR specifically induces claudin-2 endocytosis, but not claudin-1 endocytosis [113]. Whether claudin-2 turnover induced by EGFR occurs by a spike-mediated pathway is not known at present.

Claudin endocytosis is a regulated process. Moreover, different claudins are internalized by different endocytic pathways [105], which provide mechanisms to regulate barrier function by differential regulation of endocytosis. For instance, claudin-1, claudin-2 and claudin-4 are internalized by clathrin-mediated endocytosis, however claudin-5 is preferentially internalized by caveolar endocytosis [105,107,113]. Since claudins form complexes, it is likely that lateral claudin-claudin interactions can influence the endocytic pathways that mediate claudin turnover [33,35,114].

Stimulation of acinar epithelial cell mAChR with carbachol induces claudin-4 phosphorylation, resulting in formation of a complex with β -arrestin 2, subsequent internalization of claudin-4 and loss of barrier function [107]. Inhibiting clathrin-mediated endocytosis prevented the loss of claudin-4 and preserved barrier function. Involvement of tight junction spikes in this process was revealed by treatment with the proteasome inhibitor MG132, which stabilized spike-associated claudin-4 and also preserved barrier function.

2.4.2 Spikes formed in response to chronic alcohol exposure are due to impaired claudin/ZO-1 interactions

Chronic alcohol abuse is a risk factor for poor outcome in acute respiratory distress syndrome [115,116]. This is due, in part, to the deleterious effect of alcohol exposure on lung epithelial barrier function [117]. Increased paracellular leak across alveolar epithelial cell monolayers is accompanied by an increase in tight junction spikes [108] (Fig. 2.6). The effects of alcohol on alveolar epithelial tight junctions, including increased leak and stimulation of spike formation, can be recapitulated by TGF β 1 [99] and antagonizing GM-CSF [95], indicating that alcohol causes an imbalance in lung epithelial cytokine signaling.

Claudin-18 is prominently expressed by alveolar epithelial cells however, the healthy lung epithelium expresses low levels of claudin-5 [118]. In response to alcohol exposure, alveolar epithelial cells increase claudin-5 expression, which correlates with an increase in tight junction spikes containing claudin-18 [108]. Increased claudin-5 expression was both necessary and sufficient to induce spikes in alveolar epithelial cells. Using super-resolution microscopy and the proximity ligation assay to measure protein-protein interactions in situ, it was determined that

increased claudin-5 binds to claudin-18 and inhibits it from interacting with ZO-1, resulting in increased tight junction spike formation [108] (Fig. 2.7).

Although the precise mechanism by which claudin-5 affects claudin-18/ZO-1 interactions remains to be determined, it seems likely that there will be other examples of claudin-claudin interactions that affect organization of the tight junction scaffold. One possible model is that claudin-5 binding to claudin-18 causes a conformational shift in the C-terminus of claudin-18 displacing ZO-1 and enabling other, as yet unknown, factors to interact with claudin-18 (Fig. 2.7). Whether this is the case will require identifying proteins that preferentially interact with spike associated claudin-18.

2.4.3 Roles for claudins in regulating tight junction ultrastructure

Tight junctions have been examined at the ultrastructural level, using freeze fracture scanning electron microscopy, demonstrating a diversity of tight junction organization as meshworks that differ in strand number, shape and organization. By and large, tight junction permeability inversely correlates with meshwork depth and strand number (e.g. [119–121]) although this is not always the case [122]. Tight junction ruffles do not necessarily correlate with changes in ultrastructure since there are examples where ruffled junctions do [43] and do not [18] have accompanying changes in tight junction ultrastructure that can be detected by freeze fracture electron microscopy.

Claudins are required to form tight junction strands at the ultrastructural level [42,123] and the architecture of the tight junction meshwork is sensitive to claudin composition. For instance, overexpression of claudin-3 by MDCK cells causes a transition from an angular to a curved loop meshwork structure and decreased strand breaks [124]. The third transmembrane domain of

claudin-3 has a unique bent conformation that has been directly linked to the control of tight junction strand morphology by altering claudin packing [125]. Increased claudin-4 expression by MDCK cells produces tight junctions that have a reticular network of parallel strands, whereas high levels of claudin-2 expression are associated with curved stands that are diffuse [122].

Imaging using conventional confocal immunofluorescence microscopy has a limit of resolution of 200 nm. This is not sufficient resolution to detect strand breaks in the range of 20 nm-200 nm, which are associated with increased paracellular leak due to changes in claudin expression [124,126]. Super-resolution fluorescence microscopy has the capacity to image tight junction strands at high enough resolution to reveal differences in the ultrastructural meshwork formed by different claudins; this was demonstrated by analysis of claudin-null HEK293 cells transfected to express claudin-3 or claudin-5, which showed differences in tight junction ultrastructure that could be detected by freeze fracture electron microscopy and Spectral Position Determination Microscopy [127]. In native alveolar epithelial cells, tight junction spikes were detected by stochastic optical reconstruction microscopy (STORM) [108]. However, alveolar epithelial cells are squamous and have a limited tight junction meshwork architecture [128,129], so STORM did not detect any meshwork changes associated with tight junction spikes. Using super-resolution microscopy to assess ultrastructural changes formed by native claudins in cuboidal epithelia is feasible using current technology, but likely challenging, since it will require super-resolution in the x-z axis in addition to the x-y plane.

2.5 Summary and future directions

Tight junction assembly and function are influenced by protein composition, post-translational modifications and the internal and external mechanical forces they are subjected to. Most models emphasize the impact of actin and the cytosolic scaffold on the assembly and behavior of claudins. However, evidence is emerging that this is a reciprocal relationship, where claudins themselves can be active determinants of scaffold protein conformation and function.

Claudins associated with ruffles are assembled into tight junctions. However, it is not known whether claudins associated with tight junction spikes are assembled into bona fide tight junctions. Cells forming tight junction spikes show evidence that intact tight junctions are maintained when they were engulfed by one cell from another [104,108]. However, it is also possible that spikes contain a pool of non-junction associated claudins. One method to distinguish whether spike associated claudins are fully integrated into tight junctions is to use Fluorescence Recovery After Photobleaching (FRAP) analysis of YFP-tagged claudins which can differentiate junction associated claudins from non-junctional pools, based on rate and extent of recovery [48]. If spike associated claudins are not junctional, they could serve other roles. For instance, non-junctional pools of claudin-7 along the lateral plasma membrane regulate tumor cell growth and migration [130,131].

Since most approaches to measure epithelial permeability are based on overall measurements of an intact monolayer or tissue, the impact of tight junction morphological changes on paracellular permeability have not been well elucidated. Electrophysiologic methods that rely on scanning live cell monolayers to map local paracellular ion permeability have been developed, although these are difficult to use and correlate with tight junction morphology because they are low throughput [132,133].

Several imaging approaches have been established that enable local permeability to be measured. This includes a fluorescence barrier permeability assay based on plating cells on a biotinylated substrate that are subsequently probed with fluorescently tagged streptavidin and imaged by fluorescence microscopy (XPerT assay) [134]. The XPerT assay has been successfully used to identify sites of localized barrier dysfunction, primarily in endothelial cell monolayers [78,135–137]. The ZnUMBA assay based on zinc permeability and a fluorescent reporter molecule represents another approach to visualize localized barrier permeability [138]. Coupling imaging methods with cells expressing fluorescently tagged tight junction proteins will enable sites of paracellular leak to be identified relative to areas where tight junctions are not linear.

Many advances have been made in defining the tight junction proteome, including the use of BioID to identify proteins that are in close proximity to ZO-1, claudin-4 and occludin [74,139]. The utility of this approach is underscored by the finding that the N- and C-terminal domains of ZO-1 interact with different proteins [139]. Further expanding the use of BioID to identify proteins that interact with other claudins comparing conditions where tight junctions are linear, ruffled or forming spikes are anticipated to help define mechanisms where claudins control tight junction morphology and could help identify new proteins specific to ruffled or spike morphologies.

The ability of claudins to influence their own assembly and integration into tight junctions is beginning to be appreciated. Claudin-1, claudin-2 and claudin-5 have been associated with linear, ruffled and spiked tight junctions respectively. The ability of other claudins to influence tight junction morphology is less well established. In addition, the effect of claudins on tight junction morphology is likely to be context sensitive, especially due to interactions with other claudins present in tight junctions, and remains to be determined.

Undoubtedly, C-terminal domains of different claudins bind to different protein substrates, however, evidence is now emerging that claudins can influence the behavior of scaffold and other proteins. By analogy with connexins [140–142], the C-terminal domains of claudins are likely to be intrinsically disordered having significant structural plasticity. ZO-1 also has intrinsically disordered domains, is mechanosensitive and can exist in different phase states [143], underscoring the concept that tight junction assembly is highly context dependent with respect to both local protein composition and biophysical mechanical state. Taken together, we propose a model where complexes between different claudin C-terminal domains and scaffold proteins influence each other to fold into unique conformations. One implication of this model is that determining the regulation of epithelial paracellular barrier function will require taking into account how the reciprocal interplay between claudins, scaffold proteins and cytoskeletal tension affect tight junction assembly and function.

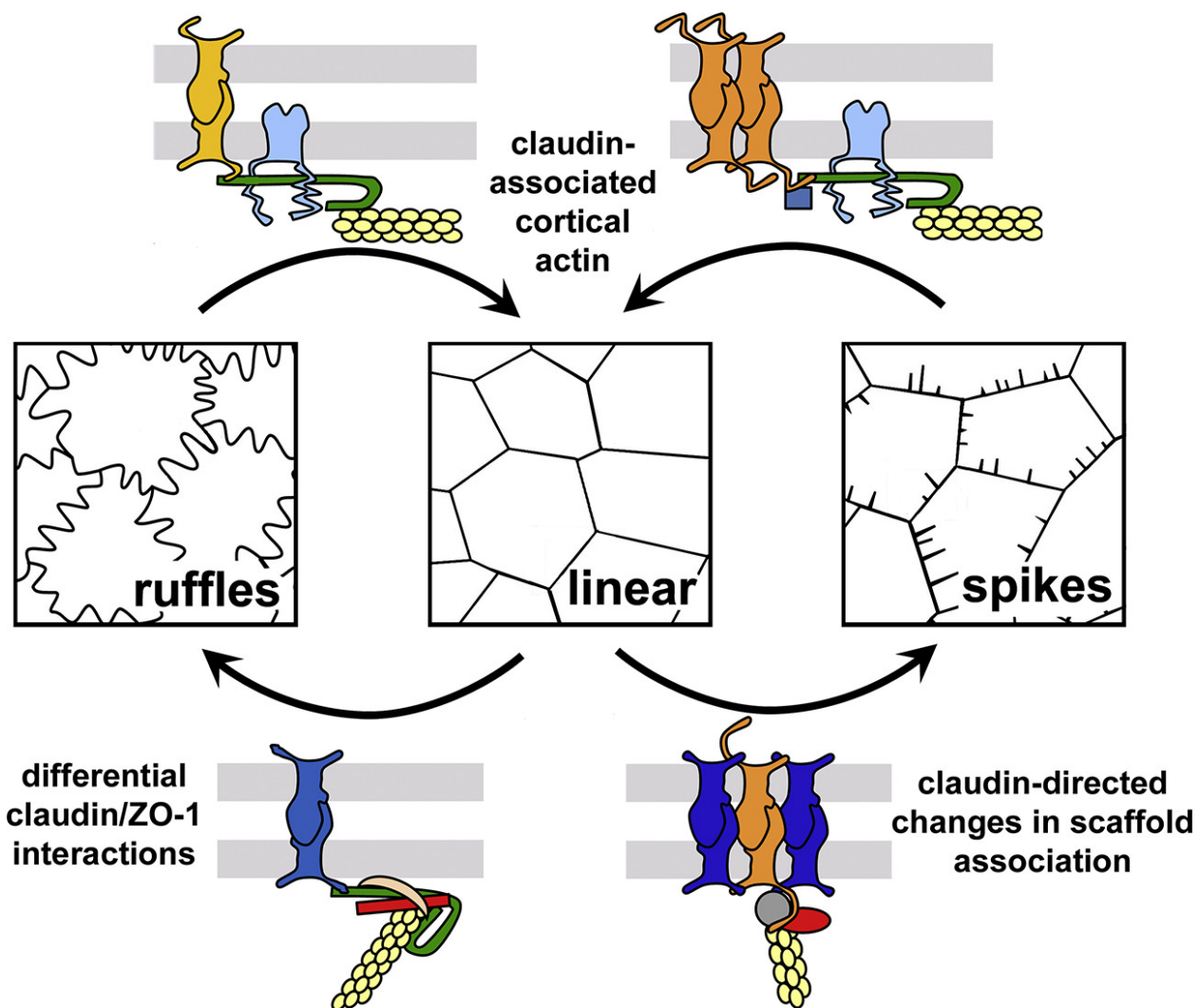


Figure 2.1. Graphical abstract.

Tight junctions show hallmark morphological changes, ruffles and spikes, in response to stimuli that cause paracellular leak. Ruffling and spike formation are due to claudin-directed regulation of tight junction scaffold protein engagement of the actin cytoskeleton. Tight junction ruffling requires ZO-1. Symmetric and asymmetric changes in tension preferentially induce ruffles and spikes, respectively.

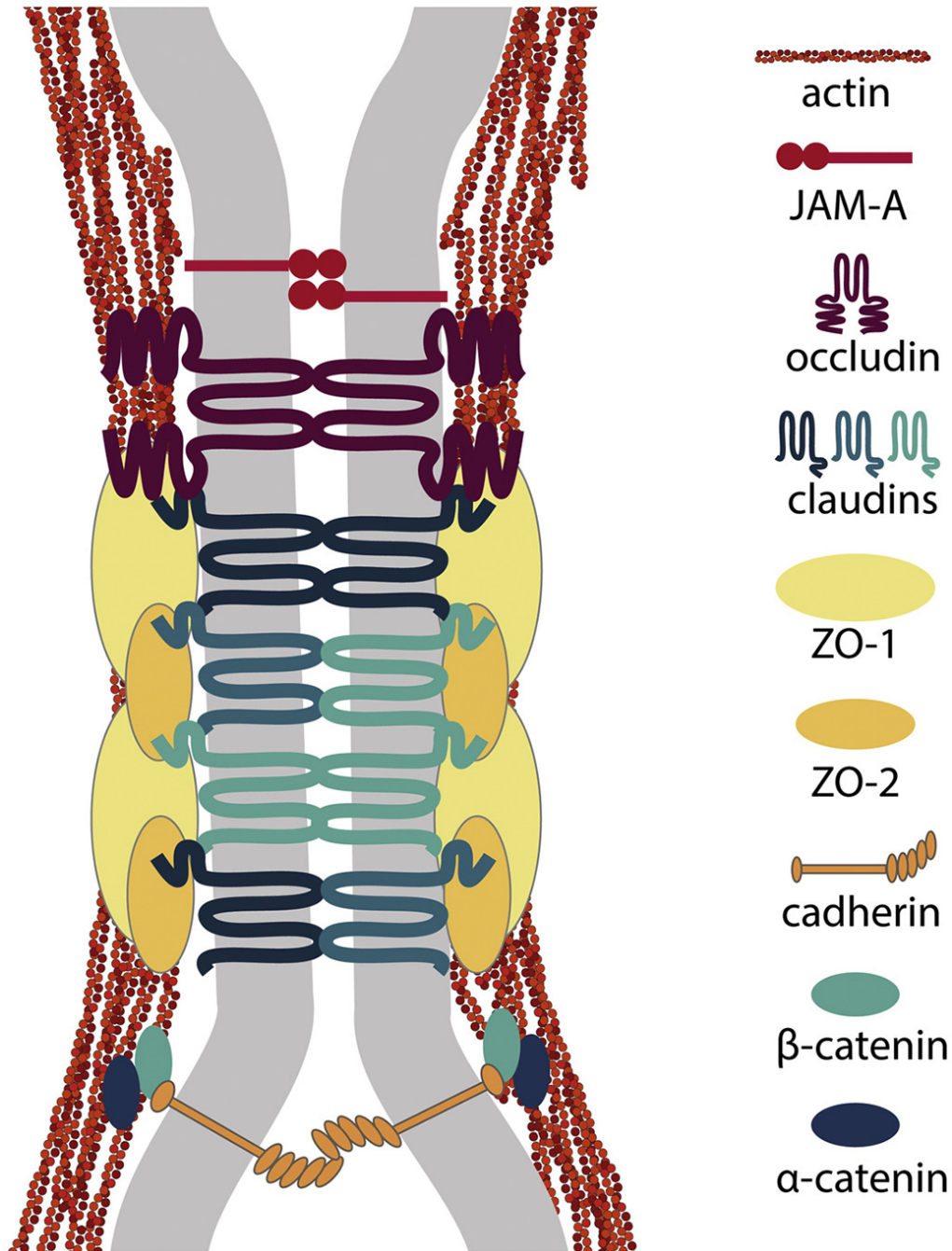


Figure 2.2. Protein composition of tight junctions and adherens junctions.

Shown is a subset of transmembrane, cytosolic scaffold and cytoskeletal proteins associated with tight junctions (occludin, claudin, ZO-1, ZO-1) and adherens junctions (cadherin, α -catenin, β -catenin).

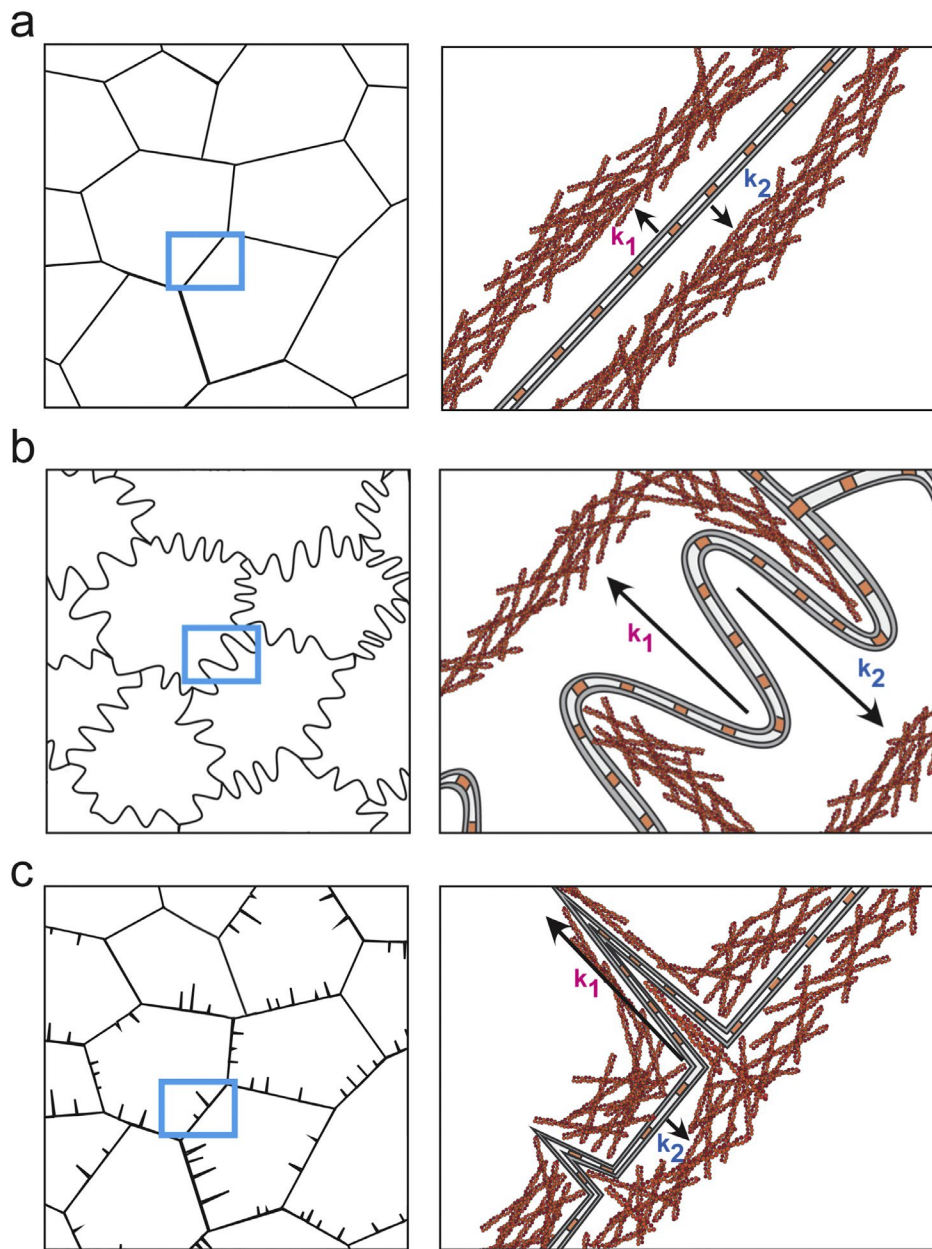


Figure 2.3. Roles for actin control of tight junction morphology.

(A) Linear tight junctions showing cortical actin and symmetrical forces perpendicular to the plane of the membrane ($k_1 = k_2$). (B) Tight junction ruffles, with tight junctions tethered to actin perpendicular to cortical actin and subjected to higher, symmetrical forces than linear junctions. (C) Tight junction spikes subjected to asymmetrical tension ($k_1 > k_2$), and oriented along actin stress fibers.

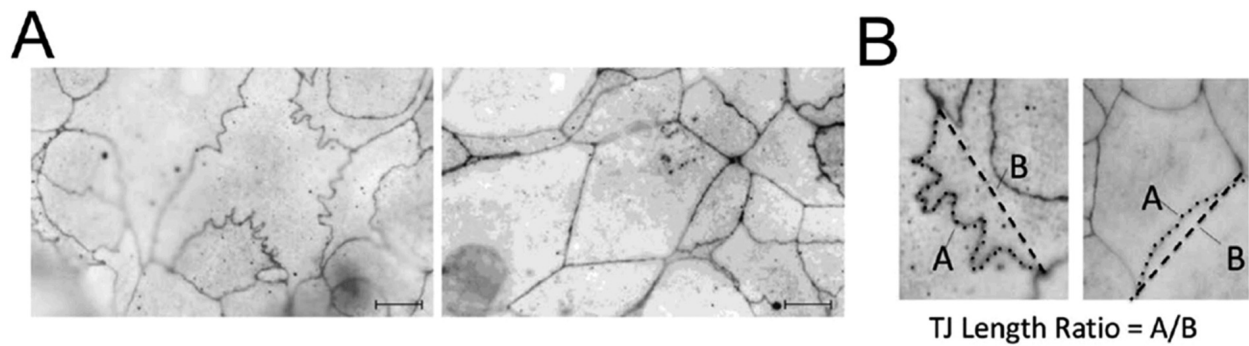


Figure 2.4. Quantitation of tight junction ruffles.

(A) ZO-1 in HIF1 β deficient Caco2 cells has a ruffled appearance. Transfection to overexpress claudin-1 cDNA normalizes ZO1 distribution to a linear morphology. (B) Quantification of tight junction ruffling was performed by dividing the actual junction length (dotted line A) by the distance between tricellular junctions (dashed line B). Examples of ruffled (left) and linear (right) tight junction morphology are shown. Reproduced from [27] with permission.

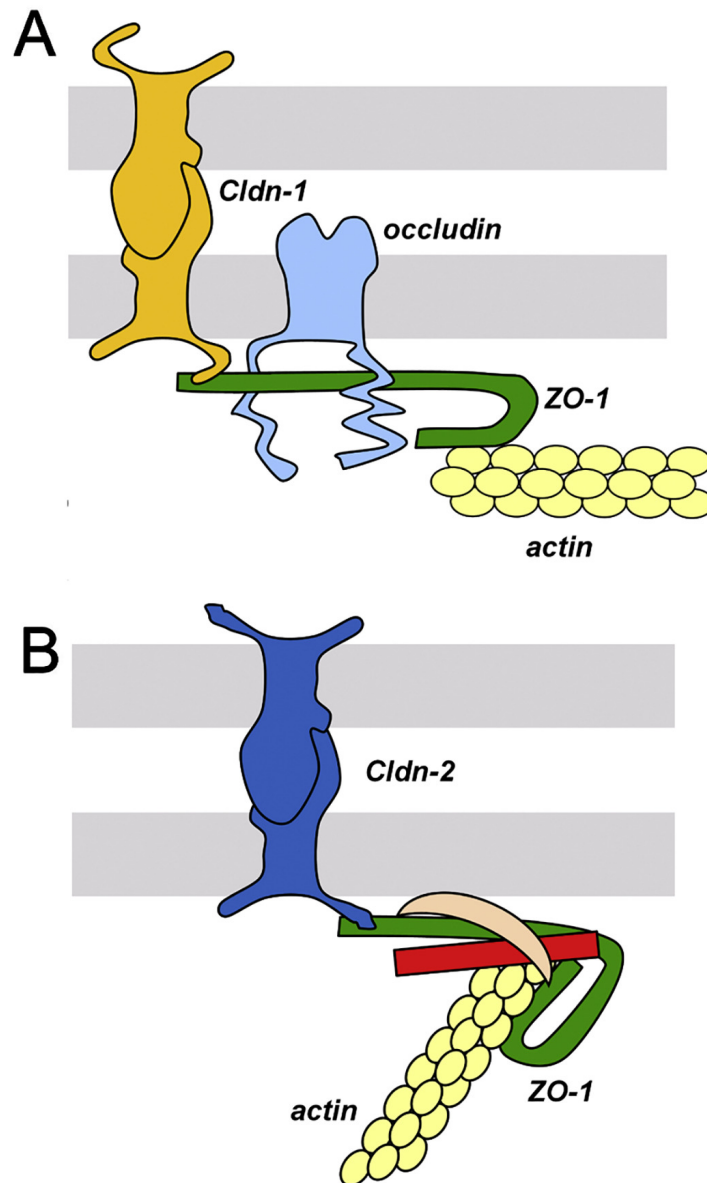


Figure 2.5. Model for claudin-directed changes in ZO-1 conformation.

(A) Claudin-1 binds to ZO-1 in a conformation enabling interactions with occludin that promote association with actin in a cortical orientation, parallel to the plane of the plasma membrane. (B) ZO-1 associated with claudin-2 is proposed to have an alternative conformation. Shown here are induced interactions with TOCA-1 (crescent) and WASP (red bar), potentially reorienting actin/ZO-1 interactions into a conformation that favors tight junction ruffling.

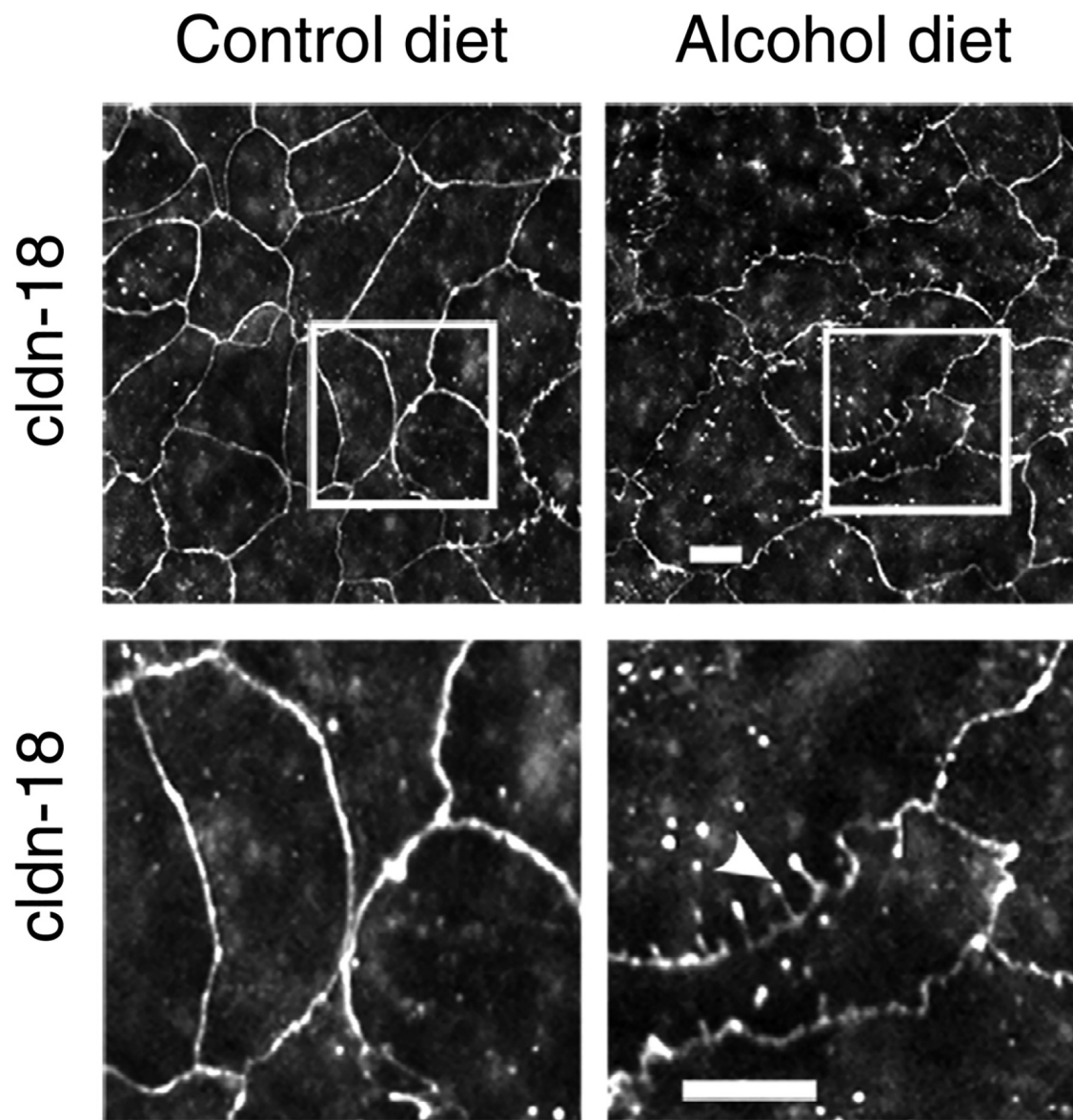


Figure 2.6. Tight junction spikes induced in lung epithelial cells.

Alveolar epithelial cells isolated from alcohol or control-fed rats were cultured for 7 days on Transwell permeable supports and immunolabeled for claudin-18. Cells from alcohol fed rats showed enhancement of tight junction spikes, that are claudin-18 projections perpendicular to the cell-cell interface (arrowhead). Square regions in the top panels correspond to magnified images below. Note strand breaks, puncta and other discontinuities in claudin-18 present in cells from alcohol-fed rats (Bar, 10 μm). Reproduced from [108] under CC BY 4.0.

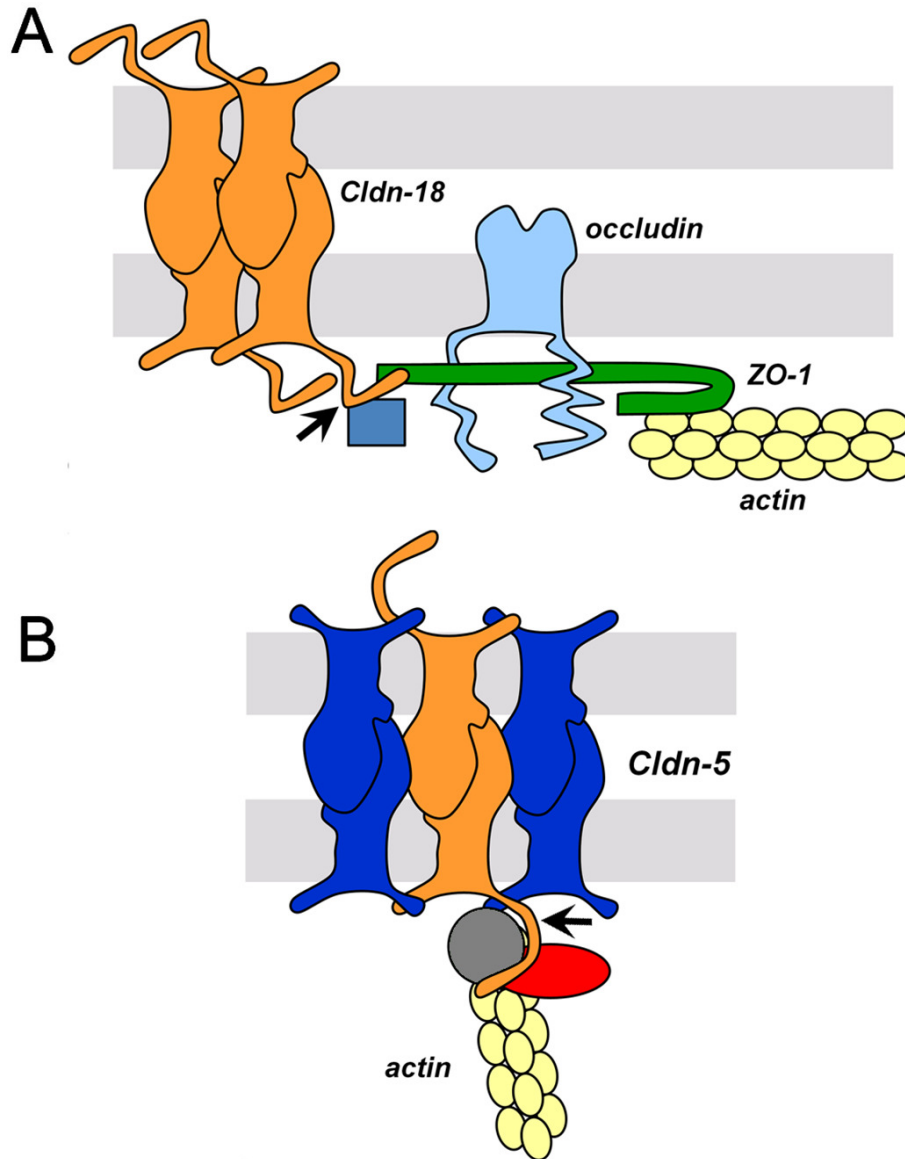


Figure 2.7. Model for claudin-claudin interactions affecting scaffold protein binding.

(A) Tight junctions enriched for claudin-18 show significant binding with ZO-1, as well as other associated proteins, indicated by the blue square, and actin in a cortical orientation (equivalent to Fig. 2.5A). (B) Increased claudin-5 interacts with claudin-18 to prevent an interaction with ZO-1. The red oval and grey circle denote putative C-terminal interacting proteins that bind to claudin-18 in the absence of ZO-1. In this model, claudin-5 is proposed to induce a conformational change in the C terminal domain of claudin-18 (arrows).

Stimulus	Effect on claudins	Effect on TER	Effect on paracellular flux	Reference
High expression of ZO-1	Cldn-2 high, cldn-1, cldn-7 low	No significant change	Variable degrees of changes in permeability, but no real pattern	Tokuda, et al. [20]
ZO-1 truncation mutants	nd	nd	nd	Fanning, et al. [19,43]
TOCA-1 expression	No change in cldn-2	No significant change	Increase 3 kDa Dextran	Van Itallie, et al. [54]
KD HIF1B knockdown	Decrease cldn-1	Decrease	Increase FITC dextran (3, 10, 40 kDa)	Saeedi, et al. [27]
KD HIF-2a knockdown	nd	Decrease	nd	Glover, et al. [31]
Reoxygenation after anoxia injury	Increase in cldn-4	Decrease	Increase FITC-dextran	Jin, et al. [21]
MLCK activation	Local decreases in cldn-1	Decrease	Increase insulin, mannitol	Shen, et al. [18]
Cyclic stretch	nd	nd	Increase insulin	Samak, et al. [23]
VAV3 inactivation	nd	Decrease	nd	Hilfenhaus, et al. [60]
Nanostructure contact	Decrease cldn-1, cldn-4	Decrease	Increase FITC-BSA, FITC-IgG, Etanercept	Kam, et al. [16], Walsh, et al. [17], Stewart, et al. [11]

Table 2.1. Stimuli inducing ruffled tight junctions.

References:

1. M. Quiros, A. Nusrat, RhoGTPases, actomyosin signaling and regulation of the epithelial Apical Junctional Complex, *Semin. Cell Dev. Biol.* 36 (2014) 194–203.
2. S. Tsukita, M. Furuse, M. Itoh, Multifunctional strands in tight junctions, *Nat. Rev. Mol. Cell Biol.* 2 (2001) 285–293.
3. Q. Wang, B. Margolis, Apical junctional complexes and cell polarity, *Kidney Int.* 72 (2007) 1448–1458.
4. L. Gonzalez-Mariscal, J. Miranda, H. Gallego-Gutierrez, M. Cano-Cortina, E. Amaya, Relationship between apical junction proteins, gene expression and cancer, *Biochim. Biophys. Acta Biomembr.* (2020) 183278.
5. T. Yano, H. Kanoh, A. Tamura, S. Tsukita, Apical cytoskeletons and junctional complexes as a combined system in epithelial cell sheets, *Ann. N. Y. Acad. Sci.* 1405 (2017) 32–43.
6. S.M. Krug, J.D. Schulzke, M. Fromm, Tight junction, selective permeability, and related diseases, *Semin. Cell Dev. Biol.* 36 (2014) 166–176.
7. J.M. Anderson, C.M. Van Itallie, Physiology and function of the tight junction, *Cold Spring Harb. Perspect. Biol.* 1 (2009) a002584.
8. D. Gunzel, Claudins: vital partners in transcellular and paracellular transport coupling, *Pflugers Arch.* 469 (2017) 35–44.
9. A.A. Bhat, N. Syed, L. Therachiyil, S. Nisar, S. Hashem, M.A. Macha, S.K. Yadav, R. Krishnankutty, S. Muralitharan, H. Al-Naemi, P. Bagga, R. Reddy, P. Dhawan, A. Akobeng, S. Uddin, M.P. Frenneaux, W. El-Rifai, M. Haris, Claudin-1, a double-edged sword in cancer, *Int. J. Mol. Sci.* 21 (2020).

10. B. Zhou, P. Flodby, J. Luo, D.R. Castillo, Y. Liu, F.X. Yu, A. McConnell, B. Varghese, G. Li, N.O. Chinge, M. Sunohara, M.N. Koss, W. Elatre, P. Conti, J.M. Liebler, C. Yang, C.N. Marconett, I.A. Laird-Offringa, P. Minoo, K. Guan, B.R. Stripp, E.D. Crandall, Z. Borok, Claudin-18-mediated YAP activity regulates lung stem and progenitor cell homeostasis and tumorigenesis, *J. Clin. Invest.* 128 (2018) 970–984.
11. T. Stewart, W.T. Koval, S.A. Molina, S.M. Bock, J.W. Lillard Jr., R.F. Ross, T.A. Desai, M. Koval, Calibrated flux measurements reveal a nanostructure-stimulated transcytotic pathway, *Exp. Cell Res.* 355 (2017) 153–161.
12. E.E. Schneeberger, R.D. Lynch, The tight junction: a multifunctional complex, *Am. J. Physiol. Cell Physiol.* 286 (2004) C1213–C1228.
13. H. Sasaki, C. Matsui, K. Furuse, Y. Mimori-Kiyosue, M. Furuse, S. Tsukita, Dynamic behavior of paired claudin strands within apposing plasma membranes, *Proc. Natl. Acad. Sci. U. S. A.* 100 (2003) 3971–3976.
14. S.M. Krug, S. Amasheh, J.F. Richter, S. Milatz, D. Gunzel, J.K. Westphal, O. Huber, J.D. Schulzke, M. Fromm, Tricellulin forms a barrier to macromolecules in tricellular tight junctions without affecting ion permeability, *Mol. Biol. Cell* 20 (2009) 3713–3724.
15. T. Higashi, S. Tokuda, S. Kitajiri, S. Masuda, H. Nakamura, Y. Oda, M. Furuse, Analysis of the ‘angulin’ proteins LSR, ILDR1 and ILDR2–tricellulin recruitment, epithelial barrier function and implication in deafness pathogenesis, *J. Cell Sci.* 126 (2013) 966–977.

16. K.R. Kam, L.A. Walsh, S.M. Bock, M. Koval, K.E. Fischer, R.F. Ross, T.A. Desai, Nanostructure-mediated transport of biologics across epithelial tissue: enhancing permeability via nanotopography, *Nano Lett.* 13 (2013) 164–171.
17. L. Walsh, J. Ryu, S. Bock, M. Koval, T. Mauro, R. Ross, T. Desai, Nanotopography facilitates in vivo transdermal delivery of high molecular weight therapeutics through an integrin-dependent mechanism, *Nano Lett.* 15 (2015) 2434–2441.
18. L. Shen, E.D. Black, E.D. Witkowski, W.I. Lencer, V. Guerriero, E.E. Schneeberger, J.R. Turner, Myosin light chain phosphorylation regulates barrier function by remodeling tight junction structure, *J. Cell Sci.* 119 (2006) 2095–2106.
19. A.S. Fanning, T.Y. Ma, J.M. Anderson, Isolation and functional characterization of the actin binding region in the tight junction protein ZO-1, *FASEB J.* 16 (2002) 1835–1837.
20. S. Tokuda, T. Higashi, M. Furuse, ZO-1 knockout by TALEN-mediated gene targeting in MDCK cells: involvement of ZO-1 in the regulation of cytoskeleton and cell shape, *PLoS One* 9 (2014) e104994.
21. Y. Jin, A.T. Blikslager, Myosin light chain kinase mediates intestinal barrier dysfunction via occludin endocytosis during anoxia/reoxygenation injury, *Am. J. Phys. Cell Physiol.* 311 (2016) C996–C1004.
22. A.I. Ivanov, D. Hunt, M. Utech, A. Nusrat, C.A. Parkos, Differential roles for actin polymerization and a myosin II motor in assembly of the epithelial apical junctional complex, *Mol. Biol. Cell* 16 (2005) 2636–2650.
23. G. Samak, R. Gangwar, L.M. Crosby, L.P. Desai, K. Wilhelm, C.M. Waters, R. Rao, Cyclic stretch disrupts apical junctional complexes in Caco-2 cell monolayers by a

- JNK-2-, c-Src-, and MLCK-dependent mechanism, *Am. J. Physiol. Gastrointest. Liver Physiol.* 306 (2014) G947–G958.
24. L. Gonzalez-Mariscal, A. Avila-Flores, A. Betanzos, The relationship between structure and function of tight junctions, in: J.M. Anderson, M. Cereijido (Eds.), *Tight Junctions*, Second edition, CRC Press, Place Published, 2001, pp. 89–120.
 25. C.M. Van Itallie, A.S. Fanning, A. Bridges, J.M. Anderson, ZO-1 stabilizes the tight junction solute barrier through coupling to the perijunctional cytoskeleton, *Mol. Biol. Cell* 20 (2009) 3930–3940.
 26. S. Angelow, R. El-Husseini, S.A. Kanzawa, A.S. Yu, Renal localization and function of the tight junction protein, claudin-19, *Am. J. Physiol. Ren. Physiol.* 293 (2007) F166–F177.
 27. B.J. Saeedi, D.J. Kao, D.A. Kitzenberg, E. Dobrinskikh, K.D. Schwisow, J.C. Masterson, A.A. Kendrick, C.J. Kelly, A.J. Bayless, D.J. Kominsky, E.L. Campbell, K.A. Kuhn, G.T. Furuta, S.P. Colgan, L.E. Glover, HIF-dependent regulation of claudin-1 is central to intestinal epithelial tight junction integrity, *Mol. Biol. Cell* 26 (2015) 2252–2262.
 28. S. Awadia, F. Huq, T.R. Arnold, S.M. Goicoechea, Y.J. Sun, T. Hou, G. Kreider-Letterman, P. Massimi, L. Banks, E.J. Fuentes, A.L. Miller, R. Garcia-Mata, SGEF forms a complex with Scribble and Dlg1 and regulates epithelial junctions and contractility, *J. Cell Biol.* 218 (2019) 2699–2725.
 29. M. Abercrombie, The crawling movement of metazoan cells, *Proc. R. Soc. Lond. B Biol. Sci.* 207 (1980) 129–147.

30. J.V. Small, T. Stradal, E. Vignal, K. Rottner, The lamellipodium: where motility begins, *Trends Cell Biol.* 12 (2002) 112–120.
31. L.E. Glover, B.E. Bowers, B. Saeedi, S.F. Ehrentraut, E.L. Campbell, A.J. Bayless, E. Dobrinskikh, A.A. Kendrick, C.J. Kelly, A. Burgess, L. Miller, D.J. Kominsky, P. Jedlicka, S.P. Colgan, Control of creatine metabolism by HIF is an endogenous mechanism of barrier regulation in colitis, *Proc. Natl. Acad. Sci. U. S. A.* 110 (2013) 19820–19825.
32. K.R. Kam, L.A. Walsh, S.M. Bock, J.D. Ollerenshaw, R.F. Ross, T.A. Desai, The effect of nanotopography on modulating protein adsorption and the fibrotic response, *Tissue Eng. Part A* 20 (2014) 130–138.
33. G. Krause, J. Protze, J. Piontek, Assembly and function of claudins: structure-function relationships based on homology models and crystal structures, *Semin. Cell Dev. Biol.* 42 (2015) 3–12.
34. C.M. Van Itallie, J.M. Anderson, Claudin interactions in and out of the tight junction, *Tissue Barriers* 1 (2013) e25247.
35. M. Koval, Differential pathways of claudin oligomerization and integration into tight junctions, *Tissue Barriers* 1 (2013) e24518.
36. S. Gowrikumar, A.B. Singh, P. Dhawan, Role of claudin proteins in regulating cancer stem cells and chemoresistance-potential implication in disease prognosis and therapy, *Int. J. Mol. Sci.* 21 (2019).
37. D.N. Kotton, Claudin-18: unexpected regulator of lung alveolar epithelial cell proliferation, *J. Clin. Invest.* 128 (2018) 903–905.

38. M. Itoh, M. Furuse, K. Morita, K. Kubota, M. Saitou, S. Tsukita, Direct binding of three tight junction-associated MAGUKs, ZO-1, ZO-2, and ZO-3, with the COOH termini of claudins, *J. Cell Biol.* 147 (1999) 1351–1363.
39. J.C. Herve, M. Derangeon, D. Sarrouilhe, N. Bourmeyster, Influence of the scaffolding protein Zonula Occludens (ZOs) on membrane channels, *Biochim. Biophys. Acta* 1838 (2014) 595–604.
40. S. Takahashi, N. Iwamoto, H. Sasaki, M. Ohashi, Y. Oda, S. Tsukita, M. Furuse, The E3 ubiquitin ligase LNX1p80 promotes the removal of claudins from tight junctions in MDCK cells, *J. Cell Sci.* 122 (2009) 985–994.
41. P. Yin, Y. Li, L. Zhang, Sec24C-dependent transport of Claudin-1 regulates hepatitis C virus entry, *J. Virol.* 91 (2017) (pii: e00629-17).
42. T. Otani, T.P. Nguyen, S. Tokuda, K. Sugihara, T. Sugawara, K. Furuse, T. Miura, K. Ebnet, M. Furuse, Claudins and JAM-A coordinately regulate tight junction formation and epithelial polarity, *J. Cell Biol.* 218 (2019) 3372–3396.
43. A.S. Fanning, B.P. Little, C. Rahner, D. Utepbergenov, Z. Walther, J.M. Anderson, The unique-5 and -6 motifs of ZO-1 regulate tight junction strand localization and scaffolding properties, *Mol. Biol. Cell* 18 (2007) 721–731.
44. A.W. McGee, S.R. Dakoji, O. Olsen, D.S. Bredt, W.A. Lim, K.E. Prehoda, Structure of the SH3-guanylate kinase module from PSD-95 suggests a mechanism for regulated assembly of MAGUK scaffolding proteins, *Mol. Cell* 8 (2001) 1291–1301.
45. B.R. Stevenson, J.M. Anderson, D.A. Goodenough, M.S. Mooseker, Tight junction structure and ZO-1 content are identical in two strains of Madin-Darby canine kidney cells which differ in transepithelial resistance, *J. Cell Biol.* 107 (1988) 2401–2408.

46. R. Rosenthal, S. Milatz, S.M. Krug, B. Oelrich, J.D. Schulzke, S. Amasheh, D. Gunzel, M. Fromm, Claudin-2, a component of the tight junction, forms a paracellular water channel, *J. Cell Sci.* 123 (2010) 1913–1921.
47. C.M. Van Itallie, J. Holmes, A. Bridges, J.L. Gookin, M.R. Coccaro, W. Proctor, O.R. Colegio, J.M. Anderson, The density of small tight junction pores varies among cell types and is increased by expression of claudin-2, *J. Cell Sci.* 121 (2008) 298–305.
48. C.T. Capaldo, A.E. Farkas, R.S. Hilgarth, S.M. Krug, M.F. Wolf, J.K. Benedik, M. Fromm, M. Koval, C. Parkos, A. Nusrat, Proinflammatory cytokine-induced tight junction remodeling through dynamic self-assembly of claudins, *Mol. Biol. Cell* 25 (2014) 2710–2719.
49. S. Tokuda, M. Furuse, Claudin-2 knockout by TALEN-mediated gene targeting in MDCK cells: claudin-2 independently determines the leaky property of tight junctions in MDCK cells, *PLoS One* 10 (2015) e0119869.
50. C.M. Van Itallie, K.F. Lidman, A.J. Tietgens, J.M. Anderson, Newly synthesized claudins but not occludin are added to the basal side of the tight junction, *Mol. Biol. Cell* 30 (2019) 1406–1424.
51. C.M. Van Itallie, O.R. Colegio, J.M. Anderson, The cytoplasmic tails of claudins can influence tight junction barrier properties through effects on protein stability, *J. Membr. Biol.* 199 (2004) 29–38.
52. L.S. Rodgers, M.T. Beam, J.M. Anderson, A.S. Fanning, Epithelial barrier assembly requires coordinated activity of multiple domains of the tight junction protein ZO-1, *J. Cell Sci.* 126 (2013) 1565–1575.

53. A.S. Fanning, M.F. Lye, J.M. Anderson, A. Lavie, Domain swapping within PDZ2 is responsible for dimerization of ZO proteins, *J. Biol. Chem.* 282 (2007) 37710–37716.
54. C.M. Van Itallie, A.J. Tietgens, E. Krystofiak, B. Kachar, J.M. Anderson, A complex of ZO-1 and the BAR-domain protein TOCA-1 regulates actin assembly at the tight junction, *Mol. Biol. Cell* 26 (2015) 2769–2787.
55. A.I. Ivanov, C.A. Parkos, A. Nusrat, Cytoskeletal regulation of epithelial barrier function during inflammation, *Am. J. Pathol.* 177 (2010) 512–524.
56. W.Q. He, J. Wang, J.Y. Sheng, J.M. Zha, W.V. Graham, J.R. Turner, Contributions of myosin light chain kinase to regulation of epithelial paracellular permeability and mucosal homeostasis, *Int. J. Mol. Sci.* 21 (2020).
57. D. Spadaro, S. Le, T. Laroche, I. Mean, L. Jond, J. Yan, S. Citi, Tension-dependent stretching activates ZO-1 to control the Junctional localization of its interactors, *Curr. Biol.* 27 (2017) 3783–3795 e3788.
58. C. Crone, O. Christensen, Electrical resistance of a capillary endothelium, *J. Gen. Physiol.* 77 (1981) 349–371.
59. W.N. Duran, F.A. Sanchez, J.W. Breslin, Microcirculatory exchange function, in: R.F. Tuma, W.N. Duran, K. Ley (Eds.), *Handbook of Physiology: Microcirculation*, Academic Press, Place Published, 2008, pp. 81–124.
60. G. Hilfenhaus, D.P. Nguyen, J. Freshman, D. Prajapati, F. Ma, D. Song, S. Ziyad, M. Cuadrado, M. Pellegrini, X.R. Bustelo, M.L. Iruela-Arispe, Vav3-induced cytoskeletal dynamics contribute to heterotypic properties of endothelial barriers, *J. Cell Biol.* 217 (2018) 2813–2830.

61. A. Carreau, B. El Hafny-Rahbi, A. Matejuk, C. Grillon, C. Kieda, Why is the partial oxygen pressure of human tissues a crucial parameter? *Small molecules and hypoxia*, *J. Cell. Mol. Med.* 15 (2011) 1239–1253.
62. J. Karhausen, G.T. Furuta, J.E. Tomaszewski, R.S. Johnson, S.P. Colgan, V.H. Haase, Epithelial hypoxia-inducible factor-1 is protective in murine experimental colitis, *J. Clin. Invest.* 114 (2004) 1098–1106.
63. B. Bedogni, S.M. Welford, D.S. Cassarino, B.J. Nickoloff, A.J. Giaccia, M.B. Powell, The hypoxic microenvironment of the skin contributes to Akt-mediated melanocyte transformation, *Cancer Cell* 8 (2005) 443–454.
64. P.J. Ratcliffe, HIF-1 and HIF-2: working alone or together in hypoxia? *J. Clin. Invest.* 117 (2007) 862–865.
65. G.L. Semenza, Oxygen homeostasis, *Wiley Interdiscip. Rev. Syst. Biol. Med.* 2 (2010) 336–361.
66. L.E. Glover, S.P. Colgan, Epithelial barrier regulation by hypoxia-inducible factor, *Ann. Am. Thorac Soc.* 14 (2017) S233–S236.
67. K. Fluck, J. Fandrey, Oxygen sensing in intestinal mucosal inflammation, *Pflugers Arch.* 468 (2016) 77–84.
68. J.C. Masterson, K.A. Biette, J.A. Hammer, N. Nguyen, K.E. Capocelli, B.J. Saeedi, R.F. Harris, S.D. Fernando, L.B. Hosford, C.J. Kelly, E.L. Campbell, S.F. Ehrentraut, F.N. Ahmed, H. Nakagawa, J.J. Lee, E.N. McNamee, L.E. Glover, S.P. Colgan, G.T. Furuta, Epithelial HIF-1 α /claudin-1 axis regulates barrier dysfunction in eosinophilic esophagitis, *J. Clin. Invest.* 129 (2019) 3224–3235.

69. R. Rosenthal, D. Gunzel, D. Theune, C. Czichos, J.D. Schulzke, M. Fromm, Water channels and barriers formed by claudins, *Ann. N. Y. Acad. Sci.* 1397 (2017) 100–109.
70. M. Simian, M.J. Bissell, Organoids: a historical perspective of thinking in three dimensions, *J. Cell Biol.* 216 (2017) 31–40.
71. Y.A. Kadry, D.A. Calderwood, Chapter 22: structural and signaling functions of integrins, *Biochim. Biophys. Acta Biomembr.* (2020) 183206.
72. M.B. Aldrich, F.C. Velasquez, S. Kwon, A. Azhdarinia, K. Pinkston, B.R. Harvey, W. Chan, J.C. Rasmussen, R.F. Ross, C.E. Fife, E.M. Sevick-Muraca, Lymphatic delivery of etanercept via nanotopography improves response to collagen-induced arthritis, *Arthritis Res. Ther.* 19 (2017) 116.
73. S. Kwon, F.C. Velasquez, J.C. Rasmussen, M.R. Greives, K.D. Turner, J.R. Morrow, W.J. Hwu, R.F. Ross, S. Zhang, E.M. Sevick-Muraca, Nanotopography-based lymphatic delivery for improved anti-tumor responses to checkpoint blockade immunotherapy, *Theranostics* 9 (2019) 8332–8343.
74. K. Fredriksson, C.M. Van Itallie, A. Aponte, M. Gucek, A.J. Tietgens, J.M. Anderson, Proteomic analysis of proteins surrounding occludin and claudin-4 reveals their proximity to signaling and trafficking networks, *PLoS One* 10 (2015) e0117074.
75. G. Kale, A.P. Naren, P. Sheth, R.K. Rao, Tyrosine phosphorylation of occludin attenuates its interactions with ZO-1, ZO-2, and ZO-3, *Biochem. Biophys. Res. Commun.* 302 (2003) 324–329.

76. R.K. Rao, S. Basuroy, V.U. Rao, K.J. Karnaky Jr., A. Gupta, Tyrosine phosphorylation and dissociation of occludin-ZO-1 and E-cadherin-beta-catenin complexes from the cytoskeleton by oxidative stress, *Biochem. J.* 368 (2002) 471–481.
77. B.C. Elias, T. Suzuki, A. Seth, F. Giorgianni, G. Kale, L. Shen, J.R. Turner, A. Naren, D.M. Desiderio, R. Rao, Phosphorylation of Tyr-398 and Tyr-402 in occludin prevents its interaction with ZO-1 and destabilizes its assembly at the tight junctions, *J. Biol. Chem.* 284 (2009) 1559–1569.
78. M.J. Song, N. Davidovich, G.G. Lawrence, S.S. Margulies, Superoxide mediates tight junction complex dissociation in cyclically stretched lung slices, *J. Biomech.* 49 (2016) 1330–1335.
79. M. Takeichi, Dynamic contacts: rearranging adherens junctions to drive epithelial remodelling, *Nat. Rev. Mol. Cell Biol.* 15 (2014) 397–410.
80. T.S. Malinova, S. Huveneers, Sensing of cytoskeletal forces by asymmetric adherens junctions, *Trends Cell Biol.* 28 (2018) 328–341.
81. Y.L. Dorland, T.S. Malinova, A.M. van Stalborch, A.G. Grieve, D. van Geemen, N.S. Jansen, B.J. de Kreuk, K. Nawaz, J. Kole, D. Geerts, R.J. Musters, J. de Rooij, P.L. Hordijk, S. Huveneers, The F-BAR protein pacsin2 inhibits asymmetric VE-cadherin internalization from tensile adherens junctions, *Nat. Commun.* 7 (2016) 12210.
82. S. Huveneers, J. Oldenburg, E. Spanjaard, G. van der Krogt, I. Grigoriev, A. Akhmanova, H. Rehmann, J. de Rooij, Vinculin associates with endothelial VE-cadherin junctions to control force-dependent remodeling, *J. Cell Biol.* 196 (2012) 641–652.

83. K.M. Gray, J.W. Jung, C.T. Inglut, H.C. Huang, K.M. Stroka, Quantitatively relating brain endothelial cell-cell junction phenotype to global and local barrier properties under varied culture conditions via the Junction Analyzer Program, *Fluids Barriers CNS* 17 (2020) 16.
84. M.A. McGill, R.F. McKinley, T.J. Harris, Independent cadherin-catenin and bazooka clusters interact to assemble adherens junctions, *J. Cell Biol.* 185 (2009) 787–796.
85. Y. Kakei, M. Akashi, T. Shigeta, T. Hasegawa, T. Komori, Alteration of cell-cell junctions in cultured human lymphatic endothelial cells with inflammatory cytokine stimulation, *Lymphat. Res. Biol.* 12 (2014) 136–143.
86. H. Schnittler, M. Taha, M.O. Schnittler, A.A. Taha, N. Lindemann, J. Seebach, Actin filament dynamics and endothelial cell junctions: the Ying and Yang between stabilization and motion, *Cell Tissue Res.* 355 (2014) 529–543.
87. P. Baluk, J. Fuxe, H. Hashizume, T. Romano, E. Lashnits, S. Butz, D. Vestweber, M. Corada, C. Molendini, E. Dejana, D.M. McDonald, Functionally specialized junctions between endothelial cells of lymphatic vessels, *J. Exp. Med.* 204 (2007) 2349–2362.
88. S.N. Stahley, M. Saito, V. Faundez, M. Koval, A.L. Matheyses, A.P. Kowalczyk, Desmosome assembly and disassembly are membrane raft-dependent, *PLoS One* 9 (2014) e87809.
89. Y. Wang, 2015, Two-Color Fluorescent Analysis of Connexin 36 Turnover and Trafficking - Relationship to Functional Plasticity, *Ophthalmology & Visual Science*, University of Texas Health Science Center, Houston, UT GSBS Dissertations and Theses (Open Access) http://digitalcommons.library.tmc.edu/utgsbs_dissertations/589, pp. 132.

90. B.R. Stevenson, D.A. Begg, Concentration-dependent effects of cytochalasin D on tight junctions and actin filaments in MDCK epithelial cells, *J. Cell Sci.* 107 (Pt 3) (1994) 367–375.
91. L. Shen, J.R. Turner, Actin depolymerization disrupts tight junctions via caveolae-mediated endocytosis, *Mol. Biol. Cell* 16 (2005) 3919–3936.
92. K.H. Ogawa, C.M. Troyer, R.G. Doss, F. Aminian, E.C. Balreira, J.M. King, Mathematical classification of tight junction protein images, *J. Microsc.* 252 (2013) 100–110.
93. K.M. Gray, D.B. Katz, E.G. Brown, K.M. Stroka, Quantitative phenotyping of cell-cell junctions to evaluate ZO-1 presentation in brain endothelial cells, *Ann. Biomed. Eng.* 47 (2019) 1675–1687.
94. H. Brezovjakova, C. Tomlinson, N. Mohd Naim, P. Swiatlowska, J.C. Erasmus, S. Huveneers, J. Gorelik, S. Bruche, V.M. Braga, Junction mapper is a novel computer vision tool to decipher cell-cell contact phenotypes, *Elife* 8 (2019) (pii: e45413).
95. C. Ward, B. Schlingmann, A.A. Stecenko, D.M. Guidot, M. Koval, NF-kappa B inhibitors impair lung epithelial tight junctions in the absence of inflammation, *Tissue Barriers* 3 (2015) e982424.
96. L.L. Pontani, I. Jorjadze, J. Brujic, Cis and trans cooperativity of E-cadherin mediates adhesion in biomimetic lipid droplets, *Biophys. J.* 110 (2016) 391–399.
97. Y. Wu, X. Jin, O. Harrison, L. Shapiro, B.H. Honig, A. Ben-Shaul, Cooperativity between trans and cis interactions in cadherin-mediated junction formation, *Proc. Natl. Acad. Sci. U. S. A.* 107 (2010) 17592–17597.

98. J.R. Turner, Molecular basis of epithelial barrier regulation: from basic mechanisms to clinical application, *Am. J. Pathol.* 169 (2006) 1901–1909.
99. C.E. Overgaard, B. Schlingmann, S. Dorsainvil White, C. Ward, X. Fan, S. Swarnakar, L.A. Brown, D.M. Guidot, M. Koval, The relative balance of GM-CSF and TGF-beta1 regulates lung epithelial barrier function, *Am. J. Phys. Lung Cell. Mol. Phys.* 308 (2015) L1212–L1223.
100. J. Zhao, E.S. Krystofiak, A. Ballesteros, R. Cui, C.M. Van Itallie, J.M. Anderson, C. Fenollar-Ferrer, B. Kachar, Multiple claudin-claudin cis interfaces are required for tight junction strand formation and inherent flexibility, *Commun. Biol.* 1 (2018) 50.
101. A. Hartsock, W.J. Nelson, Adherens and tight junctions: structure, function and connections to the actin cytoskeleton, *Biochim. Biophys. Acta* 1778 (2008) 660–669.
102. K. Shigetomi, Y. Ono, T. Inai, J. Ikenouchi, Adherens junctions influence tight junction formation via changes in membrane lipid composition, *J. Cell Biol.* 217 (2018) 2373–2381.
103. A. Nusrat, C.A. Parkos, P. Verkade, C.S. Foley, T.W. Liang, W. Innis-Whitehouse, K.K. Eastburn, J.L. Madara, Tight junctions are membrane microdomains, *J. Cell Sci.* 113 (2000) 1771–1781.
104. M. Matsuda, A. Kubo, M. Furuse, S. Tsukita, A peculiar internalization of claudins, tight junction-specific adhesion molecules, during the intercellular movement of epithelial cells, *J. Cell Sci.* 117 (2004) 1247–1257.
105. D. Zwanziger, C. Staat, A.V. Andjelkovic, I.E. Blasig, Claudin-derived peptides are internalized via specific endocytosis pathways, *Ann. N. Y. Acad. Sci.* 1257 (2012) 29–37.

106. B.L. Daugherty, M. Mateescu, A.S. Patel, K. Wade, S. Kimura, L.W. Gonzales, S. Guttentag, P.L. Ballard, M. Koval, Developmental regulation of claudin localization by fetal alveolar epithelial cells, *Am. J. Phys. Lung Cell. Mol. Phys.* 287 (2004) L1266–L1273.
107. X. Cong, Y. Zhang, J. Li, M. Mei, C. Ding, R.L. Xiang, L.W. Zhang, Y. Wang, L.L. Wu, G.Y. Yu, Claudin-4 is required for modulation of paracellular permeability by muscarinic acetylcholine receptor in epithelial cells, *J. Cell Sci.* 128 (2015) 2271–2286.
108. B. Schlingmann, C.E. Overgaard, S.A. Molina, K.S. Lynn, L.A. Mitchell, S. Dorsainvil White, A.L. Mattheyses, D.M. Guidot, C.T. Capaldo, M. Koval, Regulation of claudin/zonula occludens-1 complexes by hetero-claudin interactions, *Nat. Commun.* 7 (2016) 12276.
109. A.W. Vogl, M. Du, X.Y. Wang, J.S. Young, Novel clathrin/actin-based endocytic machinery associated with junction turnover in the seminiferous epithelium, *Semin. Cell Dev. Biol.* 30 (2014) 55–64.
110. M. Du, J. Young, M. De Asis, J. Cipollone, C. Roskelley, Y. Takai, P.K. Nicholls, P.G. Stanton, W. Deng, B.B. Finlay, A.W. Vogl, A novel subcellular machine contributes to basal junction remodeling in the seminiferous epithelium, *Biol. Reprod.* 88 (2013) 60.
111. K. Lyon, A. Adams, M. Piva, P. Asghari, E.D. Moore, A.W. Vogl, Ca²⁺ signaling machinery is present at intercellular junctions and structures associated with junction turnover in rat Sertoli cells, *Biol. Reprod.* 96 (2017) 1288–1302.
112. G. Caldieri, E. Barbieri, G. Nappo, A. Raimondi, M. Bonora, A. Conte, L. Verhoef, S. Confalonieri, M.G. Malabarba, F. Bianchi, A. Cuomo, T. Bonaldi, E. Martini, D. Mazza, P. Pinton, C. Tacchetti, S. Polo, P.P. Di Fiore, S. Sigismund, Reticulon 3-

- dependent ER-PM contact sites control EGFR nonclathrin endocytosis, *Science* 356 (2017) 617–624.
113. A. Ikari, A. Takiguchi, K. Atomi, J. Sugatani, Epidermal growth factor increases clathrin-dependent endocytosis and degradation of claudin-2 protein in MDCK II cells, *J. Cell. Physiol.* 226 (2011) 2448–2456.
114. N. Rajagopal, F.J. Irudayanathan, S. Nangia, Computational nanoscopy of tight junctions at the blood-brain barrier Interface, *Int. J. Mol. Sci.* 20 (2019) (pii: E5583).
115. M. Moss, P.E. Parsons, K.P. Steinberg, L.D. Hudson, D.M. Guidot, E.L. Burnham, S. Eaton, G.A. Cotsonis, Chronic alcohol abuse is associated with an increased incidence of acute respiratory distress syndrome and severity of multiple organ dysfunction in patients with septic shock, *Crit. Care Med.* 31 (2003) 869–877.
116. A.J. Mehta, D.M. Guidot, Alcohol and the lung, *Alcohol Res.* 38 (2017) 243–254.
117. P. Smith, L.A. Jeffers, M. Koval, Effects of different routes of endotoxin injury on barrier function in alcoholic lung syndrome, *Alcohol* 80 (2019) 81–89.
118. B. Schlingmann, S.A. Molina, M. Koval, Claudins: gatekeepers of lung epithelial function, *Semin. Cell Dev. Biol.* 42 (2015) 47–57.
119. H. Schmitz, C. Barmeyer, M. Fromm, N. Runkel, H.D. Foss, C.J. Bentzel, E.O. Riecken, J.D. Schulzke, Altered tight junction structure contributes to the impaired epithelial barrier function in ulcerative colitis, *Gastroenterology* 116 (1999) 301–309.
120. P. Claude, D.A. Goodenough, Fracture faces of zonulae occludentes from “tight” and “leaky” epithelia, *J. Cell Biol.* 58 (1973) 390–400.
121. D. Hayashi, A. Tamura, H. Tanaka, Y. Yamazaki, S. Watanabe, K. Suzuki, K. Suzuki, K. Sentani, W. Yasui, H. Rakugi, Y. Isaka, S. Tsukita, Deficiency of claudin-18 causes

- paracellular H⁺ leakage, up-regulation of interleukin-1beta, and atrophic gastritis in mice, *Gastroenterology* 142 (2012) 292–304.
122. O.R. Colegio, C. Van Itallie, C. Rahner, J.M. Anderson, Claudin extracellular domains determine paracellular charge selectivity and resistance but not tight junction fibril architecture, *Am. J. Phys. Cell Physiol.* 284 (2003) C1346–C1354.
123. M. Furuse, H. Sasaki, K. Fujimoto, S. Tsukita, A single gene product, claudin-1 or -2, reconstitutes tight junction strands and recruits occludin in fibroblasts, *J. Cell Biol.* 143 (1998) 391–401.
124. S. Milatz, S.M. Krug, R. Rosenthal, D. Gunzel, D. Muller, J.D. Schulzke, S. Amasheh, M. Fromm, Claudin-3 acts as a sealing component of the tight junction for ions of either charge and uncharged solutes, *Biochim. Biophys. Acta* 1798 (2010) 2048–2057.
125. S. Nakamura, K. Irie, H. Tanaka, K. Nishikawa, H. Suzuki, Y. Saitoh, A. Tamura, S. Tsukita, Y. Fujiyoshi, Morphologic determinant of tight junctions revealed by claudin-3 structures, *Nat. Commun.* 10 (2019) 816.
126. S. Zeissig, N. Burgel, D. Gunzel, J. Richter, J. Mankertz, U. Wahnschaffe, A.J. Kroesen, M. Zeitz, M. Fromm, J.D. Schulzke, Changes in expression and distribution of claudin 2, 5 and 8 lead to discontinuous tight junctions and barrier dysfunction in active Crohn's disease, *Gut* 56 (2007) 61–72.
127. R. Kaufmann, J. Piontek, F. Grull, M. Kirchgessner, J. Rossa, H. Wolburg, I.E. Blasig, C. Cremer, Visualization and quantitative analysis of reconstituted tight junctions using localization microscopy, *PLoS One* 7 (2012) e31128.
128. E.E. Schneeberger, M.J. Karnovsky, Substructure of intercellular junctions in freeze-fractured alveolar-capillary membranes of mouse lung, *Circ. Res.* 38 (1976) 404–411.

129. H. Bartels, H.J. Oestern, G. Voss-Wermbter, Communicating-occluding junction complexes in the alveolar epithelium. A freeze-fracture study, *Am. Rev. Respir. Dis.* 121 (1980) 1017–1024.
130. Z. Lu, D.H. Kim, J. Fan, Q. Lu, K. Verbanac, L. Ding, R. Renegar, Y.H. Chen, A non-tight junction function of claudin-7-interaction with integrin signaling in suppressing lung cancer cell proliferation and detachment, *Mol. Cancer* 14 (2015) 120.
131. S. Kuhn, M. Koch, T. Nubel, M. Ladwein, D. Antolovic, P. Klingbeil, D. Hildebrand, G. Moldenhauer, L. Langbein, W.W. Franke, J. Weitz, M. Zoller, A complex of EpCAM, claudin-7, CD44 variant isoforms, and tetraspanins promotes colorectal cancer progression, *Mol. Cancer Res.* 5 (2007) 553–567.
132. L. Zhou, Y. Gong, A. Sunq, J. Hou, L.A. Baker, Capturing rare conductance in epithelia with potentiometric-scanning ion conductance microscopy, *Anal. Chem.* 88 (2016) 9630–9637.
133. C.R. Weber, G.H. Liang, Y. Wang, S. Das, L. Shen, A.S. Yu, D.J. Nelson, J.R. Turner, Claudin-2-dependent paracellular channels are dynamically gated, *Elife* 4 (2015) e09906.
134. O. Dubrovskiy, A.A. Birukova, K.G. Birukov, Measurement of local permeability at subcellular level in cell models of agonist and ventilator-induced lung injury, *Lab. Investig.* 93 (2013) 254–263.
135. N. Klusmeier, H.J. Schnittler, J. Seebach, A novel microscopic assay reveals heterogeneous regulation of local endothelial barrier function, *Biophys. J.* 116 (2019) 1547–1559.

136. M. Ghim, P. Alpresa, S.W. Yang, S.T. Braakman, S.G. Gray, S.J. Sherwin, M. van Reeuwijk, P.D. Weinberg, Visualization of three pathways for macromolecule transport across cultured endothelium and their modification by flow, *Am. J. Physiol. Heart Circ. Physiol.* 313 (2017) H959–H973.
137. P. Belvitch, M.E. Brown, B.N. Brinley, E. Letsiou, A.N. Rizzo, J.G.N. Garcia, S.M. Dudek, The ARP 2/3 complex mediates endothelial barrier function and recovery, *Pulm. Circ.* 7 (2017) 200–210.
138. R.E. Stephenson, T. Higashi, I.S. Erofeev, T.R. Arnold, M. Leda, A.B. Goryachev, A.L. Miller, Rho flares repair local tight junction leaks, *Dev. Cell* 48 (2019) 445–459.
139. C.M. Van Itallie, A. Aponte, A.J. Tietgens, M. Gucek, K. Fredriksson, J.M. Anderson, The N and C termini of ZO-1 are surrounded by distinct proteins and functional protein networks, *J. Biol. Chem.* 288 (2013) 13775–13788.
140. G. Spagnol, M. Al-Mugotir, J.L. Kopanic, S. Zach, H. Li, A.J. Trease, K.L. Stauch, R. Grosely, M. Cervantes, P.L. Sorgen, Secondary structural analysis of the carboxyl-terminal domain from different connexin isoforms, *Biopolymers* 105 (2016) 143–162.
141. B.J. Hirst-Jensen, P. Sahoo, F. Kieken, M. Delmar, P.L. Sorgen, Characterization of the pH-dependent interaction between the gap junction protein connexin43 carboxyl terminus and cytoplasmic loop domains, *J. Biol. Chem.* 282 (2007) 5801–5813.
142. D. Bouvier, F. Kieken, A. Kellezi, P.L. Sorgen, Structural changes in the carboxyl terminus of the gap junction protein connexin 40 caused by the interaction with c Src and zonula occludens-1, *Cell Commun. Adhes.* 15 (2008) 107–118.

143. C. Schwyer, S. Shamipour, K. Pranjic-Ferscha, A. Schauer, M. Balda, M. Tada, K. Matter, C.P. Heisenberg, Mechanosensation of tight junctions depends on ZO-1 phase separation and flow, *Cell* 31 (2019) 937–952.

Chapter 3: Above the matrix: functional roles for apically localized integrins

This chapter is a manuscript that was submitted as a review with the same name to *Frontiers in Cell and Developmental Biology* and was authored by Raven J. Peterson and Michael Koval.

3.1 Abstract

Integrins are transmembrane proteins that are most typically thought of as integrating adhesion to the extracellular matrix with intracellular signaling and cell regulation. Traditionally, integrins are found at basolateral and lateral cell surfaces where they facilitate binding to the ECM and intercellular adhesion through cytosolic binding partners that regulate organization of actin microfilaments. However, evidence is accumulating that integrins also are apically localized, either endogenously or due to an exogenous stimulus. Apically localized integrins have been shown to regulate several processes by interacting with proteins such as connexins, tight junction proteins, and polarity complex proteins. Integrins can also act as receptors to mediate endocytosis. Here we review these newly appreciated roles for integrins localized to the apical cell surface.

3.2 Introduction

Integrins are classically thought of as mediating intercellular interactions and binding to the extracellular matrix (ECM), so their role in cell adhesion is well characterized [1,2]. Integrin mediated adhesion regulates the actin cytoskeleton, enabling mechanosensation, by coordinating cell responses to force transmitted from the extracellular environment [3-6]. Integrins are linked to the actin cytoskeleton via scaffold proteins (including talin, kindlin, paxillin) which also form

signaling hubs that facilitate intracellular signaling [7,8]. Signaling through integrins is unique in that it is bidirectional, as it can be initiated by external ligand binding (outside-in signaling) or by the interactions with cytosolic scaffold proteins (inside-out signaling) [1,8-10].

Much of what is known about integrins and their function comes from studying cell-cell interactions between leukocytes [11,12] and cell/ECM adhesion localized to basolateral cell surfaces [2,4]. Examples of apically localized integrins have been reported in a variety of fields yet remain under studied. In this review we consolidate examples of apically localized integrins that exist in various cell and tissue types allowing us to describe functional roles for apical integrins. We discuss the implications of these functions and questions that can be examined in the future.

3.2.1 Integrin structure

Integrins are single pass transmembrane glycoproteins found as obligate α/β heterodimer pairs. In humans, there are 18 different α subunits and 8 different β subunits that together form 24 different, specific integrin heterodimers. Different integrin heterodimers bind different ligands, including RGD receptors, collagen receptors, laminin receptors, and leukocyte specific receptors [1]. Integrin expression is cell dependent and the different α/β subunit pairings formed dictate the types of external ligands that cells can bind, which has an influence on their differentiation and behavior.

Integrin structure and conformation are key to each part of its functionality, from adhesion to signaling (Figure 3.1). The α subunit has a head domain, upper and lower leg domains [13,14]. Half of the α subunits have an I-domain inserted in the head domain, which allows them to coordinate divalent metal ions which can act as an activation switch [13,14]. Much like the α

subunit, the β subunit has upper and lower leg domains, and a head domain with a cation binding I-like domain [13,14]. As a result of this structure, both α and β subunits are able to adopt conformations with bent and extended head groups [13,14]. At inactive states, integrins are found in a bent conformation [9,13,15].

The conformational change that allows the head group to swing out into an extended conformation correlates with activation [9,15]. Activation is a requirement for integrin binding to ligands and to mediate intracellular signaling. Upon activation, integrins have a higher affinity for ligand binding [9,13]. Reflecting differences in ligand affinity for different conformations, integrins in the extended conformation are called active integrins, while integrins in the bent conformation are called inactive integrins. Though the extended head group is a hallmark of activated integrins, they can also adopt intermediate conformations such as an extended closed conformation where the headgroup is swung out but still maintains a low affinity for binding ligand [6,9,16].

3.2.2 Sensing and manipulating integrin activation using monoclonal antibodies

Though changes in integrin activity are largely a result of ligand binding or recruitment of cytosolic scaffold proteins, activity state can also be manipulated or stabilized by specific monoclonal antibodies that are conformation sensitive and can be categorized by their functionality as either activating or blocking antibodies [14,16-18]. Generally, activating antibodies promote ligand binding, while blocking antibodies prevent ligand binding [18]. Though these two classes of antibodies have functional outcomes, the mechanism of action is different.

Blocking antibodies typically allosterically regulate the ligand binding site, stabilizing integrins in the inactive state and preventing ligand binding [16,18-22]. The epitopes that many

blocking antibodies bind are called Ligand Attenuated Binding Sites (LABS) and are often found very close to ligand binding sites [18,23].

Activating antibodies are classified by the type of epitope they bind [18,23]. Ligand Induced Binding Site (LIBS) antibodies recognize epitopes that are only exposed when integrins are in the active conformation, though not necessarily only when ligand is bound, as the presence of cations (such as Mn^{2+}) can induce this conformation and subsequent antibody binding [18,23,24]. The binding of antibodies to the LIBS epitope stabilizes the integrin in the active state and increases the amount of ligand that can be bound by the integrins [16,18,24,25]. By contrast, non-LIBS antibodies are activating antibodies that recognize epitopes that are exposed in a conformation independent fashion, and as a result can bind in the presence or absence of ligand [18,23,26]. While LIBS antibodies stabilize the open conformation of integrins thus promoting ligand binding, the activation stimulated by non-LIBS antibodies likely primes the integrin for a conformation change to the active state in order to bind ligands [16,18,23]. Interestingly, the non-LIBS activating antibody TS2/16 epitope partially overlaps with blocking antibodies AIIB2 and A1-A5, suggesting that functionally distinct epitopes are often in very close proximity [27]. Because LIBS antibodies can only bind integrins that are already in the active conformation, they can both detect integrin activity state and promote a functional outcome. Unlike non-LIBS or blocking antibodies that just regulate function.

3.2.3 Roles for divalent ions and disulfide bonds in integrin conformation

Metal ion coordination in the I-domain of present in some α integrins plays a direct role regulating integrin activity by mediating changes in integrin conformation that increase binding affinity. On the other hand, metal ion coordination in the I-like domain of β integrins is less well

defined and may be more important for the control of α/β heterodimers lacking an α I-domain, such as $\alpha\nu\beta 1$ [22,28]. As a result, changes in the extracellular concentration of divalent ions can promote the adoption of a specific conformation state. Excess Mg^{2+} and Mn^{2+} can displace Ca^{2+} within the I-domain and promote the adoption of open head group conformations and support ligand binding activity [13,22,28,29]. Interestingly, when cells are treated with excess Mn^{2+} the affinity state achieved by compatible integrins is higher than that observed when integrins are activated by other means, providing further evidence for multiple different open integrin conformations [9,13]. On the other hand, excess Ca^{2+} inhibits ligand binding, as it keeps integrins in a closed conformation [13,14,22,29].

Integrin conformation and activity states can also be regulated by extracellular reducing agents acting on extracellular disulfide bonds of β subunits [9,30-32]. The addition of dithiothreitol (DTT) and to a lesser extent 2,3-dimercapto-1-propanesulfonic acid (DMPA) are able to stimulate integrin activity [31,32], in a manner independent from ion chelation [30]. DTT and DMPA appear to have an independent mechanism of activation from ion induced activation, as they can cause integrins to adopt multiple affinity states that occur at a much more gradual rate than the rapid activation of cation activation [32].

The importance of disulfide bonds also has been demonstrated when ligand binding was inhibited in response to treatment with N-ethylmaleimide, that blocks cysteines or the oxidizing agent phenylarsine oxide [33,34]. N-ethylmaleimide treatment was noteworthy in that it prevented ligand binding to $\alpha 4\beta 7$ (VLA-4) but still allowed cell adhesion, meaning that these two integrin-mediated processes can be mediated by different integrin conformations [33]. Disulfide formation/reduction in $\alpha 2\beta 1$ has also been linked to enhancing affinity to collagen [35]. Taken

together these results support the regulation of integrin function by redox circuits as a physiological control mechanism [36].

3.3 Function of apical integrins

Despite the fact that most integrins localize to the basolateral or lateral surfaces of the cell, it is becoming well documented that integrins localize to the apical surface of the cell to serve functional roles (Table 3.1). Endogenous pools of apical integrins have been documented in many cell types and there are also examples of apical integrin localization induced by stimuli or cell phenotype. The apical localization of integrins is mainly due to redistribution of the protein as opposed to resulting from increased expression of β integrin [37,38]. While newly synthesized integrins are trafficked to apical and basolateral domains in the cells, they are stabilized at the basolateral surface by the coordinated actions of extracellular ligand binding and signaling through β integrin cytoplasmic domain interactions with the actin cytoskeleton [39]. Mechanisms that target integrins to the apical surface are less well understood, however, there is evidence suggesting that extracellular ligands, such as galectin-3, and cytosolic proteins, such as Vav3 regulate and stabilize apical localization of $\beta 1$ integrin [40,41].

Apically localized integrins have been found in many different types of cells and have ligand-dependent and ligand-independent functions. Examples of stimuli that increase apical localization of integrins and their different functions are described below.

3.3.1 Reproduction and control of cell phenotype

There is abundant evidence that apical pools of integrins, particularly $\beta 1$, play important roles in reproduction, particularly in implantation (reviewed in [42-44]). Integrins $\alpha 3\beta 1$, $\alpha 6\beta 1$, and

$\alpha 6\beta 4$ have been identified on the apical surface at the head of sperm where they play roles during acrosomal exocytosis and help mediate initial interactions with the egg surface [45]. In blastocysts and endometrial cells, the apical localization of integrin $\beta 3$ has been determined to be crucial for embryo implantation [44], and apoptosis of follicular cells in the ovary [46].

As one example of differential integrin localization associated with tissue phenotype, expression levels of $\alpha 2\beta 1$ were found to change during mammary tissue differentiation, as does the apical integrin localization [47]. There is apical localization of $\alpha 2$ integrin during maturation and puberty, but it decreases during pregnancy and lactation, suggesting a role for apical integrins in mammary tissue growth and proliferation associated with the ability to produce milk [47].

Application of a type I collagen hydrogel to the apical surface of human umbilical vein endothelial cells (HUVECs) induces the reorganization of $\alpha 2\beta 1$ integrins to the apical surface of the cells [48]. It was further demonstrated that the activation of $\alpha 2\beta 1$ integrins was an important step in rapid tube formation and angiogenesis [48].

Schoenenberger, et al. demonstrated that MDCK II cells that have been transformed by *K-ras* expression and exhibit apical polarity defects also have apical localization of $\alpha 2\beta 1$ and $\alpha 3\beta 1$ integrin [49]. MDCK cells were also used to identify that apical integrins are a definitive requirement for the formation of tubulocysts as blocking collagen type I, type IV, and laminin interactions with integrin $\beta 1$ by using AIIB2 blocking antibodies prevents the formation of tubulocysts all together [50,51], as does the AJ2 blocking antibody [50]. Interestingly the study by Zuk and Matlin shows that the addition of collagen overlay on the apical surface of the cell does not have an effect on the relative size of apical pools of $\beta 1$ integrin [51]. This suggests that the presence of apical integrins themselves does not have an effect on polarity, but rather interactions between apical integrins and external ECM components promote a reorientation of the

apical/basolateral polarity axis [50,51]. This was evidenced by the loss of gp135 at the membrane [50], the random redistribution of p58 at the membrane [51], and the loss of microvilli [50] after exposure to apical collagen overlays.

In rat osteoblasts, $\beta 1$ integrins are localized equally to apical and basolateral surfaces, but treatment with IGF-I, which stimulates linear bone growth, causes a significant increase of the $\beta 1$ integrin localized to the apical surface [52]. Likewise, when osteoblasts are treated with corticosterone, which is known to inhibit bone growth in part by blocking IGF-I production, there is a decrease of integrin subunits on both the apical and basolateral surfaces, suggesting that the apical localization of integrins may play a role in regulating bone growth [52].

Studies in transgenic mouse models expressing mutant cystic fibrosis transmembrane regulator (CFTR) have shown that CF bronchial epithelial cells are enriched with $\beta 1$ integrin at the luminal surface, a characteristic absent in bronchial epithelial cells from wild type mice [53]. Studies in primary human airway epithelial cells have also confirmed the enrichment of apical $\beta 1$ integrin in cells from CF patients [41]. Apical localization of $\beta 1$ integrin in CF has been linked to increased Vav3 expression which stabilizes integrin localization at the plasma membrane [41]. Increases in apically localized $\beta 1$ integrin in CF were associated with increased bacterial infection through multiple pathways, including disruption of sphingolipid metabolism leading to decreased sphingosine-mediated bacterial killing [53] and increased apical fibronectin which enhances bacterial adhesion to the airway cells [41].

3.3.2 Apical integrins as bacterial receptors

The infection of epithelial cells by *Yersinia* is due to adhesion mediated by bacterial protein invasins binding to integrin $\beta 1$ [54-56]. The highest risk for infection is thought to be after

neutrophil migration to the monolayer where access to integrin $\beta 1$ at the basolateral surface is highest [54]. However, high rates of neutrophil transmigration in columnar intestinal epithelial cells have been demonstrated to allow for apical localization of integrin $\beta 1$, likely due to disruption of the apical junctional complex. Interestingly, pools of apical integrins remain even after the epithelial barrier is restored [54].

In T84 intestinal cells, apical integrins alone do not increase susceptibility to bacterial infection [54], however apical integrins appear to be sufficient for increased infection in studies using MDCK and Caco-2 cells [56]. These studies showed bacterial adhesion to apically localized $\beta 1$ integrin subunits was crucial in disrupting barrier function, assembly of TJ proteins, and opening the barrier to make the basolateral integrins more accessible to the bacteria [56]. The proximity of apical $\beta 1$ integrin to cell junctions seemingly played an important role in bacterial infection as they provided a spot for bacterial adhesion adjacent to the junctional proteins that are targeted by bacterial cytotoxins [56]. Interestingly, there is evidence that *Yersinia* infection in both Caco-2 cells and human ileal tissue promotes an increase in apical localization of integrin $\beta 1$ [57].

As a potential way to target integrin mediated infection, the apical localization of $\beta 1$ integrin in intestinal epithelial cells has been shown to be regulated by oxygen tension, since hypoxia decreases apically localized $\beta 1$ leading to decreased internalization of *Yersinia* [58]. The decrease in apical $\beta 1$ integrin was associated with an increase in HIF-1 α . Cells that were treated with dimethyloxalylglycine, a HIF-1 α stabilizing agent, also had reduced apical localization of $\beta 1$ integrins, suggesting that HIF-1 α might be a regulator of integrin expression and localization at either a transcriptional or post-translational level [58].

3.3.3 Regulation of epithelial barrier function

Garbi et al. demonstrated that application of collagen overlays to rat thyroid monolayers resulted in a decrease in TER, loss of E-cadherin basal polarity, and the formation of a cystic structure where the cells reoriented to form a lumen [59]. This is attributed to apical pools of $\alpha 1\beta 1$ integrins, since blocking anti- $\beta 1$ integrin with antibodies prolonged the time it took to see a decrease in TER [59].

Contact between thin plastic films imprinted with nanostructured patterns and $\alpha \nu \beta 1$ integrins at the apical surface of Caco-2 cell monolayers has also been shown to increase epithelial permeability as measured by both decreased TER and increased paracellular flux of macromolecules [60-63]. Paracellular leak induced by nanostructured films was accompanied by a hallmark change in tight junction morphology from a linear to ruffled appearance [64], as evidenced by ZO-1 immunofluorescence. Nanostructure stimulation was MLCK-dependent, associated with changes in organization of the actin cytoskeleton, and also induced changes in the integrin associated protein talin [61,63]. Apically added RGD peptides further mimicked the effects of nanostructures on epithelial barrier function, which further supports a role for integrins in regulating tight junctions [61].

Studies in Caco-2 cells have demonstrated that chitosan coated nanoparticles bind to apically localized $\alpha \nu \beta 3$ integrin, which leads to an opening of tight junctions and loss of junction associated ZO-1 and claudin-4 [65]. Anionic silica nanoparticles have also been shown to increase paracellular leak to macromolecules and decrease TER by interacting with $\alpha 6$ or αV integrin to stimulate an MLCK-dependent pathway that did not affect actin organization [66]. Whether integrin-stimulated reorganization of tight junctions by particles is strictly due to apical integrins

specifically regulating the cytoskeleton or whether it also requires nanoparticle internalization remains an open question.

3.3.4 Regulation of Cell Migration

It is well established that integrins in contact with the ECM can directly regulate cell migration, but there are several examples where integrins on the upper cell surface indirectly regulate cell migration.

Retinal pigment epithelial (RPE) cells are enriched with both $\alpha\text{v}\beta\text{5}$ and $\alpha\text{5}\beta\text{1}$ integrins that are localized to the apical surface of the cell [67,68]. While there is evidence that these integrins play roles attaching RPE cells to the neuroretina and during photoreceptor outer segment fragment endocytosis, they are also involved in RPE migration after wound healing [67]. Antagonizing $\alpha\text{5}\beta\text{1}$ in RPE cells prevented cell migration and proliferation, possibly as a result of disrupting F-actin and ZO-1 organization [67].

K-ras transformation of MDCK II cells caused the apical localization of pools of $\alpha\text{2}\beta\text{1}$ and $\alpha\text{3}\beta\text{1}$ integrin [49]. *K-ras* activation has been shown to regulate the overall both integrin expression levels and play a role in cell invasion [69,70]. While there is not direct evidence that *K-ras* transformation driven apical localization of integrins is involved in metastasis, it is an interesting consideration. Non-transformed MDCK cells also share some similar characteristics with developing and mechanically damaged kidney epithelium, so the fact that apical β1 integrins have been identified in these cell monolayers and can bind fibronectin suggests that apical localization of integrins plays a role in development and/or wound healing [71]. On the other hand, enhanced apical localization of collagen binding integrins, such as $\alpha\text{3}\beta\text{1}$, have been associated

with epithelial to mesenchyme transition [72] and might act as a switch associated with a cancer phenotype as opposed to productive wound healing.

Integrins are highly dynamic and traffic from the bottom surface to the top in rapidly migrating cells through a pathway where they are internalized and recycled to the bottom of the cell at the leading edge [73]. This pool of integrins is also likely to have a signaling function, since integrins on the top surface of human lung and skin fibroblasts has been shown to bind fibronectin [74]. Disruption of integrin ligand binding with blocking antibodies to either $\alpha 5$ or $\beta 1$ decreases cell adhesion and promotes cell migration [74]. Consistent with this model, integrins on the upper surface of migrating skin fibroblasts are highly mobile, as measured by FRAP, whereas they are clustered into structures referred to as fibrillar streaks in stationary cells [75].

Consistent with this observation, when apical pools of $\beta 1$ integrins on F98 cells are in the closed conformation, the cells are highly migratory [76]. However, when cells are treated with ligand that both clusters and activates the apical $\beta 1$ subunits there is a reduction of focal adhesions and cell elongation that in turn inhibits migration [76]. Taken together, these studies suggest that engagement between apical integrins and specific ligands provides a molecular switch that regulates cell motility.

3.3.5 Mechanosensing

In lens epithelial tissue, studies have shown $\alpha 6\beta 1$ integrin localized to the apical surface [77]. When the $\alpha 6\beta 1$ heterodimer in lens epithelial tissue is activated by fluid flow shear stress, it causes the opening of Cx50 hemichannels as a pathway to enable metabolite permeation into this avascular tissue [77]. The activation of $\beta 1$ integrin by activating antibody TS2/16 causes a similar opening of Cx50 hemichannels, but this activation appears to be entirely dependent on $\alpha 6$

participation, as blocking $\alpha 6$ prevents opening of Cx50 by either activating $\beta 1$ antibody or fluid flow shear stress. This suggests that there are mechanosensing roles for apical integrins that are ligand independent. Moreover, Cx50 and $\alpha 6$ co-immunoprecipitated, indicating they were part of a multimeric complex that required motifs present in the C terminus of Cx50 [77].

A similar pathway has been demonstrated in osteocytes, where the $\alpha 5\beta 1$ heterodimer opens Cx43 hemichannels under conditions of mechanical force that cause flow of interstitial fluid [78]. As was the case in lens cells, treatment of osteocytes with the activating antibody TS2/16 caused a force independent opening of Cx43 and $\alpha 5$ formed a precipitable complex with Cx43 [78].

The vasculature is also sensitive to mechanical stimulation due to blood flow. Consistent with a role for integrins in sensing flow, bovine aortic endothelial cells (BAECs) have apically localized $\beta 1$ integrins that respond to shear stimulation [79]. Interestingly apical $\beta 1$ integrin response to shear stress in BAEC cells was actin-independent and was instead associated with caveolae and eNOS stimulation, which distinguishes it from integrins mediating cell adhesion to the ECM [79].

$\beta 2$ integrin at the apical surface of HUVECs also regulates leukocyte translocation in a tunable manner. At basal levels of expression $\beta 2$ integrin mediates leukocyte adhesion, however transmigration requires the added mechanical stimulus of flow or chemokine activation [80]. However, high levels of activated $\beta 2$ integrin expressed at the apical surface of HUVECs enables neutrophil transmigration in the absence of flow, which might contribute to excessive inflammation [80].

3.4 Summary and future directions

Apically localized integrins have been found in many cell types. Integrins can be localized to the apical surface either endogenously or due to external stimuli. Evidence is accumulating that apical integrins play roles that are distinct from basolaterally and laterally localized integrins, although they participate in many similar processes such as mechanosensing, cell migration, development, and establishment of cell polarity. Though it has been demonstrated that specific apical pools of integrins exist [50,54,59], it is unclear whether there is an obligate intermixing of apical and basolateral integrins or whether they are independently regulated.

Much like their basolaterally localized counterparts, apically localized integrins interact with the actin cytoskeleton [41,56,61,67,76,79,81]. One possible explanation for the differential roles for apical and basal integrins is that the apical integrins access unique pools of actin that are distinct from actin interacting with integrins associated with focal adhesions. For instance, Bisaria, et al. identified a membrane proximal pool of F-actin [82], and if apical integrins mainly access this pool of actin this could explain why apical integrins are involved with processes such as apical signal transduction, mechanosensing, and regulation of barrier function. Identifying specific pools of actin that are preferentially regulated by apical integrins will help refine hypotheses linking them to the regulation of other actin-binding proteins, such as tight junction associated ZO-1 [83].

Critical to understanding how apical integrins interact with the actin cytoskeleton is to determine how scaffold proteins may be recruited by stimulation of apical integrins. Currently, there is a paucity of information on how stimulating apical integrins affect interactions with scaffold proteins like kindlin, vinculin, or focal adhesion kinase, although there is indirect evidence showing a reorganization of talin in response to stimulation with apically applied nanostructured surfaces [63].

In addition to the actin cytoskeleton, apical integrins have also been linked to changes in plasma membrane lipid composition, enriching ceramide and diminishing sphingosine [53]. Likewise, data linking caveolin, eNOS and connexin hemichannels to apical integrin mediated mechanosensing [77-79] expands the scope of integrin-interacting proteins beyond actin and classical integrin scaffold proteins.

Clustering of apical integrins, particularly activated integrins, appears to be a key component in inducing cell responses ranging from cell migration to increases in permeability [41,48,50,51,53,59,60-62,76]. Apical integrin clustering can also drive endocytosis which can be physiological, in the case of integrin turnover during cell migration, but also has the pathological consequences of facilitating infection by bacteria using apical integrins as receptors.

Most studies defining roles for apical integrins in driving reversal of apical/basolateral polarity relied on substrate overlay techniques to stimulate apical integrins [48,50,51,59,61]. While these techniques demonstrate that clustering of apical integrins has a functional outcome, they are difficult to interpret as integrin-specific because the substrate has contact with the entire apical surface of the cells likely leading to stimulation of other receptors. Increased permeability and tight junction reorganization seen in cells treated apically with nanostructured surfaces are subject to a similar complication [60-62].

A more specific approach was used by Turner, et al., who showed that targeting apical integrins with antibody coated polystyrene beads replicates tube formation in a way comparable to collagen hydrogel exposure [48]. This suggests that at least in some situations, apical integrin stimulation alone is sufficient to induce the same results seen with a substrate overlay technique.

How clustering of apical integrins is linked to integrin conformation and activation is not well defined. Several studies have demonstrated that integrin activation, usually through ligand

binding [41,48,50,51,53,59,76], but not necessarily clustering [65] were necessary to cause cells to respond. Recent evidence demonstrates that $\beta 1$ integrins associated with focal adhesions contain nanoclusters with distinct populations of both active and inactive integrins suggesting two independent pools depending on activation state [84]. Given the transition from freely mobile integrins to clustered, immobile integrins that is associated with cells becoming stationary [75], it is likely that clustering and integrin activation state are interconnected at the apical surface as well. Taking advantage of tools such activation state sensitive antibodies, novel approaches to specifically promote integrin clustering and super-resolution imaging techniques will help define mechanisms by which apical integrins influence cell function.

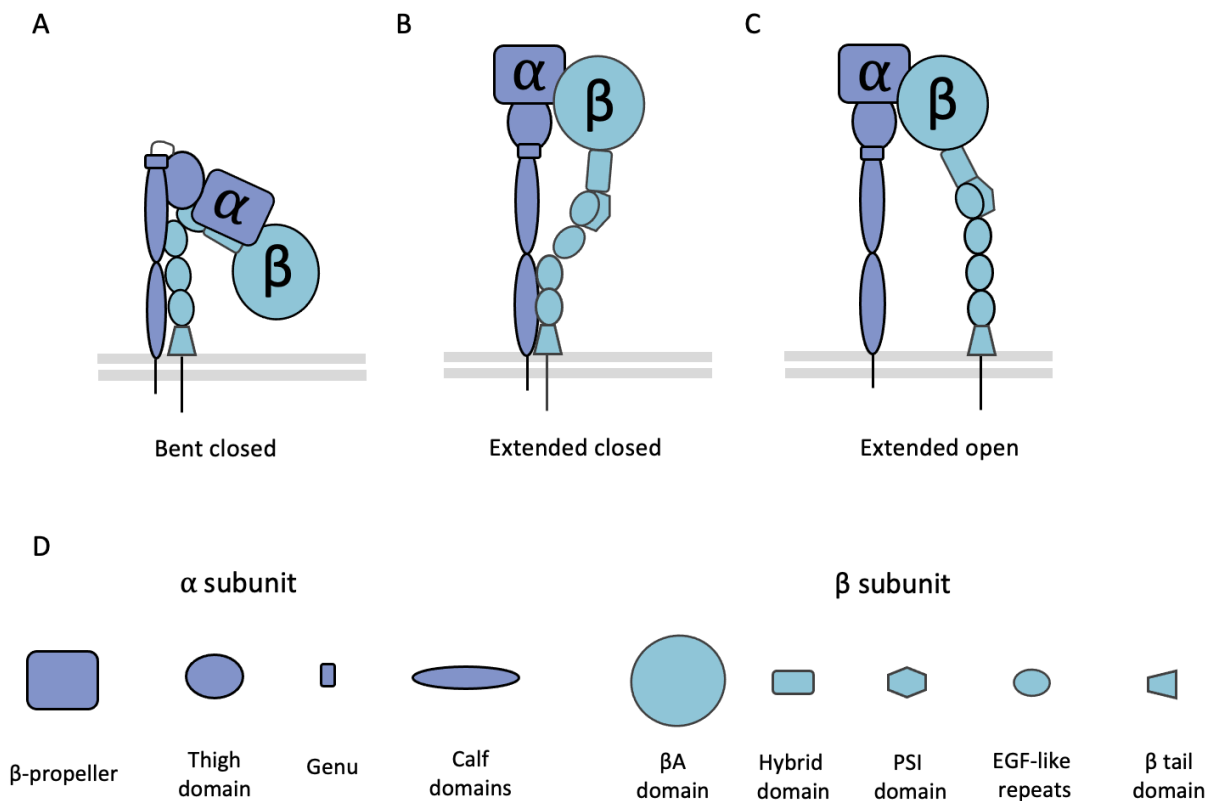


Figure 3.1. Overview of integrin conformation and domain composition.

Integrins can adopt a range of conformation structures from (A) bent closed conformation that is inactive with a low affinity for external ligands, to (B) extended closed conformation, an intermediate conformation in that is active but has a low affinity for external ligands, and (C) extended open conformation that is active with a high affinity for external ligands. (D) Structural domains of each integrin subunit. Integrins $\alpha 1$, $\alpha 2$, $\alpha 10$, $\alpha 11$, αD , αE , αL , αM , αX have an I-domain in their β -propeller subunit. PSI: Plexin, Semaphorin, Integrin domain, EGF: Epidermal Growth Factor domain. Adapted from [13,14].

Cell/tissue	Integrins	Role	Reference
Kidney			
MDCK cells	$\beta 1$	Hypothesized role in wound healing	Praetorius and Spring, [71]
MDCK I cells	$\beta 1$	Regulating tight junction associated actin, receptor for bacterial invasion	Tafazoli, et al., [56]
MDCK II cells	$\alpha 2\beta 1, \alpha 3\beta 1$ $\alpha 5\beta 1$	Polarity, tubulocyst formation Apical localization demonstrated	Zuk and Matlin, [51] Gut, et al., [39]
K-ras transformed MDCK II cells	$\beta 1$	Apical localization demonstrated	Honig, et al., [40]
MDCK clone 8 cells	$\alpha 2\beta 1, \alpha 3\beta 1$	Cell migration/metastasis, Apical polarity defects	Schoenberger, et al., [49]
Medullary collecting duct (rat)	$\alpha 2, \alpha 3, \alpha 6, \beta 1$	Polarity reversal	Ojakian and Schwimmer, [50]
	$\beta 1$	Hypothesized role in wound healing	Praetorius and Spring, [71]
Intestine			
Caco2 cells	$\beta 1$ $\alpha \nu \beta 1$ $\beta 1$	Receptor for bacterial invasion Increased transepithelial permeability Apical localization demonstrated, increased in hypoxia by HIF-1 α	Ragnarsson, et al., [57] Walsh, et al., [61] Zeitouni, et al., [58]
	$\alpha \nu \beta 3$	Targeted nanoparticles internalized, increased tight junction permeability	Xu, et al., [65]
	$\alpha 6, \alpha \nu$	Anionic nanoparticle binding increased tight junction permeability	Lamson, et al., [66]
T84 cells	$\beta 1$	Wound healing after neutrophil transmigration, increased tight junction leak	McCormick, et al., [54]
M-like cells	$\alpha 2\beta 1$	Apical localization demonstrated due to redistribution from basal surface	Hamazaoui, et al., [38]
M cells (mouse) ileum	$\beta 1$ $\beta 1$ $\alpha 2, \alpha 4$	Hypothesized to be receptor for bacterial invasion Receptor for bacterial invasion Hypothesized roles in cell/matrix and cell/cell interactions	Clark, et al., [55] Ragnarsson, et al., [57] Beaulieu, [37]
Bone			
Osteoblasts (rat)	$\beta 1$	Bone growth/remodeling	Gohel, et al., [52]
MLO-Y4 cells (mouse)	$\alpha 5\beta 1$	Mechanosensing fluid flow shear stress opens Cx43 hemichannels	Batra, et al., [78]
Lung			
Bronchial airway (mouse), primary airway epithelial cells, Calu-3 cells	$\beta 1$	CFTR knockdown and Fdel508/Fdel508 genotype increases apical $\beta 1$ expression, associated with increased ceramide/sphingosine ratio, impaired bacterial clearance	Badaoui, et al., [41]; Grassme, et al., [53]
Lung tissue (rat)	$\alpha \nu \beta 3$	Apical localization demonstrated in lung endothelium	Singh, et al., [85]
Eye			
Lens epithelial cells (mouse)	$\alpha 6\beta 1$	Mechanosensing fluid flow shear stress opens Cx50 hemichannels	Liu, et al., [77]
Lens epithelium (chicken)	$\alpha 3\beta 1$	Epithelial to mesenchymal transition	Zuk and Hay, [72]
Retinal pigment epithelial cells	$\alpha \nu \beta 5$ $\alpha 5\beta 1$	Hypothesized roles in ligand stabilization and photoreceptor outer segment fragment endocytosis Hypothesized roles in attachment to neuroretina, photoreceptor outer segment fragment endocytosis, cell migration	Mallavarapu, et al., [68] Li, et al., [67]

Cell/tissue	Integrins	Role	Reference
Endothelium			
Aortic Endothelial Cells (bovine)	$\beta 1$	Mechanosensing fluid flow shear stress, may activate TRPV4 channels	Yang and Rizzo, [79]
HUVECs	$\alpha 2\beta 1$ $\beta 2$	Hypothesized role in angiogenesis High levels of apical integrin allow neutrophil migration to take place independent of shear signals. Activation state of integrin matters	Turner, et al., [48] Cinamon, et al., [80]
Other			
FRT thyroid cells (rat)	$\alpha 1\beta 1$	Collagen binding causes polarity reversal, increases tight junction leak	Garbi, et al., [59]
Mammary tissue (mouse)	$\alpha 2\beta 1$	Tissue development, growth, proliferation	Keely, et al., [47]
F98 glioma cells	$\beta 1$	Regulation of cell migration/metastasis	Mang, et al., [76]
Splenic sinus endothelial cells (rat)	$\alpha v\beta 5$	Co-localized near vesicles hypothesize they play a role in endocytosis	Uehara and Uehara, [81]
NCI-N87 gastric carcinoma cells	$\alpha 5\beta 1$	Apical localization demonstrated	Feige, et al., [86]

Table 3.1. Cells and tissues with apically oriented integrins.

References

1. Hynes, R.O. (2002). Integrins: bidirectional, allosteric signaling machines. *Cell* 110(6), 673-687. doi: 10.1016/s0092-8674(02)00971-6
2. Geiger, B., and Yamada, K.M. (2011). Molecular architecture and function of matrix adhesions. *Cold Spring Harb Perspect Biol* 3(5). doi: 10.1101/cshperspect.a005033.
3. Brakebusch, C., and Fassler, R. (2003). The integrin-actin connection, an eternal love affair. *EMBO J* 22(10), 2324-2333. doi: 10.1093/emboj/cdg245.
4. Schwartz, M.A. (2010). Integrins and extracellular matrix in mechanotransduction. *Cold Spring Harb Perspect Biol* 2(12), a005066. doi: 10.1101/cshperspect.a005066.
5. Weber, G.F., Bjerke, M.A., and DeSimone, D.W. (2011). Integrins and cadherins join forces to form adhesive networks. *J Cell Sci* 124(Pt 8), 1183-1193. doi: 10.1242/jcs.064618.
6. Li, J., and Springer, T.A. (2017). Integrin extension enables ultrasensitive regulation by cytoskeletal force. *Proc Natl Acad Sci U S A* 114(18), 4685-4690. doi: 10.1073/pnas.1704171114.
7. Sun, Z., Costell, M., and Fassler, R. (2019). Integrin activation by talin, kindlin and mechanical forces. *Nat Cell Biol* 21(1), 25-31. doi: 10.1038/s41556-018-0234-9.
8. Kadry, Y.A., and Calderwood, D.A. (2020). Chapter 22: Structural and signaling functions of integrins. *Biochim Biophys Acta Biomembr* 1862(5), 183206. doi: 10.1016/j.bbamem.2020.183206.

9. Ye, F., Kim, C., and Ginsberg, M.H. (2012). Reconstruction of integrin activation. *Blood* 119(1), 26-33. doi: 10.1182/blood-2011-04-292128.
10. Humphries, J.D., Chastney, M.R., Askari, J.A., and Humphries, M.J. (2019). Signal transduction via integrin adhesion complexes. *Curr Opin Cell Biol* 56, 14-21. doi: 10.1016/j.ceb.2018.08.004
11. Chigaev, A., and Sklar, L.A. (2012). Aspects of VLA-4 and LFA-1 regulation that may contribute to rolling and firm adhesion. *Front Immunol* 3, 242. doi: 10.3389/fimmu.2012.00242.
12. Martin-Cofreces, N.B., Vicente-Manzanares, M., and Sanchez-Madrid, F. (2018). Adhesive Interactions Delineate the Topography of the Immune Synapse. *Front Cell Dev Biol* 6, 149. doi: 10.3389/fcell.2018.00149.
13. Luo, B.H., Carman, C.V., and Springer, T.A. (2007). Structural basis of integrin regulation and signaling. *Annu Rev Immunol* 25, 619-647. doi: 10.1146/annurev.immunol.25.022106.141618.
14. Campbell, I.D., and Humphries, M.J. (2011). Integrin structure, activation, and interactions. *Cold Spring Harb Perspect Biol* 3(3). doi: 10.1101/cshperspect.a004994.
15. Takagi, J., Petre, B.M., Walz, T., and Springer, T.A. (2002). Global conformational rearrangements in integrin extracellular domains in outside-in and inside-out signaling. *Cell* 110(5), 599-511. doi: 10.1016/s0092-8674(02)00935-2.
16. Su, Y., Xia, W., Li, J., Walz, T., Humphries, M.J., Vestweber, D., et al. (2016). Relating conformation to function in integrin alpha5beta1. *Proc Natl Acad Sci U S A* 113(27), E3872-3881. doi: 10.1073/pnas.1605074113.

17. Takada, Y., and Puzon, W. (1993). Identification of a regulatory region of integrin beta 1 subunit using activating and inhibiting antibodies. *J Biol Chem* 268(23), 17597-17601.
18. Byron, A., Humphries, J.D., Askari, J.A., Craig, S.E., Mould, A.P., and Humphries, M.J. (2009). Anti-integrin monoclonal antibodies. *J Cell Sci* 122(Pt 22), 4009-4011. doi: 10.1242/jcs.056770.
19. Werb, Z., Tremble, P.M., Behrendtsen, O., Crowley, E., and Damsky, C.H. (1989). Signal transduction through the fibronectin receptor induces collagenase and stromelysin gene expression. *J Cell Biol* 109(2), 877-889. doi: 10.1083/jcb.109.2.877.
20. Hall, D.E., Reichardt, L.F., Crowley, E., Holley, B., Moezzi, H., Sonnenberg, A., et al. (1990). The alpha 1/beta 1 and alpha 6/beta 1 integrin heterodimers mediate cell attachment to distinct sites on laminin. *J Cell Biol* 110(6), 2175-2184. doi: 10.1083/jcb.110.6.2175.
21. Mould, A.P., Akiyama, S.K., and Humphries, M.J. (1996). The inhibitory anti-beta1 integrin monoclonal antibody 13 recognizes an epitope that is attenuated by ligand occupancy. Evidence for allosteric inhibition of integrin function. *J Biol Chem* 271(34), 20365-20374. doi: 10.1074/jbc.271.34.20365.
22. Takagi, J., and Springer, T.A. (2002). Integrin activation and structural rearrangement. *Immunol Rev* 186, 141-163. doi: 10.1034/j.1600-065x.2002.18613.x.
23. Humphries, M.J. (2004). Monoclonal antibodies as probes of integrin priming and activation. *Biochem Soc Trans* 32(Pt3), 407-411. doi: 10.1042/BST0320407.
24. Bazzoni, G., Shih, D.T., Buck, C.A., and Hemler, M.E. (1995). Monoclonal antibody 9EG7 defines a novel beta 1 integrin epitope induced by soluble ligand and manganese,

- but inhibited by calcium. *J Biol Chem* 270(43), 25570-25577. doi: 10.1074/jbc.270.43.25570.
25. Luque, A., Gomez, M., Puzon, W., Takada, Y., Sanchez-Madrid, F., and Cabanas, C. (1996). Activated conformations of very late activation integrins detected by a group of antibodies (HUTS) specific for a novel regulatory region (355-425) of the common beta 1 chain. *J Biol Chem* 271(19), 11067-11075. doi: 10.1074/jbc.271.19.11067.
 26. Tsuchida, J., Ueki, S., Saito, Y., and Takagi, J. (1997). Classification of 'activation' antibodies against integrin beta1 chain. *FEBS Lett* 416(2), 212-216. doi: 10.1016/s0014-5793(97)01206-4.
 27. van de Wiel-van Kemenade, E., van Kooyk, Y., de Boer, A.J., Huijbens, R.J., Weder, P., van de Kastele, W., et al. (1992). Adhesion of T and B lymphocytes to extracellular matrix and endothelial cells can be regulated through the beta subunit of VLA. *J Cell Biol* 117(2), 461-470. doi: 10.1083/jcb.117.2.461.
 28. Shimaoka, M., Takagi, J., and Springer, T.A. (2002). Conformational regulation of integrin structure and function. *Annu Rev Biophys Biomol Struct* 31, 485-516. doi: 10.1146/annurev.biophys.31.101101.140922.
 29. Tiwari, S., Askari, J.A., Humphries, M.J., and Bulleid, N.J. (2011). Divalent cations regulate the folding and activation status of integrins during their intracellular trafficking. *J Cell Sci* 124(Pt 10), 1672-1680. doi: 10.1242/jcs.084483.
 30. Edwards, B.S., Curry, M.S., Southon, E.A., Chong, A.S., and Graf, L.H., Jr. (1995). Evidence for a dithiol-activated signaling pathway in natural killer cell avidity regulation of leukocyte function antigen-1: structural requirements and relationship to phorbol ester- and CD16-triggered pathways. *Blood* 86(6), 2288-2301.

31. Yan, B., and Smith, J.W. (2001). Mechanism of integrin activation by disulfide bond reduction. *Biochemistry* 40(30), 8861-8867. doi: 10.1021/bi002902i.
32. Chigaev, A., Zwartz, G.J., Buranda, T., Edwards, B.S., Prossnitz, E.R., and Sklar, L.A. (2004). Conformational regulation of alpha 4 beta 1-integrin affinity by reducing agents. "Inside-out" signaling is independent of and additive to reduction-regulated integrin activation. *J Biol Chem* 279(31), 32435-32443. doi: 10.1074/jbc.M404387200.
33. Pujades, C., Teixido, J., Bazzoni, G., and Hemler, M.E. (1996). Integrin alpha 4 cysteines 278 and 717 modulate VLA-4 ligand binding and also contribute to alpha 4/180 formation. *Biochem J* 313 (Pt 3), 899-908. doi: 10.1042/bj3130899.
34. Edwards, B.S., Southon, E.A., Curry, M.S., Salazar, F., Gale, J.M., Robinson, M.K., et al. (1998). Oxidant inhibition of alphaLbeta2 integrin adhesion: evidence for coordinate effects on conformation and cytoskeleton linkage. *J Leukoc Biol* 63(2), 190-202. doi: 10.1002/jlb.63.2.190.
35. Lahav, J., Wijnen, E.M., Hess, O., Hamaia, S.W., Griffiths, D., Makris, M., et al. (2003). Enzymatically catalyzed disulfide exchange is required for platelet adhesion to collagen via integrin alpha2beta1. *Blood* 102(6), 2085-2092. doi: 10.1182/blood-2002-06-1646.
36. Jones, D.P. (2008). Radical-free biology of oxidative stress. *Am J Physiol Cell Physiol* 295(4), C849-868. doi: 10.1152/ajpcell.00283.2008.
37. Beaulieu, J.F. (1992). Differential expression of the VLA family of integrins along the crypt-villus axis in the human small intestine. *J Cell Sci* 102 (Pt 3), 427-436.

38. Hamzaoui, N., Kerneis, S., Caliot, E., and Pringault, E. (2004). Expression and distribution of beta1 integrins in in vitro-induced M cells: implications for Yersinia adhesion to Peyer's patch epithelium. *Cell Microbiol* 6(9), 817-828. doi: 10.1111/j.1462-5822.2004.00391.x.
39. Gut, A., Balda, M.S., and Matter, K. (1998). The cytoplasmic domains of a beta1 integrin mediate polarization in Madin-Darby canine kidney cells by selective basolateral stabilization. *J Biol Chem* 273(45), 29381-29388. doi: 10.1074/jbc.273.45.29381.
40. Honig, E., Ringer, K., Dewes, J., von Mach, T., Kamm, N., Kreitzer, G., et al. (2018). Galectin-3 modulates the polarized surface delivery of beta1-integrin in epithelial cells. *J Cell Sci* 131(11). doi: 10.1242/jcs.213199.
41. Badaoui, M., Zoso, A., Idris, T., Bacchetta, M., Simonin, J., Lemeille, S., et al. (2020). Vav3 Mediates Pseudomonas aeruginosa Adhesion to the Cystic Fibrosis Airway Epithelium. *Cell Rep* 32(1), 107842. doi: 10.1016/j.celrep.2020.107842.
42. Sueoka, K., Shiokawa, S., Miyazaki, T., Kuji, N., Tanaka, M., and Yoshimura, Y. (1997). Integrins and reproductive physiology: expression and modulation in fertilization, embryogenesis, and implantation. *Fertil Steril* 67(5), 799-811. doi: 10.1016/s0015-0282(97)81388-x.
43. Wang, J., and Armant, D.R. (2002). Integrin-mediated adhesion and signaling during blastocyst implantation. *Cells Tissues Organs* 172(3), 190-201. doi: 10.1159/000066970.

44. Kaneko, Y., Day, M.L., and Murphy, C.R. (2011). Integrin beta3 in rat blastocysts and epithelial cells is essential for implantation in vitro: studies with Ishikawa cells and small interfering RNA transfection. *Hum Reprod* 26(7), 1665-1674. doi: 10.1093/humrep/der128.
45. Frolikova, M., Valaskova, E., Cerny, J., Lumeau, A., Sebkova, N., Palenikova, V., et al. (2019). Addressing the Compartmentalization of Specific Integrin Heterodimers in Mouse Sperm. *Int J Mol Sci* 20(5). doi: 10.3390/ijms20051004.
46. Meehan, T.L., Kleinsorge, S.E., Timmons, A.K., Taylor, J.D., and McCall, K. (2015). Polarization of the epithelial layer and apical localization of integrins are required for engulfment of apoptotic cells in the *Drosophila* ovary. *Dis Model Mech* 8(12), 1603-1614. doi: 10.1242/dmm.021998.
47. Keely, P.J., Wu, J.E., and Santoro, S.A. (1995). The spatial and temporal expression of the alpha 2 beta 1 integrin and its ligands, collagen I, collagen IV, and laminin, suggest important roles in mouse mammary morphogenesis. *Differentiation* 59(1), 1-13. doi: 10.1046/j.1432-0436.1995.5910001.x.
48. Turner, K.R., Adams, C., Staelens, S., Deckmyn, H., and San Antonio, J. (2020). Crucial Role for Endothelial Cell alpha2beta1 Integrin Receptor Clustering in Collagen-Induced Angiogenesis. *Anat Rec (Hoboken)* 303(6), 1604-1618. doi: 10.1002/ar.24277.
49. Schoenenberger, C.A., Zuk, A., Zinkl, G.M., Kendall, D., and Matlin, K.S. (1994). Integrin expression and localization in normal MDCK cells and transformed MDCK cells lacking apical polarity. *J Cell Sci* 107 (Pt 2), 527-541.

50. Ojakian, G.K., and Schwimmer, R. (1994). Regulation of epithelial cell surface polarity reversal by beta 1 integrins. *J Cell Sci* 107 (Pt 3), 561-576.
51. Zuk, A., and Matlin, K.S. (1996). Apical beta 1 integrin in polarized MDCK cells mediates tubulocyst formation in response to type I collagen overlay. *J Cell Sci* 109 (Pt 7), 1875-1889.
52. Gohel, A.R., Hand, A.R., and Gronowicz, G.A. (1995). Immunogold localization of beta 1-integrin in bone: effect of glucocorticoids and insulin-like growth factor I on integrins and osteocyte formation. *J Histochem Cytochem* 43(11), 1085-1096. doi: 10.1177/43.11.7560891.
53. Grassme, H., Henry, B., Ziobro, R., Becker, K.A., Riethmuller, J., Gardner, A., et al. (2017). beta1-Integrin Accumulates in Cystic Fibrosis Luminal Airway Epithelial Membranes and Decreases Sphingosine, Promoting Bacterial Infections. *Cell Host Microbe* 21(6), 707-718 e708. doi: 10.1016/j.chom.2017.05.001.
54. McCormick, B.A., Nusrat, A., Parkos, C.A., D'Andrea, L., Hofman, P.M., Carnes, D., et al. (1997). Unmasking of intestinal epithelial lateral membrane beta1 integrin consequent to transepithelial neutrophil migration in vitro facilitates inv-mediated invasion by *Yersinia pseudotuberculosis*. *Infect Immun* 65(4), 1414-1421. doi: 10.1128/IAI.65.4.1414-1421.1997.
55. Clark, M.A., Hirst, B.H., and Jepson, M.A. (1998). M-cell surface beta1 integrin expression and invasin-mediated targeting of *Yersinia pseudotuberculosis* to mouse Peyer's patch M cells. *Infect Immun* 66(3), 1237-1243. doi: 10.1128/IAI.66.3.1237-1243.1998.

56. Tafazoli, F., Holmstrom, A., Forsberg, A., and Magnusson, K.E. (2000). Apically exposed, tight junction-associated beta1-integrins allow binding and YopE-mediated perturbation of epithelial barriers by wild-type Yersinia bacteria. *Infect Immun* 68(9), 5335-5343. doi: 10.1128/iai.68.9.5335-5343.2000.
57. Ragnarsson, E.G., Schoultz, I., Gullberg, E., Carlsson, A.H., Tafazoli, F., Lerm, M., et al. (2008). Yersinia pseudotuberculosis induces transepytosis of nanoparticles across human intestinal villus epithelium via invasin-dependent macropinocytosis. *Lab Invest* 88(11), 1215-1226. doi: 10.1038/labinvest.2008.86.
58. Zeitouni, N.E., Dersch, P., Naim, H.Y., and von Kockritz-Blickwede, M. (2016). Hypoxia Decreases Invasin-Mediated Yersinia enterocolitica Internalization into Caco-2 Cells. *PLoS One* 11(1), e0146103. doi: 10.1371/journal.pone.0146103.
59. Garbi, C., Negri, R., Cali, G., and Nitsch, L. (1996). Collagen interaction with apically expressed beta 1 integrins: loss of transepithelial resistance and reorganization of cultured thyroid cell monolayer. *Eur J Cell Biol* 69(1), 64-75.
60. Kam, K.R., Walsh, L.A., Bock, S.M., Koval, M., Fischer, K.E., Ross, R.F., et al. (2013). Nanostructure-mediated transport of biologics across epithelial tissue: enhancing permeability via nanotopography. *Nano Lett* 13(1), 164-171. doi: 10.1021/nl3037799.
61. Walsh, L., Ryu, J., Bock, S., Koval, M., Mauro, T., Ross, R., et al. (2015). Nanotopography facilitates in vivo transdermal delivery of high molecular weight therapeutics through an integrin-dependent mechanism. *Nano Lett* 15(4), 2434-2441. doi: 10.1021/nl504829f.

62. Stewart, T., Koval, W.T., Molina, S.A., Bock, S.M., Lillard, J.W., Jr., Ross, R.F., et al. (2017). Calibrated flux measurements reveal a nanostructure-stimulated transcytotic pathway. *Exp Cell Res* 355(2), 153-161. doi: 10.1016/j.yexcr.2017.03.065.
63. Huang, X., Shi, X., Hansen, M.E., Setiady, I., Nemeth, C.L., Celli, A., et al. (2020). Nanotopography Enhances Dynamic Remodeling of Tight Junction Proteins through Cytosolic Liquid Complexes. *ACS Nano* 14(10), 13192-13202. doi: 10.1021/acsnano.0c04866.
64. Lynn, K.S., Peterson, R.J., and Koval, M. (2020). Ruffles and spikes: Control of tight junction morphology and permeability by claudins. *Biochim Biophys Acta Biomembr* 1862(9), 183339. doi: 10.1016/j.bbamem.2020.183339.
65. Xu, Y., Xu, J., Shan, W., Liu, M., Cui, Y., Li, L., et al. (2016). The transport mechanism of integrin α v β 3 receptor targeting nanoparticles in Caco-2 cells. *Int J Pharm* 500(1-2), 42-53. doi: 10.1016/j.ijpharm.2016.01.028.
66. Lamson, N.G., Berger, A., Fein, K.C., and Whitehead, K.A. (2020). Anionic nanoparticles enable the oral delivery of proteins by enhancing intestinal permeability. *Nat Biomed Eng* 4(1), 84-96. doi: 10.1038/s41551-019-0465-5.
67. Li, R., Maminishkis, A., Zahn, G., Vossmeier, D., and Miller, S.S. (2009). Integrin α 5 β 1 mediates attachment, migration, and proliferation in human retinal pigment epithelium: relevance for proliferative retinal disease. *Invest Ophthalmol Vis Sci* 50(12), 5988-5996. doi: 10.1167/iovs.09-3591.
68. Mallavarapu, M., and Finnemann, S.C. (2010). Neural retina and MerTK-independent apical polarity of α v β 5 integrin receptors in the retinal pigment epithelium. *Adv Exp Med Biol* 664, 123-131. doi: 10.1007/978-1-4419-1399-9_15.

69. Schramm, K., Krause, K., Bittroff-Leben, A., Goldin-Lang, P., Thiel, E., and Kreuser, E.D. (2000). Activated K-ras is involved in regulation of integrin expression in human colon carcinoma cells. *Int J Cancer* 87(2), 155-164. doi: 10.1002/1097-0215(20000715)87:2<155::aid-ijc1>3.0.co;2-j.
70. Hirata, E., Ichikawa, T., Horike, S.I., and Kiyokawa, E. (2018). Active K-RAS induces the coherent rotation of epithelial cells: A model for collective cell invasion in vitro. *Cancer Sci* 109(12), 4045-4055. doi: 10.1111/cas.13816.
71. Praetorius, J., and Spring, K.R. (2002). Specific lectins map the distribution of fibronectin and beta 1-integrin on living MDCK cells. *Exp Cell Res* 276(1), 52-62. doi: 10.1006/excr.2002.5516.
72. Zuk, A., and Hay, E.D. (1994). Expression of beta 1 integrins changes during transformation of avian lens epithelium to mesenchyme in collagen gels. *Dev Dyn* 201(4), 378-393. doi: 10.1002/aja.1002010409.
73. Gu, Z., Noss, E.H., Hsu, V.W., and Brenner, M.B. (2011). Integrins traffic rapidly via circular dorsal ruffles and macropinocytosis during stimulated cell migration. *J Cell Biol* 193(1), 61-70. doi: 10.1083/jcb.201007003.
74. Akiyama, S.K., Yamada, S.S., Chen, W.T., and Yamada, K.M. (1989). Analysis of fibronectin receptor function with monoclonal antibodies: roles in cell adhesion, migration, matrix assembly, and cytoskeletal organization. *J Cell Biol* 109(2), 863-875. doi: 10.1083/jcb.109.2.863.
75. Duband, J.L., Nuckolls, G.H., Ishihara, A., Hasegawa, T., Yamada, K.M., Thiery, J.P., et al. (1988). Fibronectin receptor exhibits high lateral mobility in embryonic

- locomoting cells but is immobile in focal contacts and fibrillar streaks in stationary cells. *J Cell Biol* 107(4), 1385-1396. doi: 10.1083/jcb.107.4.1385.
76. Mang, D., Roy, S.R., Hoh, H.H., Wu, X., Zhang, J., Jin, C., et al. (2020). Self-Assembly of Integrin Ligands on the Apical Membrane Inhibits the Migration of Glioma Cells. *Langmuir* 36(14), 3750-3757. doi: 10.1021/acs.langmuir.0c00291.
77. Liu, J., Riquelme, M.A., Li, Z., Li, Y., Tong, Y., Quan, Y., et al. (2020). Mechanosensitive collaboration between integrins and connexins allows nutrient and antioxidant transport into the lens. *J Cell Biol* 219(12). doi: 10.1083/jcb.202002154.
78. Batra, N., Burra, S., Siller-Jackson, A.J., Gu, S., Xia, X., Weber, G.F., et al. (2012). Mechanical stress-activated integrin alpha5beta1 induces opening of connexin 43 hemichannels. *Proc Natl Acad Sci U S A* 109(9), 3359-3364. doi: 10.1073/pnas.1115967109.
79. Yang, B., and Rizzo, V. (2013). Shear Stress Activates eNOS at the Endothelial Apical Surface Through beta1 Containing Integrins and Caveolae. *Cell Mol Bioeng* 6(3), 346-354. doi: 10.1007/s12195-013-0276-9.
80. Cinamon, G., Shinder, V., Shamri, R., and Alon, R. (2004). Chemoattractant signals and beta 2 integrin occupancy at apical endothelial contacts combine with shear stress signals to promote transendothelial neutrophil migration. *J Immunol* 173(12), 7282-7291. doi: 10.4049/jimmunol.173.12.7282.
81. Uehara, K., and Uehara, A. (2014). Integrin alphavbeta5 in endothelial cells of rat splenic sinus: an immunohistochemical and ultrastructural study. *Cell Tissue Res* 356(1), 183-193. doi: 10.1007/s00441-014-1796-x.

82. Bisaria, A., Hayer, A., Garbett, D., Cohen, D., and Meyer, T. (2020). Membrane-proximal F-actin restricts local membrane protrusions and directs cell migration. *Science* 368(6496), 1205-1210. doi: 10.1126/science.aay7794.
83. Belardi, B., Hamkins-Indik, T., Harris, A.R., Kim, J., Xu, K., and Fletcher, D.A. (2020). A Weak Link with Actin Organizes Tight Junctions to Control Epithelial Permeability. *Dev Cell* 54(6), 792-804 e797. doi: 10.1016/j.devcel.2020.07.022.
84. Spiess, M., Hernandez-Varas, P., Oddone, A., Olofsson, H., Blom, H., Waithe, D., et al. (2018). Active and inactive beta1 integrins segregate into distinct nanoclusters in focal adhesions. *J Cell Biol* 217(6), 1929-1940. doi: 10.1083/jcb.201707075.
85. Singh, B., Fu, C., and Bhattacharya, J. (2000). Vascular expression of the alpha(v)beta(3)-integrin in lung and other organs. *Am J Physiol Lung Cell Mol Physiol* 278(1), L217-226. doi: 10.1152/ajplung.2000.278.1.L217.
86. Feige, M.H., Sokolova, O., Pickenhahn, A., Maubach, G., and Naumann, M. (2018). HopQ impacts the integrin alpha5beta1-independent NF-kappaB activation by *Helicobacter pylori* in CEACAM expressing cells. *Int J Med Microbiol* 308(5), 527-533. doi: 10.1016/j.ijmm.2018.05.003.

Chapter 4: Apical integrins as a switchable target to regulate the epithelial barrier

Abstract

The formation of selectively permeable barriers is a critical requirement that allows for specialized physiologic function in epithelia. Tight junctions are major regulators of epithelial barrier structure and function and have been shown to interact with a variety of other proteins including integrins. Recently pools of apical integrins have been identified as potential regulators of epithelial barriers, however studying integrin specific regulation of the barrier has been a challenge. In this study, we address this by using derivatized polymeric nanowires conjugated with anti-integrin $\beta 1$ antibodies that allow us to target apically localized integrins in either their closed or open conformations. We found that barrier regulation by apical integrins is conformation specific. Targeting apical integrins in the closed conformation using the nanowire platform causes junction localized zonula occludens-1 (ZO-1) to assume a ruffled morphology and was sufficient to increase epithelial barrier permeability by altering claudin assembly into tight junctions, by increasing cortical recruitment of F-actin, and by talin enrichment at junctions. Conversely, targeting apical integrins in the open conformation had the opposite effect, making junctions more linearized and was associated with decreased permeability. These data support a role for apical integrins acting as a conformation sensitive switch with the capacity to regulate epithelial barrier function.

4.1 Introduction

A key function of epithelial tissue is creating a barrier that partitions distinct cellular environments, which results from polarization on an apical/basolateral axis. Polarity is established

by cell-cell contacts mediated by the apical junctional complex (AJC) and cell attachment to the extracellular matrix. The AJC consists of tight junctions and adherens junctions that coordinate polarity complex proteins and create an adhesive meshwork between cells.

Tight junction proteins facilitate lateral adhesion between adjacent cells and regulate paracellular permeability. Claudin family transmembrane domain proteins form paracellular ion channels and are the main regulators of the paracellular barrier. Claudins work in concert with Ig superfamily and MarvelD transmembrane proteins to form tight junctions. A stable tight junction also includes cytosolic scaffold zonula occludens (ZO) proteins that crosslink integral tight junction proteins with the actin cytoskeleton and polarity complex proteins. The expression of tight junction proteins is tissue specific, allowing for organ specific permeability. Barrier function and tight junction composition also are sensitive to environmental stimuli [1].

Epithelial cell polarity is also defined by integrins, which are α/β heterodimeric transmembrane proteins that bind to the extracellular matrix to regulate the actin cytoskeleton, cell signaling and mechanosensing [2-6]. In addition to their classical role as receptors for extracellular matrix proteins, there have been several examples of integrins interacting with adherens junction [7] and tight junction proteins [8,9] suggesting that integrins might play a role in regulating apical/basolateral polarity and barrier function in epithelial cells [10]. In fact, the proximity of apically localized integrins to tight junction proteins allows for barrier disruption by bacterial infection [11].

Contact between apical integrins and large overlays such as collagen hydrogels [12] and nanostructured thin films [13-16] has been correlated with increased barrier leak as measured by increased permeability of ions and large molecules, along with corresponding changes in the morphology and localization of tight junction proteins. While these data raise the possibility that

integrin clustering and stimulation can regulate epithelial barrier function, previous research using overlays is limited by the fact that matrix overlays and nanostructured films contact the entire apical monolayer rather than specifically probing integrins.

To overcome this hurdle, we used a discrete nanowire platform [17,18] decorated with antibodies (anti-integrin nanowires), to use as a multivalent platform with the capacity to stimulate apically oriented integrins. There are many well characterized anti-integrin antibodies that can be conjugated to form anti-integrin nanowires, including classes of monoclonal antibodies (mAbs) that are sensitive to integrin conformation and activity state [19-22]. This is critically important, since integrins can assume several functionally distinct conformations ranging from an inactive bent state to an active extended state that enables high affinity ligand binding [19,23-26].

There are two classes of activating mAbs, including antibodies that bind epitopes that are only exposed when integrins are in the open conformation, called Ligand Induced Binding Site (LIBS) mAbs [19,20,27]. These antibodies can be used to detect populations of integrins in the open conformation [28,29], and they promote increased ligand binding by stabilizing the integrin in their active state [30]. On the other hand, blocking antibodies often called Ligand Attenuated Binding Site (LABS) mAbs, prevent ligand binding by allosteric regulation of the ligand binding site [19,20,31,32]. Using nanowires conjugated with either a LIBS or LABS mAb allows us to measure the impact of a multivalent ligand targeting apical integrins with different activity state on the regulation of epithelial barriers.

We show in this study that targeting apical integrins with LIBS or LABS anti-integrin antibody conjugated nanowires causes differential changes in the epithelial barrier as measured by changes in tight and adherens junction morphology and permeability. This suggests that stimulation of apical integrins is sufficient to regulate components of the AJC and that the

conformation state of clustered apical integrins plays a key role in how integrins regulate the epithelial barrier.

4.2 Materials and Methods

4.2.1 Fabrication and conjugation of nanowires

Derivatizable polycaprolactone (PCL) nanowires were fabricated from a mix of 45kDa PCL (Sigma Aldrich, 704105) and maleimidophenyl-PCL (MP-PCL) as described previously, with modifications [17,18]. Briefly, the PCL mixture (total polymer concentration 125mg/mL with MP-PCL as 30% of total polymer weight) was added to 2,2,2-trifluoroethanol (Sigma Aldrich, T63002) before being spin coated onto glass slides (Fisherbrand, 12-550C) in two stages 500 RPM for 10 sec, followed by 1000 RPM for 30 sec. Anodized alumina nanopore wafers with a 200nm pore served as the template for the nanowires (Sigma Aldrich, WHA68095502) and were placed in contact with the polymer film before heating the film to 100C for 3h to complete the templating process before cooling overnight. The wafers were then removed from the slide and etched in 5M NaOH for 30 min at 4C. The etchant was passed through a 0.22um PES filter (Corning, 431118) and rinsed first with cold distilled water, followed by a rinse with cold PBS (Corning, 21-040-CV). Nanowires were removed from the filter by rinsing with 5% poly(vinyl alcohol) (Sigma Aldrich, 475904) before being passed through 40um mesh (Corning, 352340). The filtered nanowires were centrifuged 3 times at 4000RPM for 15 min at 4C, the supernatant was discarded and the pelleted nanowires were washed with cold distilled water, cold PBS, and with reducing buffer (PBS + 0.04% w/v EDTA) respectively, and were stored in reducing buffer at 4C until use.

Nanowires were conjugated with either the AIIB2 blocking anti-integrin antibody (Millipore, MAB409T), the 9EG7 activating antibody (BD Pharmingen, 553715), or an isotype

control antibody (Thermo Fisher Scientific, 31933). To conjugate antibodies with the nanowires, the antibodies were first diluted to 0.2mg/mL before being reduced with tris(2-carboxyethyl)phosphine (Sigma Aldrich, 646547) in reducing buffer at a 4.5M excess for 1hr at 37C. Equal volume of nanowires was added to the reduced antibody where the thiol-maleimide reaction proceeded for 2hr at 25C. Conjugated nanowires were washed 3 times and centrifuged at 2500RPM for 10min at 4C allowing them to pellet while discarding supernatant and resuspending in fresh PBS. Antibody conjugated nanowires were always used within 4hr of conjugation (stored at 4C unless being used immediately), though they can be used within 36hr of conjugation if stored at 4C.

4.2.2 Cell culture

Caco-2 cells were maintained in Minimum Essential Medium (MEM) with Earle's salts and L-glutamine (Corning Cellgro, 10-010-CV) supplemented with 10% Fetal Bovine Serum (Atlanta Biologicals Premium Select, S11550), Sodium Pyruvate (Hyclone, SH30239.01), 100U/mL Penicillin/10mg/mL Streptomycin (Sigma Aldrich, P4333), 0.25ug/mL Amphoteroicin B (Thermo Fisher Scientific, 15290018), and 5ug/mL Gentamicin (Sigma Aldrich, G1397). Cells were incubated in a CO₂ incubator at 37C until they were ready to be seeded to glass coverslips for immunofluorescence experiments or Transwell permeable supports for barrier function experiments.

4.2.3 Immunofluorescence

Caco-2 cells were seeded at 200,000 cells per well on rat-tail collagen (Roche, 11179179001) coated coverslips in the supplemented MEM media described above. Cells were

incubated at 37C until they reached confluency, about 4 days. Cells were treated for 2hrs in a CO₂ incubator at 37C before being prepared for immunofluorescence. Cells were washed in PBS with calcium and magnesium (Corning, 21-030-CV), then fixed with 4% paraformaldehyde (PFA) (Electron Microscopy Solutions, 15710). In some preparations, this was followed by a methanol:acetone fixation step (Methanol: Fisher Chemical, A433F; Acetone: Fisher Chemical, A19-1). The cells were then permeabilized with 0.5% Triton X-100 (Fisher Scientific, 9002-93-1). Primary antibody (Supplemental Table 1) was diluted in 3% Bovine Serum Albumin (BSA) (Gemini Bio-Products, 700-102P) and incubated on cells overnight at 4C. Cells were washed with 3% BSA before Alexa Fluor 594 goat anti-rabbit (Thermo Fisher Scientific, A32740) and Cy2 goat anti-mouse (JacksonImmuno Research Labs, 115-225-166) secondary antibodies were diluted in 3% BSA and incubated for 1h at room temperature before washing with PBS with calcium and magnesium before mounting the coverslip to a slide with Prolong antifade with DAPI (Thermo Fisher Scientific, P36962). For F-actin visualization, rhodamine phalloidin (Thermo Fisher Scientific, R415) was diluted in PBS and incubated with cells overnight at 4C before mounting the coverslips.

Images were acquired with an Olympus IX70 microscope with a U-MWIBA filter pack (BP460-490, DM5050, BA515-550) or U-MNG filter pack (BP530-550, DM570, BA590-800). Sample identification was covered on slides before imaging to minimize bias in image collection. All images were processed in FIJI, each image had background subtracted with a rolling ball radius of 50 pixels. Minimum and maximum intensities for images of the same protein were adjusted in parallel so the intensity scale remained linear.

4.2.4 Barrier function assays

Caco-2 cells were seeded at 250,000 cells per well in the apical chamber of a 6.5mm permeable supports from either Corning (3470) or CellTreat (230635). Both brands of inserts gave comparable results. Cells were grown with 200ul of the supplemented MEM media described above in the apical chamber and 1mL of the supplemented MEM media in the basolateral chamber of the Transwell. Cells were incubated at 37C and media was changed every other day for about 7 days until cells formed a high resistance monolayer of 350 ohms x cm² or higher. Monolayer resistance was measured using an epithelial voltohmmeter (World Precision Instruments, Sarasota FL) where the measured resistance in ohms was multiplied by the area of the Transwell filter (0.33 cm²).

To ensure that changes in barrier function were not the result of cell death, we checked cell viability (Supplemental Fig. 4.1) with a colorimetric Live/Dead assay (Thermo Fisher Scientific, L3224). Cells seeded in Transwells were treated for 2hr with nanowires, soluble antibody, or antibody conjugated nanowires. After experimental treatment, cells were incubated with 4 uM of ethidium homodimer-1, 2 uM calcein-AM, and Hoechst (Thermo Fisher Scientific, H1399) for 30 min at RT. Cells were directly imaged through the Transwell on a glass bottomed 35 mm dish (MatTek, P35G-1.0-14-C) and percent viability was calculated by scoring the percentage of calcein-positive (live) and ethidium-positive (dead) cells in each field of view.

Transepithelial Electrical Resistance (TER) was measured over a time course of 2 hours using the cellZscope 2 and its accompanying software for data acquisition (nanoAnalytics, Münster, Germany). Data was pooled from 5-10 wells per treatment, where each well was normalized to a baseline TER measurement before treatment. The averages of the normalized TER for each treatment were plotted over the 2-hour time course. Significance between conditions was

determined by doing a one-way repeated measures ANOVA test with multiple comparisons and Bonferroni correction (GraphPad Prism).

Permeability for larger molecules was assessed using the dye flux assay where high resistance monolayers of Caco-2 cells seeded to 6.5mm Transwell inserts as above were equilibrated with Ringer's solution (140 mM NaCl, 2 mM CaCl₂, 1 mM MgCl₂, 10 mM glucose, and 10 mM Hepes (pH 7.3)) for 30 min at 37C before the apical buffer was replaced with fresh Ringer's containing a fluorescent probe of interest. Over a 2-hour time-course Transwell inserts were moved to new wells containing 200ul Ringer's every 30 minutes. After Transwell inserts were moved, the Ringer's solution in the basolateral chamber was collected to be read using a multichannel plate fluorimeter (BioTek-Synergy H Microplate Reader, Winooski, VT). Data was pooled from 4-6 wells per treatment, and using a standard curve, absolute flux was calculated. Significance between conditions was determined two-way ANOVA with multiple corrections to compare simple row effects between time points and Bonferroni correction (GraphPad Prism). Probes include calcein (Thermo Fisher Scientific, C481), and Alexa Fluor 488-labeled IgG (JacksonImmuno Research Labs, 711-545-152).

4.3 Results

4.3.1 Multimeric engagement of apical integrin β 1 by AIIB2 induces tight junction ruffling

We have previously observed that when the apical surface of epithelial cells is placed in contact with a film engineered with specific nanotopography, this causes ZO-1 to assume a ruffled morphology accompanied by increased paracellular leak [13-16]. Experiments using anti-integrin blockade prior to application of nanostructured films inhibits tight junction ruffling, implicating a role for integrins [14]. However, nanostructured films engage the entire apical plasma membrane

surface. To directly determine whether apical integrins influence tight junctions, we produced a discrete nanowire platform which can be derivatized with antibodies to specifically target pools of apically localized integrin β 1 (Fig. 4.1A-C). Because integrin conformation state is crucial for integrin activity, we produced anti-integrin nanowires that target integrin β 1 in either the closed state or extended state with well characterized mAbs. To do this, we used blocking mAb AIIB2, a LABS antibody that binds integrin β 1 in the bent conformation and inhibits ligand binding (Fig. 4.1A) [22,33,34] and activating mAb 9EG7, a LIBS antibody that binds the EGF repeats when integrin β 1 is in the extended conformation and promotes ligand binding (Fig. 4.1B) [20,29].

We used quantitative ZO-1 immunostaining of cells treated with anti-integrin nanowires for 2 h to determine the effect of targeting apically localized integrins on tight junction morphology (Fig. 4.1D). The most striking result was that cells acquired a robust ruffled ZO-1 morphology only when treated with the AIIB2 nanowires (Fig. 4.1E-G). Soluble reduced AIIB2 had little effect on tight junction morphology. Moreover, treating cells with either soluble reduced 9EG7 antibody or 9EG7 nanowires had the reverse effect on ZO-1, where there was a significantly smaller proportion of cells exhibiting a ruffled morphology, compared to control or untreated conditions (Fig. 4.1G). This demonstrates that anti-integrin antibodies have the capacity to alter tight junctions and that this effect depends on antibody epitope and whether the stimulus was monovalent or multivalent.

Despite robust evidence suggesting a variety of stimuli can induce ruffling of tight junctions based on ZO-1 staining, fewer studies have examined how claudins are affected in the ruffling response [1]. We thus examined the impact of anti-integrin nanowires on claudins expressed by Caco-2 cells, to determine whether they paralleled the changes to ZO-1 morphology. AIIB2 nanowires stimulated the some claudins but not others to assume a ruffled morphology.

Claudin-4 (Fig. 4.2A) and claudin-2 (Supplemental Fig. 4.2A) were both incorporated into ruffles that co-localized with ruffled ZO-1. As was observed for ZO-1, only AIIB2 nanowires stimulated claudin ruffling, however soluble 9EG7 and 9EG7 nanowires enhanced claudin-2 and claudin-4 to adopt a linear morphology.

By contrast with claudin-2 and claudin-4, we observed that nanowire targeting of apical integrin β 1 had little impact on claudin-7 (Fig. 4.2B) and claudin-1 (Supplemental Fig. 4.2B) morphology, regardless of epitope or valency. Treatment with soluble 9EG7 antibody or 9EG7 nanowires also had no apparent effect on claudin-1 or claudin-7 morphology or localization. Although claudin-1 and claudin-7 remained linear following treatment with AIIB2 nanowires, there was a decrease in localization of these proteins to tight junctions, particularly in areas containing highly ruffled ZO-1. Thus, the effect of AIIB2 nanowires was specific for different claudins, where claudin-2 and claudin-4 became ruffled and claudin-4 and claudin-7 did not.

Little has been done to determine whether adherens junctions show parallel changes in localization in cells forming ruffled tight junctions [1]. To investigate this, we determined the effect of anti-integrin nanowires on the adherens junction proteins β -catenin and E-cadherin, co-labeled with ZO-1 after 2 h of treatment with anti-integrin nanowires. There was little effect on the appearance of junction-localized E-cadherin in all cases examined (Fig. 4.3A). However, cells treated with AIIB2 nanowires showed more punctate internal localization of E-cadherin than other treatment conditions, with the exception of cells treated with bare nanowires (Fig. 4.3A). Treatment with AIIB2 nanowires also had an effect on β -catenin morphology, where β -catenin did not exhibit a ruffled morphology and instead was noticeably more dispersed (Fig. 4.3B). Interestingly, while the 9EG7 nanowires had less impact on the junctional localization of β -catenin,

there are areas in the images where β -catenin was slightly more dispersed, though β -catenin was less affected by 9EG7 nanowires than by AIIB2 nanowires.

4.3.2 The effect of targeting apical integrin β 1 subunits on barrier function depends on epitope and valency

We previously demonstrated that when cells were treated with a nanostructured surface that causes a ruffled ZO-1 morphology it was accompanied by decreases in barrier function [13-15]. However, other stimuli that induce ruffled ZO-1 do not have an impact on epithelial barriers (GG, HH). Thus, we examined the effect of anti-integrin nanowires on Caco-2 cell barrier function. Initially, measured transepithelial resistance (TER) for the duration of a 2h time course of treatment (Fig. 4.4A). Relative to bare nanowires, AIIB2 nanowires and 9EG7 had differential effects on TER, where AIIB2 nanowires caused a decrease in TER whereas 9EG7 nanowires increased TER. By contrast with AIIB2 nanowires, free reduced AIIB2 had the opposite effect on TER, which was increased, reflecting an increase in the paracellular ion barrier. Free reduced 9EG7 also increased TER. In each case, the effects of treatments on TER correlated with their effect on tight junction morphology, where AIIB2 nanowires induced morphologic changes to ZO-1 and claudins and the other treatments did not.

We then examined the effects of anti-integrin nanowires on paracellular flux, using calcein (0.63kDa, Fig. 4.4B) as a tracer. Cells treated with AIIB2 nanowires had no significant effect on the paracellular permeability of calcein. Both soluble and nanowire bound 9EG7 reduced the paracellular flux of calcein. In contrast to AIIB2 nanowires, soluble, free reduced AIIB2 decreased the flux of calcein. By and large, the effects of different stimuli on paracellular flux of calcein paralleled their effects on TER, with some subtle differences.

We then examined the impact of anti-integrin nanowires on transcytosis, using fluorescently tagged IgG as a tracer as in Stewart et al. [15]. AIIB2 nanowires enhanced the transepithelial flux of IgG as compared with bare or 9EG7 nanowires (Fig. 4.4D). On the other hand, free reduced AIIB2 and 9EG7 had little effect on IgG flux. Taken together, these data demonstrate that different modes of targeting integrins have different effects on Caco-2 barrier function. Of note, the effects of AIIB2 nanowires on TER (decreased), paracellular flux (little effect) and transcytosis (increased) matches the effects of DN2 and DN3 nanostructured films on Caco2 cells [15], meaning that an effect mediated through integrin $\beta 1$ is sufficient to explain the ability of these nanostructures to alter barrier function [14] and that no other factors are required to be engaged for their effect on epithelial cells.

4.3.3 Effect of targeting apical integrin $\beta 1$ subunits on actin depend on valency

There are several lines of evidence supporting the role of apically localized integrins regulating tight junction structure and barrier function (see Chapter 3), but little has been done to determine what links apical integrins to regulation of the epithelial barrier. Since a role for actin was implicated in the ability of nanostructured films to induce tight junction ruffling [14], we hypothesized that integrin-induced changes in actin cytoskeleton organization might be responsible for the observed cell responses to anti-integrin nanowires. Using rhodamine phalloidin to stain for F-actin reveals that treatment of cells with AIIB2 nanowires caused an overall decrease in total actin with few actin stress fibers remaining (Fig 4.5A). By contrast, treatment with 9EG7 nanowires, soluble 9EG7 and, to a lesser extent, soluble AIIB2 resulted in more prominent cortical actin as compared to cells treated with AIIB2 nanowires (Fig. 4.5A). It also appeared that cells treated with 9EG7 nanowires or soluble 9EG7 has more cortical actin than stress fibers, as opposed

to cells treated with AIIB2 nanowires or bare nanowires, where the signal from cortical actin and stress fibers was more balanced.

Talin, a scaffold protein that directly binds the cytoplasmic tail of integrin $\beta 1$ functioning as an actin crosslinker [37-39] seemed like a likely candidate to mediating these changes in cell responses to anti-AIIB2 nanowires. When we stained cells for talin 2hr after treatment, we observed that the localization of talin became more cortically localized in cells treated with AIIB2 nanowires as compared with cells treated with either bare nanowires or soluble AIIB2 (Fig. 4.5B). The enhanced cortical localization of talin is consistent with a model where it is involved in the effects AIIB2 nanowires have on actin organization.

In order to understand how cells coordinate the nanowires themselves, and see if this could provide insight into a possible mechanism of action, we quantified where cell-associated nanowires were in relation to tight junctions (Fig. 4.5C). The majority of cell-associated bare nanowires were in relation to tight junctions (Fig. 4.5C). The majority of cell-associated bare nanowires did not induce ZO-1 ruffling and were not in direct contact with cell junctions. By contrast, cells treated with AIIB2 nanowires that induced tight junction ruffling and cortical reorganization of the actin cytoskeleton were predominantly non-junctionally localized. Of the AIIB2 nanowires that were localized to cell-cell contact sites, significantly more AIIB2 nanowires were adjacent to ruffled junctions than were in direct contact with ruffles. The correlation of AIIB2 nanowire localization relative to ruffled junctions suggests that integrin regulation of tight junction structure and function due to action at a distance as opposed to local action mediated by direct contact with the junctions themselves.

4.4 Discussion

In this study we demonstrated that specifically targeting apically localized $\beta 1$ integrins is sufficient to induce changes in tight junction morphology and barrier function. Furthermore, for the first time, we have found that targeting different conformations of apical $\beta 1$ integrin subunits with antibodies results in differential regulation of epithelial barrier structure and function.

We found that nanowires decorated with an antibody classically considered to be blocking (AIIB2) caused an increase in paracellular ion permeability, based on TER, however, there was little effect of AIIB2 nanowires on paracellular flux of solutes. Moreover, AIIB2 nanowires enhanced IgG transcytosis. This profile of changes in epithelial barrier function due to AIIB2 nanowires is comparable to the impact of nanostructured films on Caco-2 cell barrier function [15], implicating a central role for integrin $\beta 1$ in the ability of nanostructured surfaces to alter epithelial barrier function by direct contact with the apical plasma membrane [14,15].

Moreover, this effect required a multivalent substrate, since monovalent AIIB2 had the opposite effect on tight junction morphology and permeability. The classification of AIIB2 as a blocking antibody reflects its ability to inhibit processes that require fully extended active integrins [22,33,34]. Our data demonstrate that, rather than being inert, closed state, apically localized integrin $\beta 1$ can influence cell function when engaged in a specific manner.

Our data also support a model where AIIB2 nanowires cause a decrease in TER by sorting claudins into two distinct pools (claudin-2/claudin-4 vs claudin-1/claudin-7) as opposed to having them all co-mingle in the same tight junction strands. In addition to altered claudin stoichiometry, an increase in tight junction length due to ruffling has the capacity to enable a net increase in the capacity to contain ion permeable claudins (such as claudin-2) as compared with linear tight junctions, thus leading to increased ion permeability (e.g. decreased TER) [40].

Though claudin/ZO-1 interactions have been implicated in the appearance of ruffled tight junctions [1], to our knowledge no work to date has shown whether claudins themselves are recruited into ruffles. Previous work primarily demonstrated a link between ruffled ZO-1 and changes in claudin expression, rather than claudin morphology. Ruffled ZO-1 resulting from various stimuli coincided with decreases in expression of claudin-1 [14,35,41], increases in claudin-2 and decreases in claudin-7 [35], consistent with our observations. Interestingly, different stimuli inducing tight ruffling could result in either increased [42] or decreased [14] claudin-4 expression. Therefore, the observation that certain claudins participate in ruffling while others do not is interesting. Claudins-2 and -4 are known compete for localization to tight junctions [43], which is consistent with their ability to participate in ruffling. On the other hand, claudins-1 and -7, which are phylogenetically similar based on their C-terminal tails [44], were not ruffle associated. Claudin-7 has the ability to directly interact with integrin $\beta 1$ [45-47] which is likely to play a role in its segregation away from ruffled tight junctions. Whether claudin-1 is affected in a comparable manner remains to be determined. Also, determining how apical integrin targeting affects the localization of non-classical claudins, which have much more diversity in their C-terminal tails, could help define roles for the C-terminus in whether they ruffle or not.

Despite evidence that apical integrins play some role in regulating the epithelial barrier [12-14], there has been no direct examination of the role that integrin conformation state plays. The use of collagen overlays to examine how apical integrins regulate barrier function and polarity suggests that there is a requirement for activated apical integrins, however our data suggests that targeting active and inactive pools of apical integrins has a differential effect on both barrier structure and function. Other work has demonstrated that changes in actin organization might regulate tight junction ruffling [41] as well as apical integrin mediated decreases in permeability

[11,16]. As with our data, talin enrichment was also observed when the apical surfaces of cells were exposed to integrin stimulating substrates [16], suggesting that targeting apical integrins with blocking AIIB2 nanowires is sufficient to trigger this cellular response. This is further evidence that inactive integrins are able to play functional/regulatory roles in the cell. However, because soluble blocking AIIB2 antibody did not have the same effect as blocking AIIB2 nanowires, the multivalent delivery might be a requirement for the regulatory activity of inactive apical integrins. Whether the mechanism of action for barrier regulation via inactive apical integrins is a result of either clustering of inactive integrins [48] driven by the nanowire acting as a multivalent ligand, or transmission of force via catch bonds [49] formed between integrin subunits and the antibody/nanowire complex, or some combination of both needs to be explored.

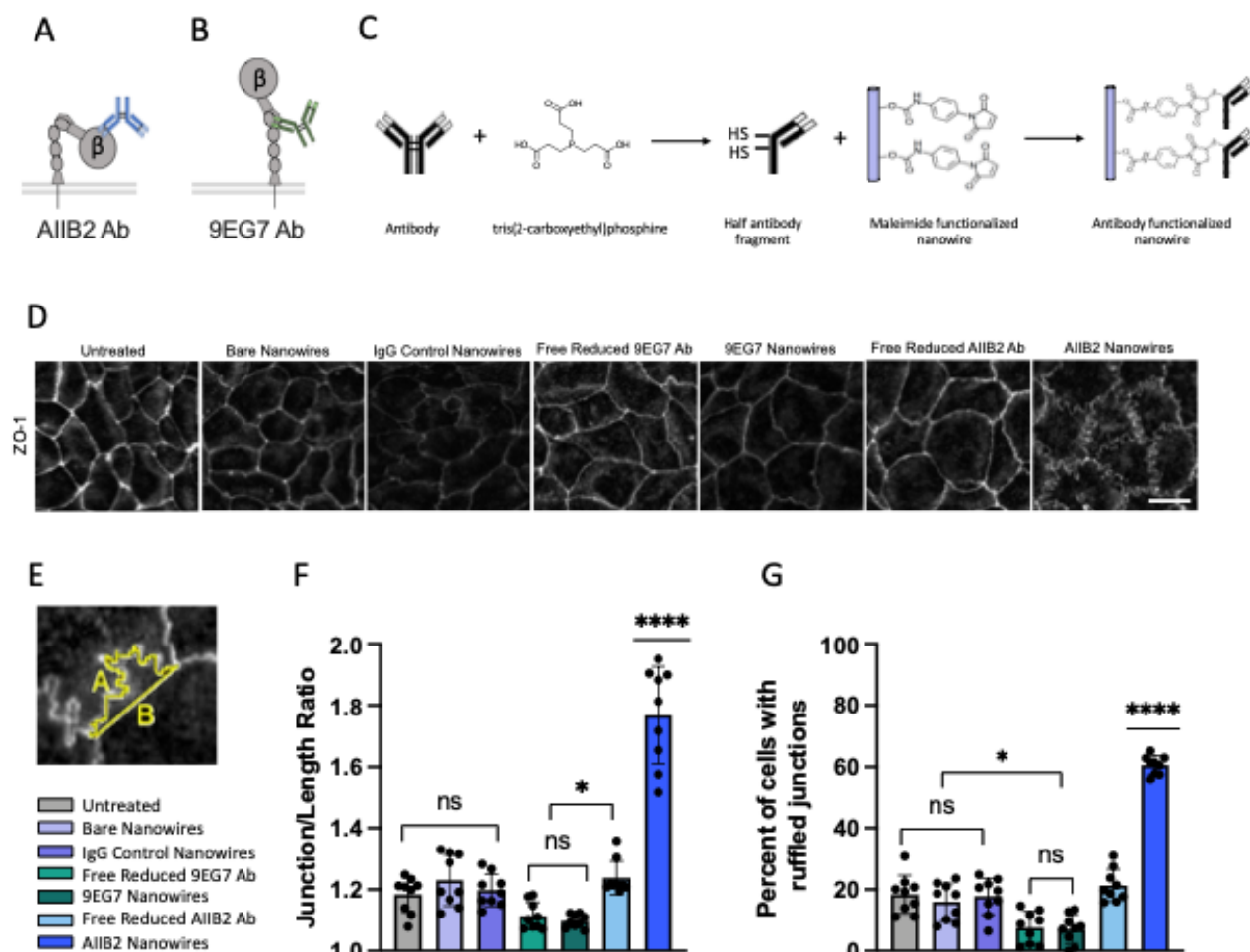


Figure 4.1. Targeting apical integrins with AIB2 nanowires produce a ruffled ZO-1 morphology.

(A) Schematic depicts the AIB2 blocking mAb (blue) binding the β A domain of the β 1 integrin subunit. (B) Schematic depicts the 9EG7 activating mAb (green) binding the EGF domain of the β 1 integrin subunit. (C) Schematic depicts the general reduction and conjugation reactions that generate the antibody decorated nanowires used in these experiments. (D) Representative immunofluorescence images of Caco-2 cells labeled with ZO-1 (grey) 2 hours after treatment with bare nanowires, IgG control nanowires, free reduced antibody (9EG7 or AIB2), or anti-integrin nanowires (9EG7 or AIB2) bar=10 μ m. (E) Changes in ZO-1 morphology are quantified by

finding the ratio between the actual length between tricellular junctions (trace A) and the linear distance between those same junctions (trace B). **(F)** Quantification of junction/length ratios for each treatment displayed as mean \pm SD (n=3 biological replicates, each point represents 25 measurements from a single field of view), treatment key on left. **(G)** Quantification of percent of cells in a field of view with one or more ruffled junctions displayed as mean \pm SD (n=3 biological replicates), treatment key on left. **(F and G)** Significance determined by one-way ANOVA with multiple comparisons and Bonferroni's correction. *p<0.05, ****p<0.0001.

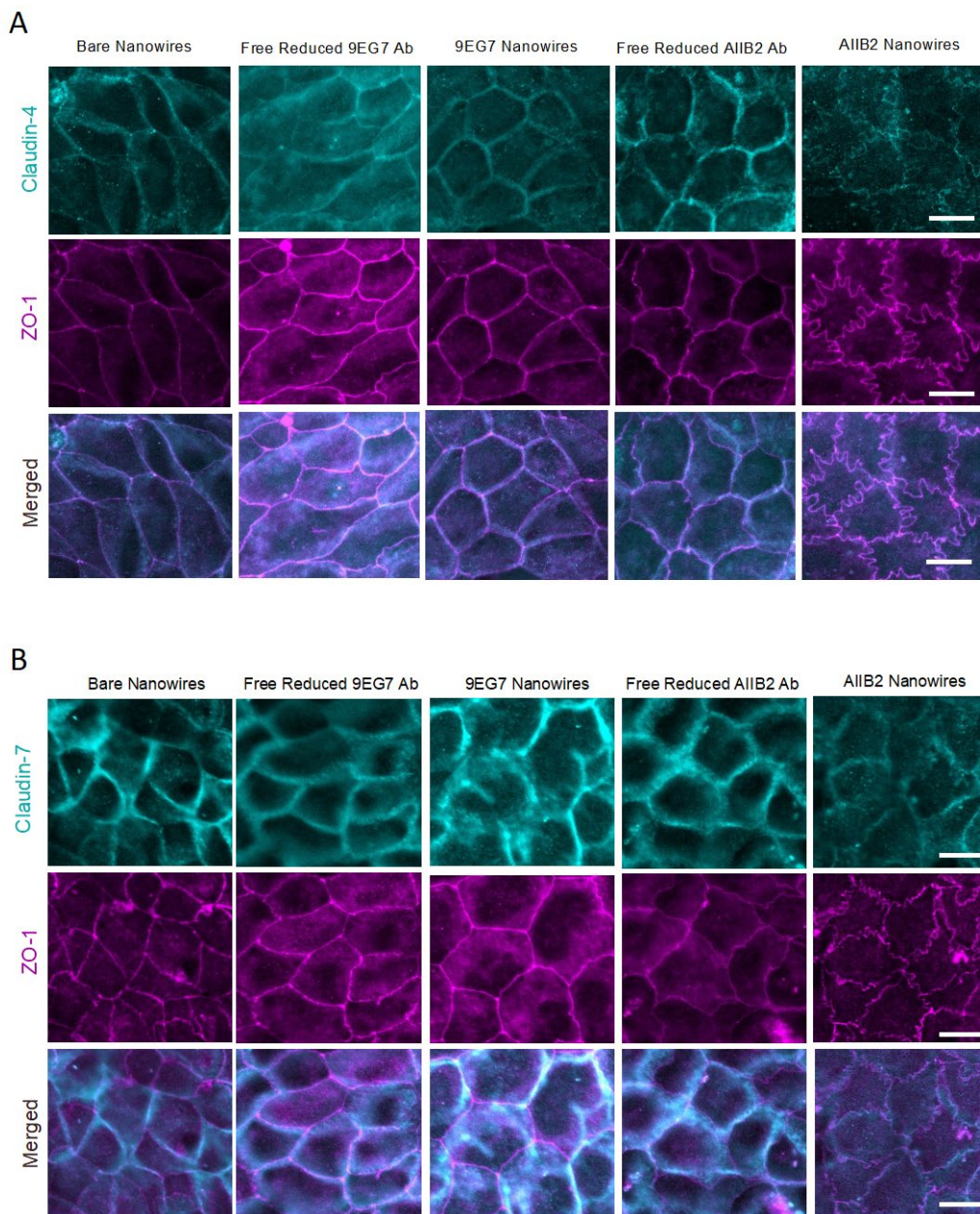


Figure 4.2. AIB2 nanowires cause differential changes in claudin morphology.

(A) Representative immunofluorescence images of Caco-2 cells co-labeled with claudin-4 (cyan) and ZO-1 (magenta) fixed 2hr after treatment, bar=10 μ m. **(B)** Representative immunofluorescence images of Caco-2 cells stained with claudin-7 (cyan) and ZO-1 (magenta) fixed 2hr after treatment, bar=10 μ m.

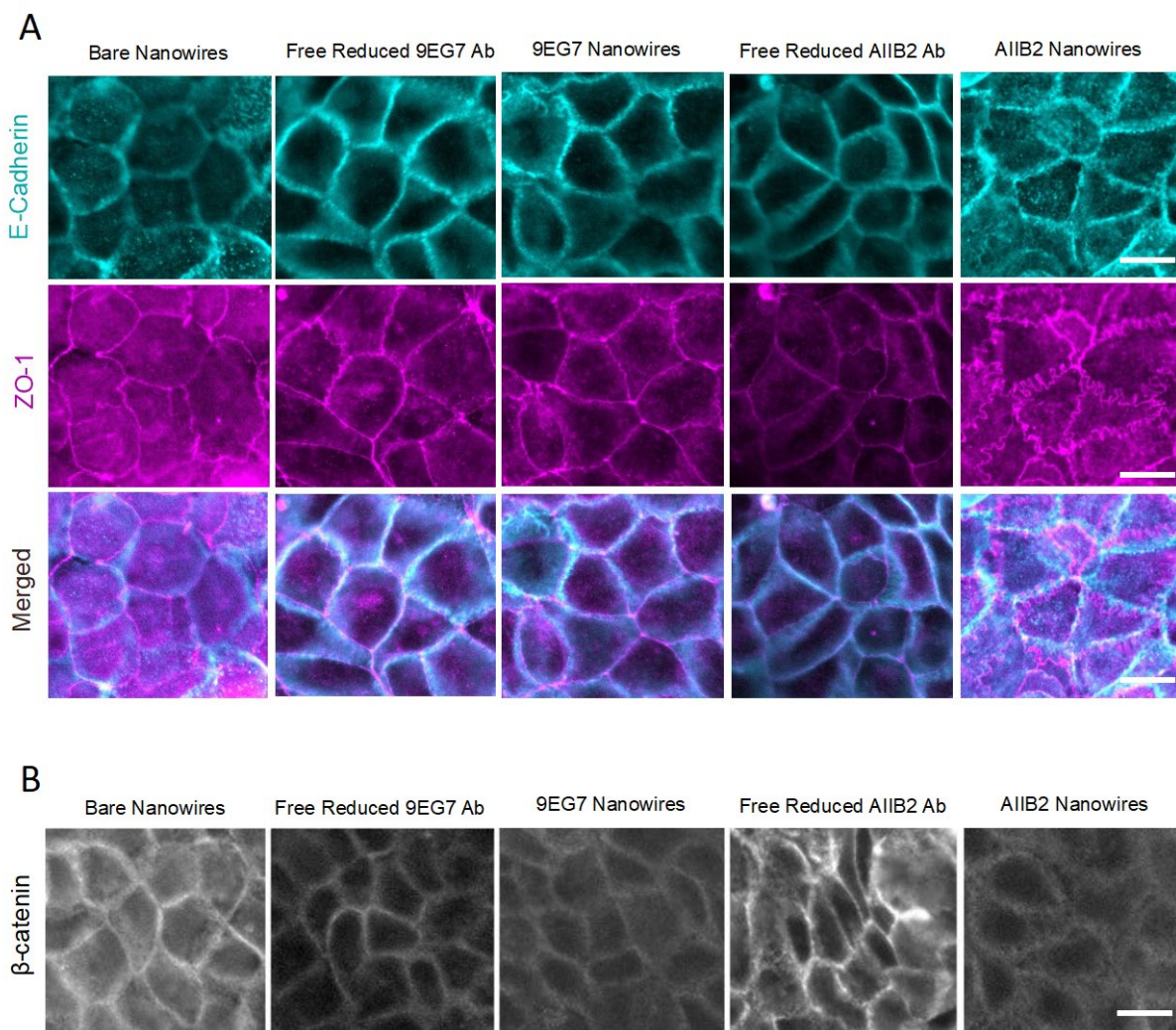


Figure 4.3. AIB2 nanowires cause changes in adherens junction protein localization.

(A) Representative immunofluorescence images of Caco-2 cells stained with E-cadherin (cyan) and ZO-1 (magenta) fixed 2hr after treatment, bar=10 μ m. **(B)** Representative immunofluorescence images of Caco-2 cells labeled with β -catenin fixed 2hr after treatment, bar=10 μ m.

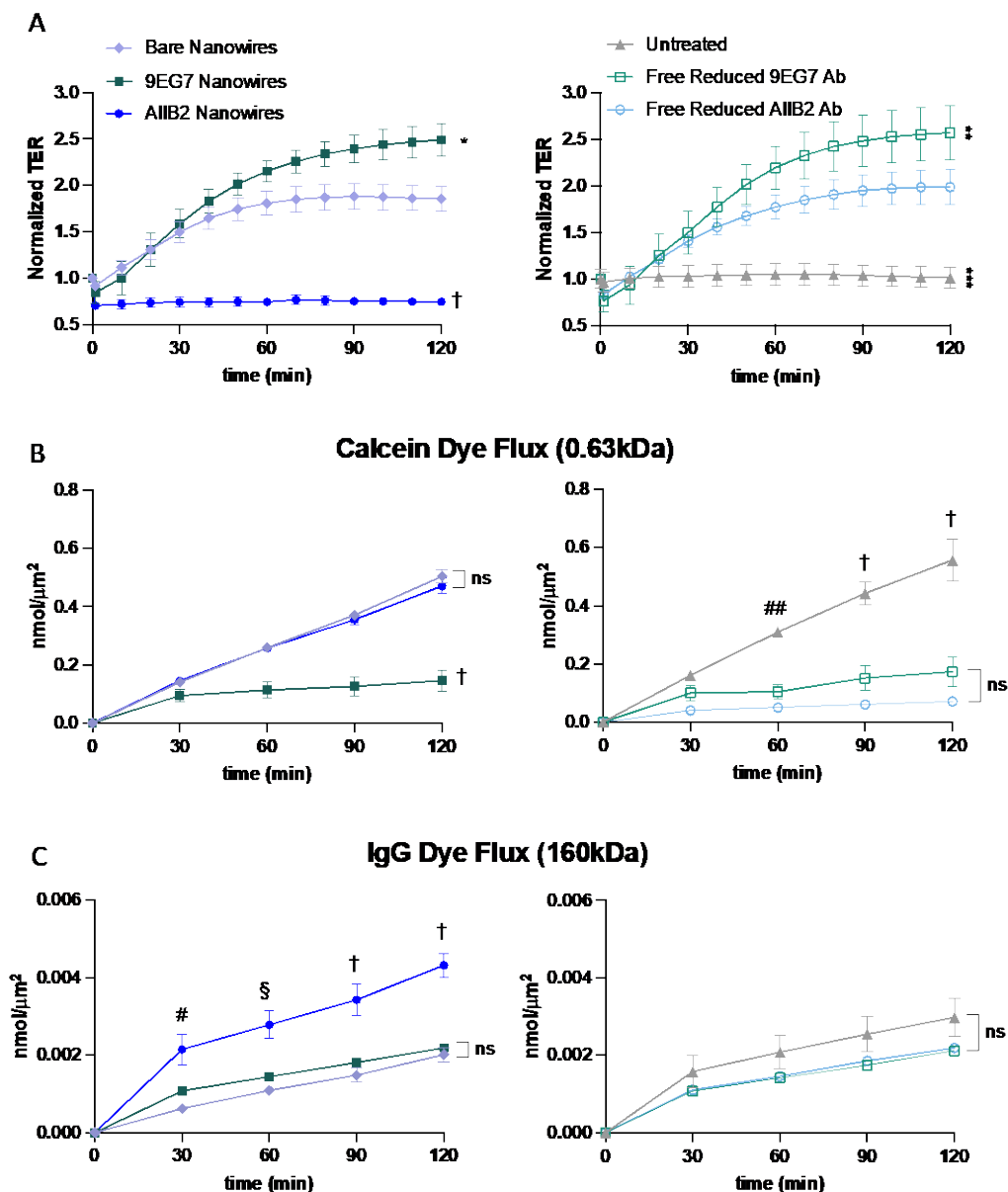


Figure 4.4 Differential effects of targeting apical integrins on ion and small molecule permeability.

(A) Transepithelial electrical resistance (TER) measurements on Caco-2 cells for 2hr following treatment. Measurements taken every 10 minutes with a cellZscope impedance system, and all points were normalized to baseline TER readings before treatment. Each point is the average TER for that treatment \pm SEM (n=5-10 wells/treatment). Significance was determined by one-way

repeated measures ANOVA with Bonferroni correction for multiple comparisons. * $p=0.0051$, ** $p=0.0024$, *** $p=0.0009$, † $p<0.0001$. **(B)** Dye flux permeability for calcein (0.63kDa). Each point is the average permeability for that treatment \pm SEM (n=4-8 wells/treatment). **(C)** Dye flux permeability for whole IgG (160kDa). Each point is the average permeability for that treatment \pm SEM (n=4-6 wells/treatment). **(B and C)** Significance was determined by two-way ANOVA with Bonferroni correction for multiple comparisons of simple row effects. # $p=0.0128$, ## $p=0.0001$, § $p=0.0013$, † $p<0.0001$.

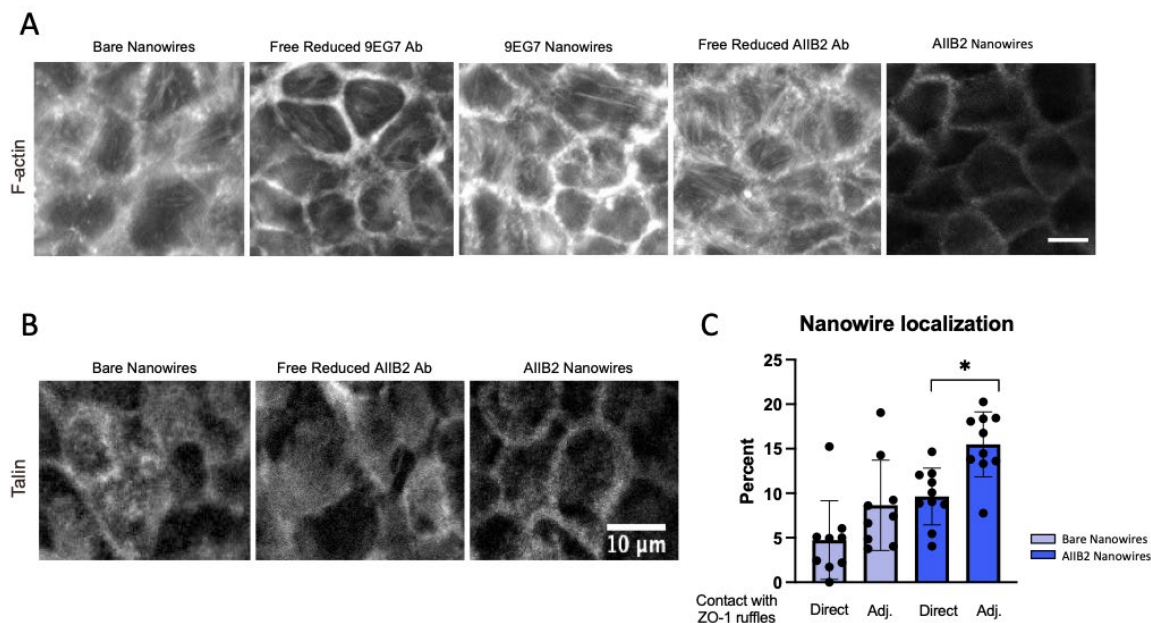
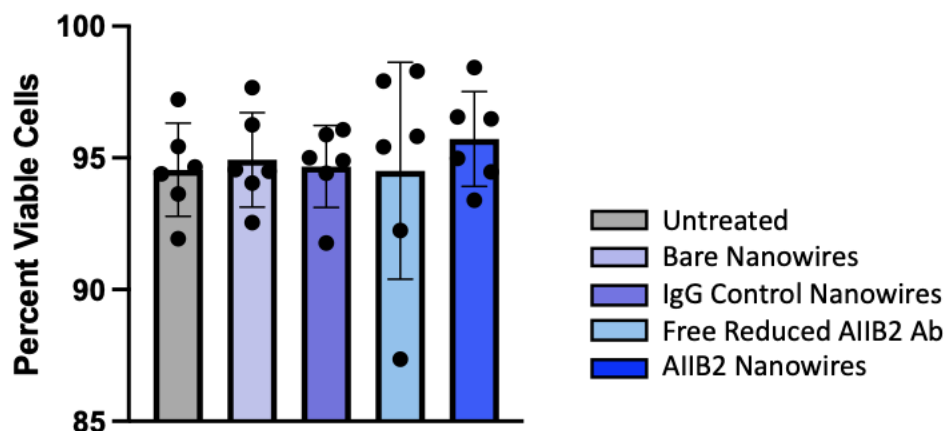


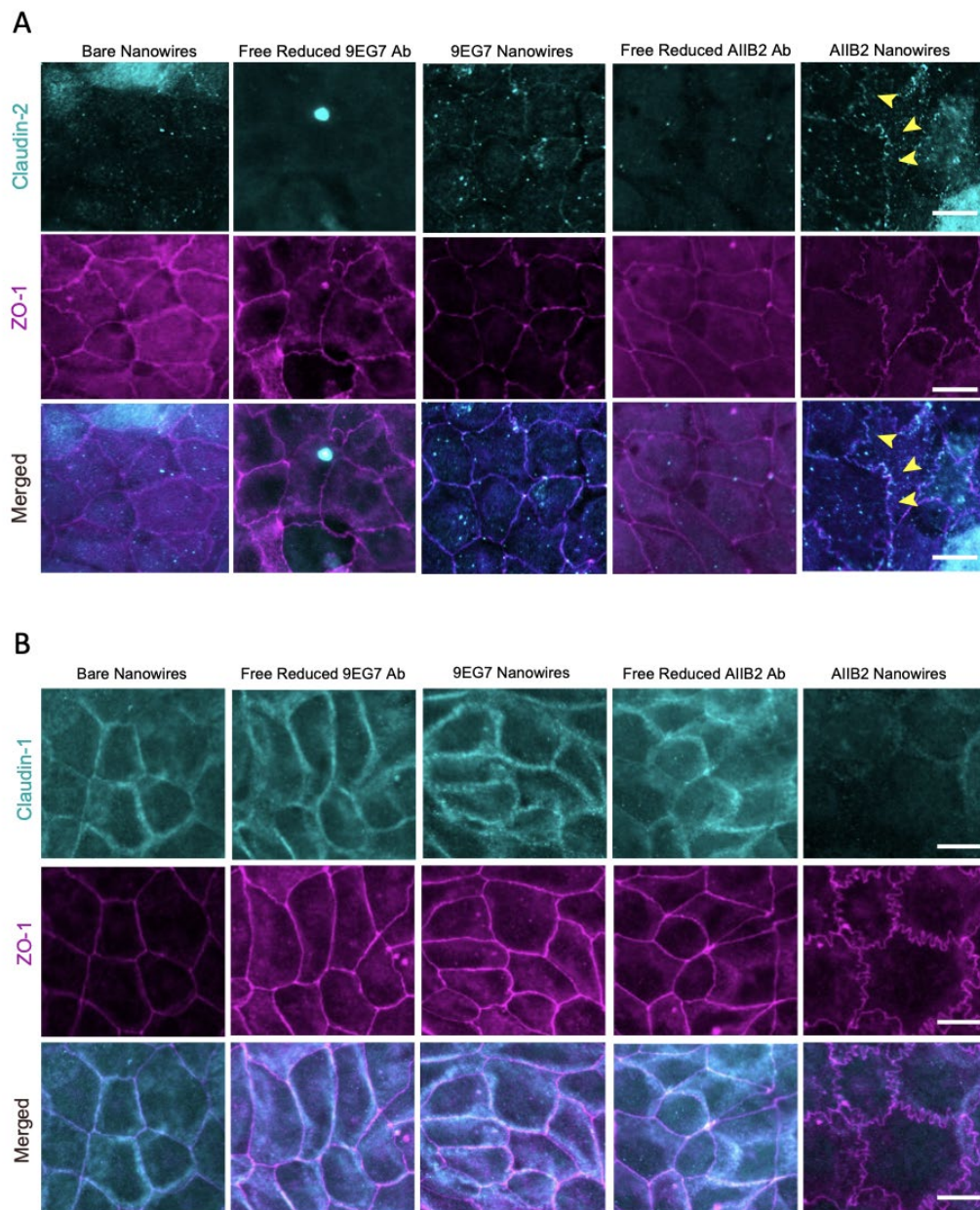
Figure 4.5. Actin reorganization and recruitment of talin in response to AIB2 nanowires.

(A) Representative immunofluorescence images of F-actin (grey) in cells fixed 2hr after treatment, bar=10 μ m. (B) Representative immunofluorescence images of talin (grey) in cells fixed 2hr after treatment, bar=10 μ m. (C) Quantification of ZO-1 associated nanowire localization either represented as either direct contact with ruffles or adjacent (adj.) contact with ruffles. Each data point represents the junctionally localized nanowires as a percent of the total cell associated nanowires in each field of view, data is displayed as mean \pm SD (n=9-10 fields of view of 3 biological replicates). Significance determined by one-way ANOVA with Bonferroni correction for multiple comparisons, *p=0.0183.



Supplemental Figure 4.1. Cell viability.

To ensure that changes in barrier function were not a result of cell death. Graph depicts quantification of the percent of viable Caco-2 cells 2hr after treatment visualized by calcein-AM. Each data point is the number of viable cells in a field of view (n=2 biological replicates, 3 fields of view each). $p > 0.9999$, significance was determined by one-way ANOVA with Bonferroni's correction for multiple comparisons.



Supplemental Figure 4.2. Targeting apical integrins with AIB2 nanowires and claudin morphology.

(A) Representative immunofluorescence images of Caco-2 cells co-labeled for claudin-2 (cyan) and ZO-1 (magenta) fixed and stained 2hr after treatment, bar=10 μ m. Yellow arrowheads indicate claudin-2 ruffling. **(B)** Representative immunofluorescence images of Caco-2 cells co-labeled for claudin-1 (cyan) and ZO-1 (magenta) fixed and stained 2hr after treatment, bar=10 μ m.

Protein	Catalog number	Fixation method	Concentration
β -catenin	BD Biosciences, 610153	4% PFA only	1:500
Claudin-1	Thermo Fisher Scientific, 51-9000	4% PFA + methanol:acetone	1:500
Claudin-2	Thermo Fisher Scientific, 51-6100	4% PFA + methanol:acetone	1:100
Claudin-4	Thermo Fisher Scientific, 36-4800	4% PFA + methanol:acetone	1:100
Claudin-7	Thermo Fisher Scientific, 34-9100	4% PFA + methanol:acetone	1:500
E-cadherin	Cell Signaling Technology, 24E10	4% PFA + methanol:acetone	1:500
Talin	Sigma Aldrich, T3287	4% PFA only	1:100
ZO-1	Thermo Fisher Scientific, 33-9100	4% PFA + methanol:acetone	1:1000

Supplemental table 4.1. Primary antibodies and fixation conditions.

References

1. Lynn KS, Peterson RJ, Koval M. Ruffles and spikes: Control of tight junction morphology and permeability by claudins. *Biochimica et Biophysica Acta-Biomembranes* 1862, 183339. (2020).
2. Hynes RO. Integrins: Bidirectional, Allosteric Signaling Machines. *Cell* 110, 673-687. (2002).
3. Schwartz MA. Integrins and Extracellular Matrix in Mechanotransduction. *Cold Spring Harbor Perspectives in Biology* 2, a005066. (2010).
4. Humphries JD, Chastney MR, Askari JA, Humphries MJ. Signal transduction via integrin adhesion complexes. *Current Opinions in Cell Biology* 56, 14-21. (2019).
5. Sun Z, Costell M, Fässler R. Integrin activation by talin, kindlin and mechanical forces. *Nature Cell Biology* 21, 25-31. (2019).
6. Kadry YA, Calderwood DA. Chapter 22: Structural and signaling functions of integrins. *Biochimica et Biophysica Acta-Biomembranes* 1862, 183206. (2020).
7. Wang Z, Symons JM, Goldstein SL, McDonald A, Miner JH, Kreidberg JA. $\alpha 3\beta 1$ integrin regulates epithelial cytoskeletal organization. *Journal of Cell Science* 112, 2925-2935. (1999).
8. Lu Z, Kim DH, Fan J, Lu Q, Verbanac K, Ding L, Renegar R, Chen YH. A non-tight junction function of claudin-7—Interaction with integrin signaling in suppressing lung cancer cell proliferation and detachment. *Molecular Cancer* 14. (2015).

9. Fredriksson K, Van Itallie CM, Aponte A, Gucek M, Tietgens AJ, Anderson JM. Proteomic analysis of proteins surrounding occludin and claudin-4 reveals their proximity to signaling and trafficking networks. *PLoS One* 10, e0117074. (2015).
10. Starchenko A, Graves-Deal R, Yang YP, Li C, Zent R, Singh B, Coffey RJ. Clustering of integrin $\alpha 5$ at the lateral membrane restores epithelial polarity in invasive colorectal cancer cells. *Molecular Biology of the Cell* 28, 1288-1300. (2017).
11. Tafazoli F, Holmström A, Forsberg Å, Magnusson KE. Apically exposed, tight junction-associated $\beta 1$ integrins allow binding and YopE-mediated perturbation of epithelial barriers by wild-type *yersinia* bacteria. *Infection and Immunity* 68, 5335-5343. (2000).
12. Garbi C, Negri R, Calì G, Nitsch L. Collagen interaction with apically expressed $\beta 1$ integrins: Loss of transepithelial resistance and reorganization of cultured thyroid cell monolayer. *European Journal of Cell Biology* 69, 64-75. (1996).
13. Kam KR, Walsh LA, Bock SM, Koval M, Fischer KE, Ross RF, Desai TA. Nanostructure-mediated transport of biologics across epithelial tissue: Enhancing permeability via nanotopography. *Nano Letters* 13, 164-171. (2013).
14. Walsh L, Ryu J, Bock S, Koval M, Mauro T, Ross R, Desai T. Nanotopography facilitates *in vivo* transdermal delivery of high molecular weight therapeutics through and integrin-dependent mechanism. *Nano Letters* 15, 2434-2441. (2015).
15. Stewart T, Koval WT, Molina SA, Bock SM, Lillard JW, Ross RF, Desai TA, Koval M. Calibrated flux measurements reveal a nanostructure-stimulated transcytotic pathway. *Experimental Cell Research* 2, 153-161. (2017).

16. Huang X, Shi X, Hansen ME, Setiady I, Nemeth CL, Celli A, Huang B, Mauro T, Koval M, Desai TA. Nanotopography enhances dynamic remodeling of tight junction proteins through cytosolic liquid complexes. *ACS Nano* 14, 13192-13202. (2020).
17. Zamecnik CR, Lowe MM, Patterson DM, Rosenblum MD, Desai TA. Injectable polymeric cytokine-binding nanowires are effective tissue-specific immunomodulators. *ACS Nano* 11, 11433-11440. (2017).
18. Zamecnik CR, Levy ES, Lowe MM, Zirak B, Rosenblum MD, Desai TA. An injectable cytokine trap for local treatment of autoimmune disease. *Biomaterials* 230, 119626. (2020).
19. Su Y, Xia W, Li J, Walz T, Humphries MJ, Vestweber D, Cabañas C, Lu C, Springer TA. Relating conformation to function in integrin $\alpha 5\beta 1$. *Proceedings of the National Academy of Science USA*, E3872-E3881. (2016).
20. Byron A, Humphries JD, Askari JA, Craig SE, Mould P, Humphries MJ. Anti-integrin monoclonal antibodies. *Journal of Cell Science* 122, 4009-4011. (2009).
21. Takada Y, Puzon W. Identification of a regulatory region of integrin beta 1 subunit using activating and inhibiting antibodies. *The Journal of Biological Chemistry* 268, 17597-17601. (1993).
22. Spiess M, Hernandez-Varas P, Oddone A, Olofsson H, Blom H, Waithe D, Lock JG, Lakadamyali M, Strömblad. Active and inactive $\beta 1$ integrins segregate into distinct nanoclusters in focal adhesions. *Journal of Cell Biology* 217, 1929-1940. (2018).
23. Ye F, Kim C, Ginsberg MH. Reconstruction of integrin activation. *Blood* 119, 26-33. (2012).

24. Luo BH, Carman CV, Springer TA. Structural basis of integrin regulation and signaling. *Annual Review of Immunology* 25, 619-647. (2007).
25. Takagi J, Petre BM, Walz T, Springer TA. Global conformational rearrangements in integrin extracellular domains in outside-in and inside-out signaling. *Cell* 110, 599-611. (2002).
26. Li J, Springer TA. Integrin extension enables ultrasensitive regulation by cytoskeletal force. *Proceedings of the National Academy of Sciences USA* 114, 4685-4690. (2017).
27. Mould AP, Garratt AN, Askari JA, Akiyama SK, Humphries MJ. Identification of a novel anti-integrin monoclonal antibody that recognizes a ligand-induced binding site epitope on the beta 1 subunit. *Federation of European Biochemical Societies Letters* 363, 118-122. (1995).
28. Tsuchida J, Ueki S, Saito Y, Takagi J. Classification of 'activation' antibodies against integrin beta1 chain. *Federation of European Biochemical Societies Letters* 416, 212-216. (1997).
29. Bazzoni G, Shih DT, Buck CA, Hemler ME. Monoclonal antibody 9EG7 defines a novel beta 1 integrin epitope induced by soluble ligand and manganese, but inhibited by calcium. *The Journal of Biological Chemistry* 270, 25570-25577. (1995).
30. Luque A, Gómez M, Puzon W, Takada Y, Sánchez-Madrid F, Cabañas C. Activated conformations of very late activation integrins detected by a group of antibodies (HUTS) specific for a novel regulatory region (355-425) of the common beta 1 chain. *The Journal of Biological Chemistry* 271, 11067-11075. (1996).
31. Mould AP, Akiyama SK, Humphries MJ. The inhibitory anti-beta1 integrin monoclonal antibody 13 recognizes an epitope that is attenuated by ligand occupancy. Evidence for

- allosteric inhibition of integrin function. *The Journal of Biological Chemistry* 271, 20365-20374. (1996).
32. Takagi J, Springer TA. Integrin activation and structural rearrangement. *Immunological Reviews* 186, 141-163. (2002).
 33. Hall DE, Reichardt LF, Crowley E, Holley B, Moezzi H, Sonnenberg A, Damsky CH. The alpha 1/beta 1 and alpha 6/beta 1 integrin heterodimers mediate cell attachment to distinct sites on laminin. *Journal of Cell Biology* 110, 2175-2184. (1990).
 34. Werb Z, Tremble PM, Behrendtsen O, Crowley E, Damsky CH. Signal transduction through the fibronectin receptor induces collagenase and stromelysin gene expression. *Journal of Cell Biology* 109, 877-889. (1989).
 35. Tokuda S, Higashi T, Furuse M. ZO-1 knockout by TALEN-mediated gene targeting in MDCK cells: Involvement of ZO-1 in the regulation of cytoskeleton and cell shape. *PLoS One* 9, e104994. (2014).
 36. Van Itallie CM, Tietgens AJ, Krystofiak E, Kachar B, Anderson JM. A complex of ZO-1 and the BAR-domain protein TOCA-1 regulates actin assembly at the tight junction. *Molecular Biology of the Cell* 26, 2769-2787. (2015).
 37. Burridge K and Connell L. A new protein of adhesion plaques and ruffling membranes. *The Journal of Cell Biology* 97, 359-367. (1983).
 38. Horwitz A, Duggan K, Buck C, Beckerle MC, Burridge K. Interaction of plasma membrane fibronectin receptor with talin—a transmembrane linkage. *Nature* 320, 531-533. (1986).

39. Ciobanasiu C, Faivre B, Le Clainche C. Integrating actin dynamics, mechanotransduction and integrin activation: The multiple functions of actin binding proteins in focal adhesions. *Eur. J. Cell Biol.* 92, 339-348 (2013).
40. L. Gonzalez-Mariscal, A. Avila-Flores, A. Betanzos, The relationship between structure and function of tight junctions, in: J.M. Anderson, M. Cereijido (Eds.), *Tight Junctions*, Second edition, CRC Press, Place Published, 2001, pp. 89-120.
41. Saeedi BJ, Kao DJ, Kitzenberg DA, Dobrinskikh E, Schwisow KD, Masterson JC, Kendrick AA, Kelly CJ, Bayless AJ, Kominsky DJ, Campbell EL, Kuhn KA, Furuta GT, Colgan SP, Glover LE. HIF-dependent regulation of claudin-1 is central to intestinal epithelial tight junction integrity. *Molecular Biology of the Cell* 26, 2252-2262. (2015).
42. Jin Y, Blikslager AT. Myosin light chain kinase mediates intestinal barrier dysfunction via occludin endocytosis during anoxia/reoxygenation injury. *American Journal of Physiology-Cell Physiology* 311, C99-C1004. (2016).
43. Capaldo CT, Farkas AE, Hilgarth RS, Krug SM, Wolf MF, Benedik JK, Fromm M, Koval M, Parkos C, Nusrat A. Proinflammatory cytokine-induced tight junction remodeling through dynamic self-assembly of claudins. *Molecular Biology of the Cell* 25, 2710-2719. (2014).
44. Krause G, Winker L, Mueller SL, Haseloff RF, Piontek J, Blasig IE. Structure and function of claudins. *Biochimica et Biophysica Acta-Biomembranes* 1778, 631-645. (2008).

45. Lu Z, Kim DH, Fan J, Lu Q, Verbanac K, Ding L, Renegar R, Chen YH. A non-tight junction function of claudin-7-Interaction with integrin signaling in suppressing lung cancer cell proliferation and detachment. *Molecular Cancer* 14. (2015).
46. Ding L, Wang L, Sui L, Zhao H, Xu X, Li T, Wang X, Li W, Zhou P, Kong L. Claudin-7 indirectly regulates the integrin/FAK signaling pathway in human colon cancer tissue. *Journal of Human Genetics* 61, 711-720. (2016).
47. Kim DH, Lu Q, Chen YH. Claudin-7 modulates cell-matrix adhesion that controls cell migration, invasion and attachment of human HCC827 lung cancer cells. *Oncology Letters* 17, 2890-2896. (2019).
48. Burridge K and Chrzanowska-Wodnicka M. Focal adhesions, contractility, and signaling. *Annual Reviews Cell and Developmental Biology* 12, 463-519. (1996).
49. Kong F, García AJ, Mould AP, Humphries MJ, Zhu C. Demonstration of catch bonds between an integrin and its ligand. *The Journal of Cell Biology* 185, 1275-1284. (2009).

Chapter 5. Impact of anti-integrin particle geometry on tight junctions

Abstract

In Chapter 4, we determined that targeting pools of apical integrins in the closed conformation using 15 μ m nanowires conjugated with anti-integrin antibodies was sufficient to increase paracellular ion permeability which correlated with a ruffled tight junction morphology and rearrangement of the actin cytoskeleton. In order to further investigate how nanoparticle targeting of apical integrins mediates the regulation of the epithelial barrier, we synthesized particles with different geometries, 2 μ m microspheres and 5 μ m nanowires, that were conjugated to anti-integrin β 1 antibodies targeting either the closed (AIIB2) or open (9EG7) conformation. Cell responses were influenced by both the aspect ratio of the particle and the functionality of the anti-integrin antibody. AIIB2 microspheres had little impact on tight junction morphology and paracellular ion permeability. By contrast, 9EG7 microspheres induced tight junction ruffling and, after a transient decrease in permeability, increased ion permeability. AIIB2 and 9EG7 5 μ m nanowires both induced tight junction ruffling, but their effect on paracellular ion permeability matched the corresponding anti-integrin microspheres. AIIB2 microspheres were the only particles tested here that increased paracellular flux to calcein and Texas Red 10 kDa dextran. These data demonstrate that particle geometry influences the effects of targeting integrin β 1 on tight junction morphology and function.

5.1 Introduction

In Chapter 4, we showed that specifically targeting pools of apical integrin $\beta 1$ in their closed conformation with antibody conjugated nanowires was sufficient to mediate changes in the epithelial barrier. This suggested that the targeting and subsequent clustering of integrin $\beta 1$ by the nanowire platform regulated junction remodeling and barrier function. These results were consistent with previous work that attributed roles for apical integrins in controlling barrier function [1-4]. However, the results in Chapter 4 were the first demonstration of the specific contributions apical integrins alone have in this process, and the first demonstration of how integrin conformation state played a role in epithelial barrier regulation. Exploration of the integrin specific contributions to the regulation of barrier function were able to be examined because we used a discrete nanowire platform.

Previous work using nanostructured films showed that nanotopography features including height, width, and pitch influenced their impact on permeation enhancement [1,3, C. Nemeth, unpublished]. Studies using discrete nanoparticles have demonstrated that they can contribute to permeation enhancement by specifically altering tight junction proteins [5], though enhancement is tunable based on particle size and charge [6]. Functionalized carbon nanotubes [7] and protein loaded nanofibers [8] have also demonstrated the ability to increase permeability through tight junctions. Likewise, studies with antibody decorated discrete nanoparticle platforms show that both aspect ratio of the particle [9] and the size of the particle [10,11] are related to cell response and ability to internalize particles. With this in mind, we wanted to further define the impact particle geometry has in eliciting apical integrin mediated regulation of the epithelial barrier.

The method that we use to synthesize the nanowires [12,13] is tunable and allows us to modulate both the size and shape of the particle with the same polymer composition. In these

experiments, we synthesized 2 μ m microspheres to serve as a shape control, and 200nm x 5 μ m nanowires to compare to the 200nm x 15 μ m nanowires used in Chapter 4. In this chapter we demonstrate that the geometry of the nanoparticle platform itself in combination with the functionality of the anti-integrin antibody decorating it are both key to coordinating apical integrin regulation of the epithelial barrier.

5.2 Materials and Methods

5.2.1 Fabrication and conjugation of nanoparticles

Derivatizable PCL nanoparticles were fabricated from a mix of 45kDa PCL (Sigma Aldrich, 704105), maleimidophenyl-PCL (MP-PCL), and Nile Red dye (Sigma Aldrich, 19123) in 2,2,2-trifluoroethanol (Sigma Aldrich, T63002). Adjustment of PCL concentration (w/v) generates nanoparticles of varying sizes, though MP-PCL makes up 30% of the total polymer weight for any size particle. For 15 μ m nanowires, total polymer concentration is 125mg/mL, for 5 μ m nanowires, concentration is 25mg/mL, and for 2 μ m microspheres, polymer concentration is 100mg/mL.

Nanowires were fabricated as described in Chapter 4. Filtered nanowires were centrifuged 3 times at 4000RPM for 15 min at 4C, the supernatant was discarded and the pelleted nanowires were washed with cold distilled water, cold PBS, and with reducing buffer (PBS + 0.04% w/v EDTA) respectively, and were stored in reducing buffer at 4C until use.

Microspheres were fabricated using a single-emulsion technique as described previously, with modifications [14]. The PCL/solvent/dye mixture was added dropwise to a 1.5% PVA solution as it was being vortexed in a 1:2 ratio of PCL:PVA. The emulsion was then sonicated on ice in 10 sec bursts for 1 min before being added to excess PVA mixing on a magnetic stir plate. Nanoparticles were then collected, and the beaker was washed with distilled water to resuspend

any particles stuck to the bottom of the beaker before spinning them down at 1400RPM for 15 min at 4C. The supernatant was discarded, and the pelleted microspheres were washed again with cold PBS and reducing buffer respectively. After final washes, microspheres were resuspended in reducing buffer and strained through 40 μ m mesh before storing at 4C before use.

Nanoparticles were conjugated as in Chapter 4 with either the AIIB2 blocking anti-integrin antibody (Millipore, MAB409T) or the 9EG7 activating antibody (BD Pharmingen, 553715). Antibody conjugated nanoparticles were always used within 4 hours of conjugation (stored at 4C unless being used immediately).

5.2.2 Cell culture

Caco-2 cells were maintained in Minimum Essential Medium with Earle's salts and L-glutamine (Corning Cellgro, 10-010-CV) supplemented with 10% Fetal Bovine Serum (Atlanta Biologicals Premium Select, S11550), Sodium Pyruvate (Hyclone, SH30239.01), 100U/mL Penicillin/10mg/mL Streptomycin (Sigma Aldrich, P4333), 0.25 μ g/mL Amphoteroicin B (Thermo Fisher Scientific, 15290018), and 5 μ g/mL Gentamicin (Sigma Aldrich, G1397). Cells were incubated in a CO₂ incubator at 37C until they were ready to be seeded to glass coverslips for immunofluorescence experiments or Transwell permeable supports for barrier function experiments.

5.2.3 Immunofluorescence

Caco-2 cells were seeded for immunofluorescence as described in Chapter 4. Treated cells were fixed and permeabilized as described in Chapter 4 using both PFA and methanol:acetone fixation steps. Primary antibody (ZO-1, Thermo Fisher Scientific 33-9100; Claudin-1, Thermo

Fisher Scientific 51-9000; β -catenin, BD Biosciences 610153) was diluted in 3% Bovine Serum Albumin (BSA) (Gemini Bio-Products, 700-102P) and incubated on cells overnight at 4C. Cells were washed with 3% BSA before Alexa Fluor 594 goat anti-rabbit (Thermo Fisher Scientific, A32740) and Cy2 goat anti-mouse (JacksonImmuno Research Labs, 115-225-166) secondary antibodies were diluted in 3% BSA and incubated for 1h at room temperature before washing with PBS with calcium and magnesium before mounting the coverslip to a slide with Prolong antifade with DAPI (Thermo Fisher Scientific, P36962). For F-actin visualization, DyLight 488 phalloidin (Thermo Fisher Scientific, 21833) was diluted in PBS and incubated with cells for 30min at room temperature before mounting the coverslips. Images were obtained and processed as described in Chapter 4.

5.2.4 Barrier function

Caco-2 cells were seeded for barrier function assays as described in Chapter 4. Transepithelial Resistance (TER) time courses were measured over a time course of 2-hours using the cellZscope 2 and its accompanying software for data acquisition as described in Chapter 4. Permeability for larger molecules was assessed using the dye flux assay as described in Chapter 4. Probes include calcein (Thermo Fisher Scientific, C481), Texas Red-labeled 10kDa dextran (Thermo Fisher Scientific, D1863).

5.3 Results

5.3.1 Effects of targeting apical integrins on junction morphology is dependent on nanoparticle aspect ratio

We have previously observed that targeting the apical integrins of Caco-2 intestinal epithelial cells with blocking anti-integrin $\beta 1$ antibody (AIIB2) conjugated nanowires 15 μm in length is sufficient to induce remodeling of tight junction proteins resulting in a ruffled morphology (Chapter 4). However, no work has been done to address how the shape and size of nanoparticles conjugated with anti-integrin antibodies impacts the ability of apical integrins to regulate tight junctions. To examine this, we adjusted the concentrations of PCL polymer and fabrication methods used to create discrete nanowires of two different sizes (5 μm and 15 μm) and 2 μm microspheres (Fig. 5.1A). These particle sizes allow us to examine whether differences in aspect ratio and total surface area (Table 5.1) are factors in cell response to apical integrin targeting.

Immunostaining for ZO-1 revealed that both 5 μm and 15 μm AIIB2 nanowires were able to stimulate a ruffled tight junction morphology. By contrast, cells treated with AIIB2 microspheres largely retained linear tight junctions (Fig. 5.1B-D). Interestingly, while both the 5 μm and 15 μm anti-integrin nanowires were able to stimulate ZO-1 reorganization, the appearance of the resulting morphology was slightly different. While the 15 μm anti-integrin nanowires generated an undulating ruffled morphology, the 5 μm anti-integrin nanowires triggered a morphology that appeared to be more spike-like projections than ruffled (Fig. 5.1D). Though the ZO-1 morphology looked different, there was no significant difference in junction length ratio when comparing cells treated with either size of AIIB2 nanowires (Fig. 5.1B).

5.3.2 Role of aspect ratio on the effects of anti-integrin particles on epithelial barrier structure

Because we hypothesize that the changes in AJC protein localization and morphology are linked to apical integrins by their effects on the actin cytoskeleton, we examined the effects of the 2 μ m anti-integrin microspheres on F-actin using 488-phalloidin. We found that cells treated with 15 μ m AIIB2 nanowires induced cortical localization of actin (Fig. 5.2A). By contrast, cells treated with 2 μ m AIIB2 microspheres did not appear to have much impact on actin organization (Fig. 5.2A). This preliminary data suggests that although the particles are targeting the same molecules in the same conformational state, the geometry of multivalent anti-integrin particles has an impact on how they mediate cell responses. Moreover, it appeared that actin surrounded the surface of AIIB2 microspheres. This raises the possibility that unlike nanowire shaped particles, the AIIB2 microspheres may be internalized. Future work will determine whether this is the case.

In the previous chapter, we observed that AIIB2 nanowires were infrequently in direct contact with the junctions themselves (Chapter 4). To better understand if differences in aspect ratio how the cells interact with particles, we imaged the fluorescent AIIB2 microspheres and 15 μ m nanowires and measured their proximity to tight junctions stained for ZO-1 (Fig. 5.2B). We found that there was a significantly higher number of cell associated AIIB2 nanowires as compared to microspheres (Fig. 5.2C), suggesting that AIIB2 nanowires were more stably associated with cells than microspheres.

5.3.3 Apical integrin conformation state and interaction with nanoparticles

In the previous chapter, we demonstrated that targeting the closed and open conformation states of apical integrins had differential effects on epithelial barrier function and structure

(Chapter 4), and we were curious to see if those same effects were conserved when activating anti-integrin antibody was conjugated to particles with different aspect ratios. Treating cells with 9EG7 microspheres for 2hr caused the appearance of tight junction ruffles, as did treatment with the 5 μ m 9EG7 nanowires (Fig. 5.3A). These results were quantified, demonstrating that the junction/length ratios of cells treated with 9EG7 microspheres or nanoparticles were significantly greater than 1, which is the junction/length ratio of cells with linear junctions (Fig. 5.3B). However, the 9EG7 microspheres induced a significantly higher percentage of cells with ruffles than cells treated with the 5 μ m 9EG7 nanowires (Fig. 5.3C). This was surprising given that soluble or 15 μ m nanowire bound 9EG7 antibody did not induce ruffling, and, in fact, trended towards promoting more linear junctions (Chapter 4, Fig. 4.1F,G). These data are also surprising in that AIIB2 microspheres did not increase the percentage of cells with one or more ruffled junctions, nor did it significantly increase junction/length ratio.

We also examined the effect of 9EG7 particles on localization of the tight junction protein claudin-1. In cells treated with activating 9EG7 microspheres, junctional claudin-1 staining appears very bright, as opposed to treatment with the activating 9EG7 5 μ m nanowires where there is much less junctional signal from claudin-1 (Fig. 5.4A). The results from the activating 9EG7 5 μ m nanowires are consistent with observations in the previous chapter—in that in areas with very ruffled ZO-1, there is less claudin-1 signal (Chapter 4, Supplemental Fig. 4.2B). Thus, it is particularly surprising to see such strong claudin-1 signal in activating 9EG7 microsphere treated cells where tight junction ruffling is particularly robust. Staining for β -catenin after treatment with both of the activating 9EG7 nanoparticles (Fig. 5.4B) was also surprising because it did not appear to have the disperse morphology we observed in experiments with blocking AIIB2 nanowires that caused ruffling (Chapter 4, Fig. 4.3B). Together these data suggest that how apical integrins

regulate the epithelial barrier depends on the conformation state of the integrin being targeted, in addition to the geometry and aspect ratio of nanoparticles.

5.3.4 Aspect ratio and integrin conformation state control how apical integrins regulate epithelial barrier function

In Chapter 4, as well as in previous work, we tested the hypothesis that the ruffling of tight junction proteins is part of the cell response that includes increased permeability [1-3]. We saw that when we specifically target apical integrins in the closed conformation with 15 μ m nanowires that induced ruffling, there was also an increase in ionic permeability as measured by TER and permeability to whole IgG tracer molecules (Chapter 4, Fig. 4.4E). Given the effects of the anti-integrin particles tested here on tight junction morphology, we examined the effect of these particles on barrier function.

First, we examined changes in TER for the duration of a 2hr time course after treatment with different sized anti-integrin nanoparticles (Fig. 5.5A). While treatment with either AIIB2 microspheres or AIIB2 5 μ m nanowires caused an initial, rapid decrease in TER, comparable to that observed when cells were treated with AIIB2 15 μ m nanowires. Unlike cells treated with 15 μ m AIIB2 nanowires, which have a fairly constant TER throughout the duration of the 2hr time course, cells treated with AIIB2 5 μ m nanowires or microspheres recovered back to baseline TER values. By contrast, cells treated with 9EG7 microspheres or 5 μ m nanowires showed a biphasic response, where there was a transient increase in TER, followed by a subsequent decrease by the 2hr endpoint (Fig. 5.5A).

To test how aspect ratio and integrin conformation state impacted paracellular permeability to soluble substrates, we also conducted dye flux assays (Fig. 5.5B,C). Despite the fact that 9EG7

5 μ m nanowires caused junction ruffling, treating cells with these particles had little impact on barrier permeability to either calcein (0.63kDa) or Texas red dextran (10kDa). Similarly, 9EG7 2 μ m microspheres did not change barrier permeability to calcein or dextran, despite causing tight junction ruffles. Interestingly, AIIB2 2 μ m microspheres, which caused junctions to remain linear, did increase barrier permeability to both calcein and dextran. Taken together these data reflect a good correlation between formation of ruffled tight junctions and a decrease in TER, however, the effect of anti-integrin nanowires and microspheres on paracellular flux is much more variable.

5.4 Discussion

Here we found that the aspect ratio of anti-integrin nanoparticles plays a role in how integrins can regulate cell responses. The results presented here also indicate that the using nanoparticles with different aspect ratios to target apical integrins in their open or closed conformation impacts integrin mediated regulation of the epithelial barrier.

We observed that microspheres targeting integrins in the closed conformation had little effect on ionic permeability and junction morphology but stimulated increased paracellular permeability to large molecules. Microspheres targeting integrins in the closed conformation may also be internalized. Short nanowires targeting integrins in the closed conformation stimulated a ruffled tight junction morphology and transiently increased ionic permeability. Alternatively, both microspheres and short nanowires targeting integrins in the open conformation caused increased ionic permeability and tight junction ruffling while having little effect on paracellular permeability. This suggests the possibility that in order to elicit a specific change in barrier function we can tune the shape and size of the nanoparticle platform, as well as integrin epitope.

While this is an interesting possibility, we need to conduct more experiments to determine why changing the geometry of the nanoparticles can make such a difference how the epithelial barrier is regulated by apical integrins. One thing that can be examined is whether this is a function of aspect ratio, total surface area, or symmetry of the particle. The 2 μ m microspheres and 15 μ m nanowires are the closest in total surface area (Table 5.1) and when conjugated with either AIB2 or 9EG7 antibody elicit different responses. We can begin to tease out if this means aspect ratio or symmetry is driving these differences by repeating these experiments with spherical anti-integrin particles of varying sizes, including on the nanoscale, as done by Jiang, et al. [10]. We have had success using a lower molecular weight PCL, changing the solvent we dissolve the PCL in, and changing the oil-phase surfactant used as the emulsifier, to generate 200nm spheres (data not shown). These particles would allow us to compare how particles with the same aspect ratio but different surface areas are coordinated by the cell and if they interact with apical integrins in the same way to regulate junctions.

To examine the role that particle symmetry plays in regulating anti-integrin nanoparticle responses, we would want to take steps ensure that the total protein concentration per experimental well is normalized across each treatment so that the number of integrins stimulated is comparable when particles of different size and geometry are compared. This would allow us to more directly attribute the differences in cell response between a symmetrical spherical particle versus an asymmetrical rod-like nanowire shaped particle to be related to substrate geometry. Together these experiments will provide necessary insight into why we see differences in barrier structure and function between particles of the same shape that target integrins in different conformation states.

The results in this chapter also present an interesting question related to how the cells react to the particles themselves. While we presented some data regarding this (Fig. 5.2), this was a

snapshot of a single time point, live cell experiments would be much more informative. For example, we could use cells that express fluorescently tagged ZO-1 as used in Huang et al., and treat them with fluorescent anti-integrin particles and watch how ZO-1 morphology changes in real time, and if/how the particles interact with tight junctions themselves [15]. Understanding the role geometry plays on cell response in nanoparticle targeting of apical integrins will help define next steps for examining the mechanism of action that allows apical integrins to regulate the epithelial barrier.

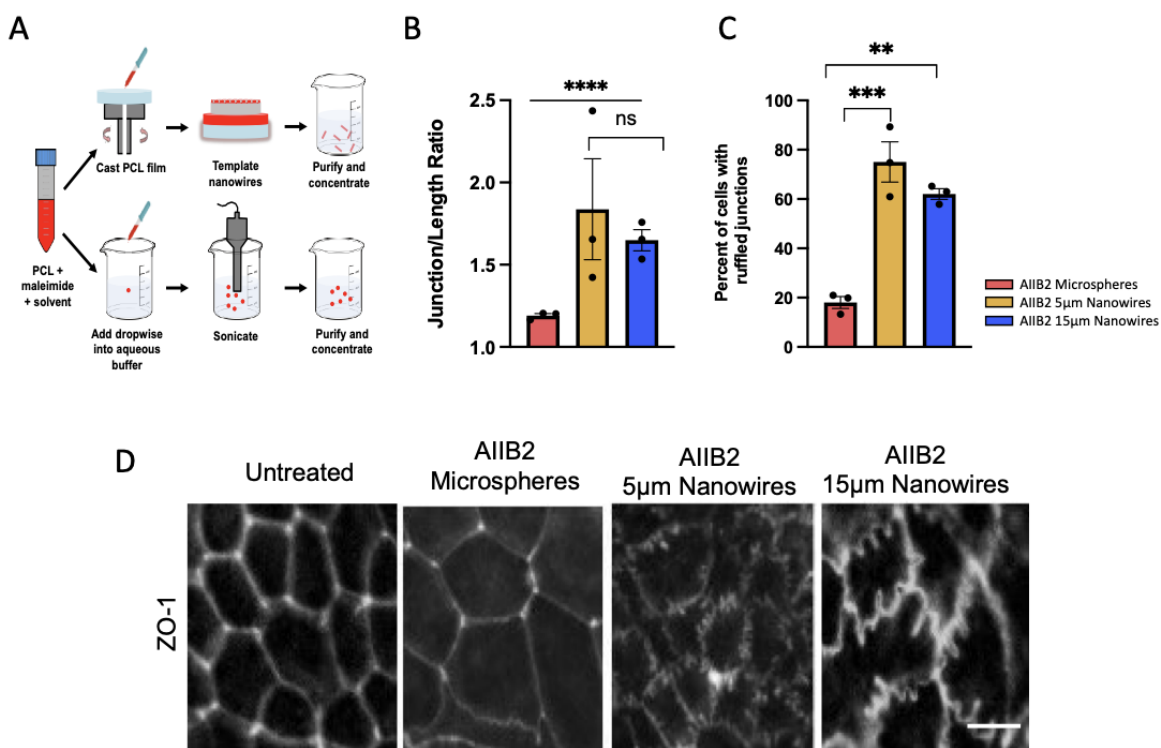


Figure 5.1. Aspect ratio of AIB2 nanoparticles is important in triggering ruffled ZO-1 morphology.

(A) Schematic depicts how different shaped nanoparticles are synthesized with polycaprolactone (PCL) polymer. (B) Quantification of junction/length ratios for each treatment, data displayed as mean ratio per field of view \pm SEM ($n=25$ measurements per field of view from 3 fields of view from 1 biological replicate), treatment key on right. **** $p<0.0001$ (C) Quantification of percent cells in a field of view with one or more ruffled junctions displayed as percent \pm SEM ($n=3$ fields of view), treatment key on right. ** $p=0.0026$, *** $p=0.0006$ (D) Representative immunofluorescence images of Caco-2 cells labeled with ZO-1 (color) 2hr after treatment with blocking AIB2 anti-integrin microspheres, long, and short nanowires, bar=10 μ m. (B and C) Significance determined by one-way ANOVA with Bonferroni's correction for multiple comparisons.

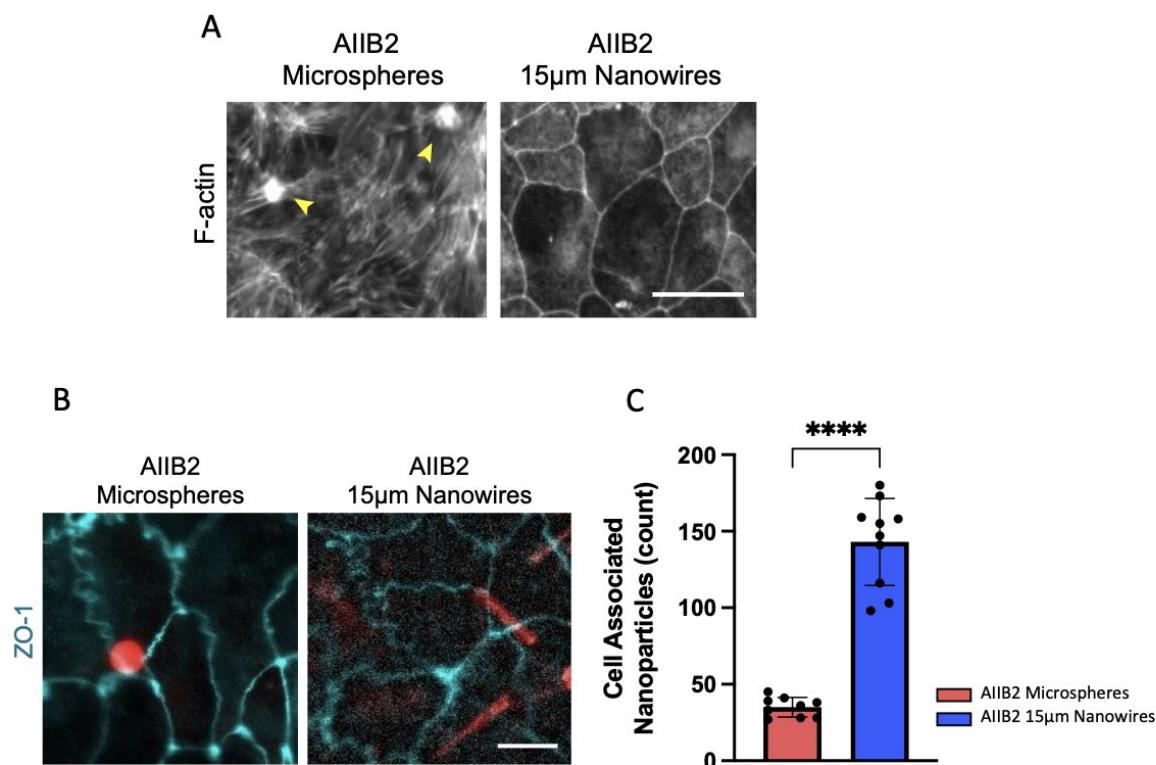


Figure 5.2. Actin reorganization depends on the geometry of AIB2 nanoparticles.

(A) Representative immunofluorescence images of Caco-2 cells labeled with 488-phalloidin to visualize F-actin (grey) 2hr after treatment, bar=10µm. Yellow arrowheads indicate likely localization of microspheres. (B) Immunofluorescence images of Caco-2 cells labeled with ZO-1 (cyan) in order to visualize Nile Red nanoparticles (red) and quantify the number of cell associated particles, bar=10µm. (C) Quantification of the number of cell-associated nanoparticles, data displayed as mean \pm SD with each point representing the number of cell associated particles counted in a single field of view (n=2 biological replicates with 4-5 fields of view each), treatment key to the right. ****p<0.0001, significance determined by one-tailed unpaired t-test.

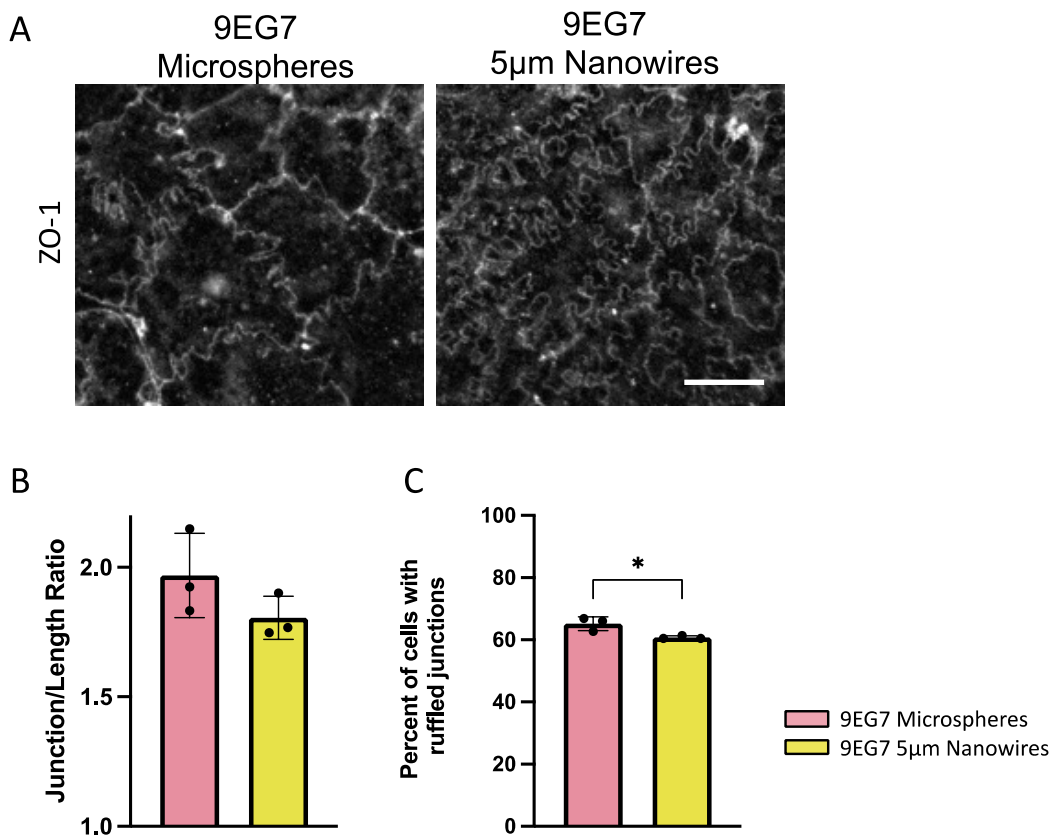


Figure 5.3. 9EG7 microspheres and 5 μ m nanowires induce ruffled ZO-1 morphology.

(A) Representative immunofluorescence images of Caco-2 cells labeled with ZO-1 (grey) 2hr after treatment, bar=10 μ m. (B) Quantification of junction/length ratios for each treatment, data displayed as mean ratio per field of view \pm SD (n=25 measurements per field of view from 3 fields of view from 1 biological replicate), p=0.0979. (C) Quantification of percent cells in a field of view with one or more ruffled junctions displayed as percent \pm SD (n=3 fields of view), *p=0.0136. (B and C) Significance determined by one-tailed unpaired t-test. Treatment key on right.

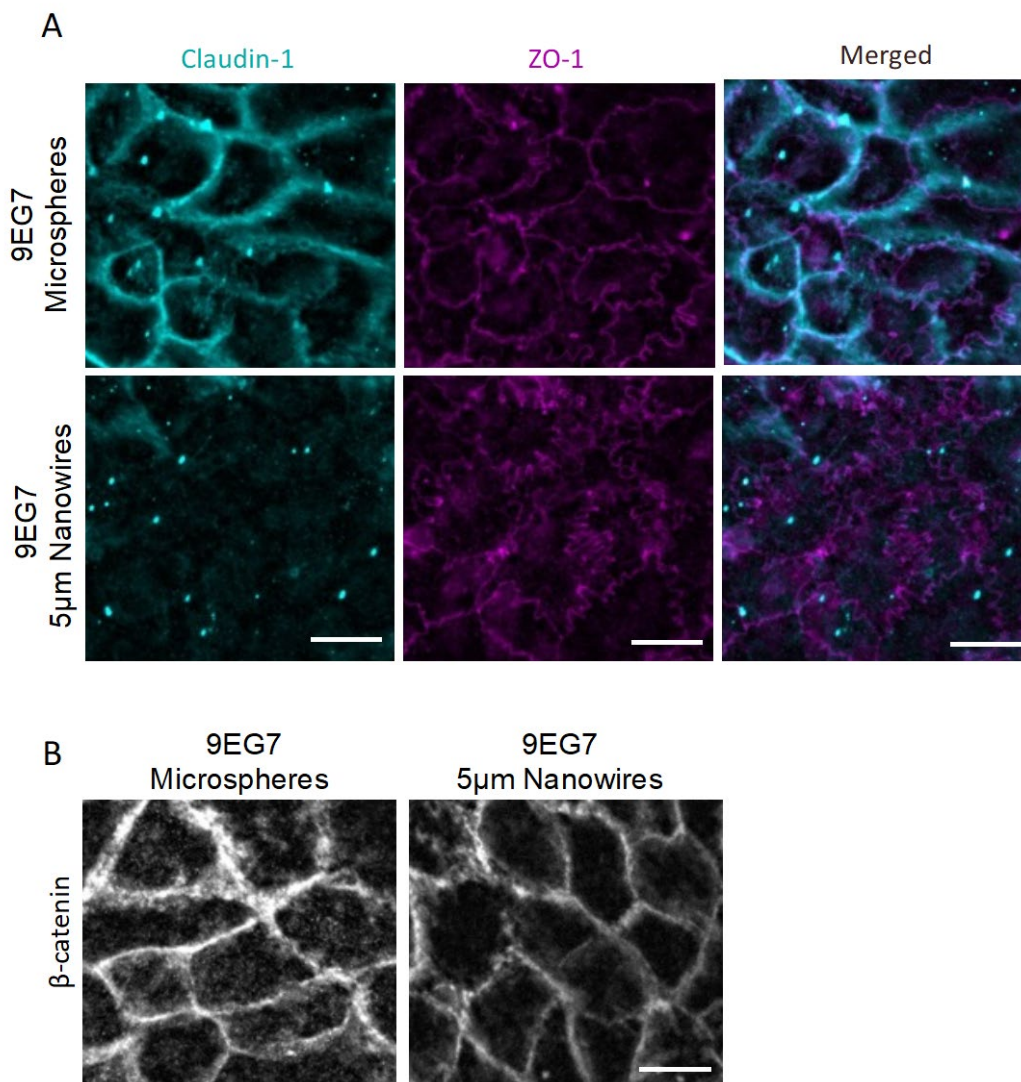


Figure 5.4. 9EG7 nanoparticles and localization of proteins in the apical junctional complex.

(A) Representative immunofluorescence images of Caco-2 cells stained for ZO-1 (magenta) and claudin-1 (cyan) 2hr after treatment, bar=10µm. **(B)** Representative immunofluorescence images of Caco-2 cells stained for β-catenin (grey) 2hr after treatment, bar=10µm.

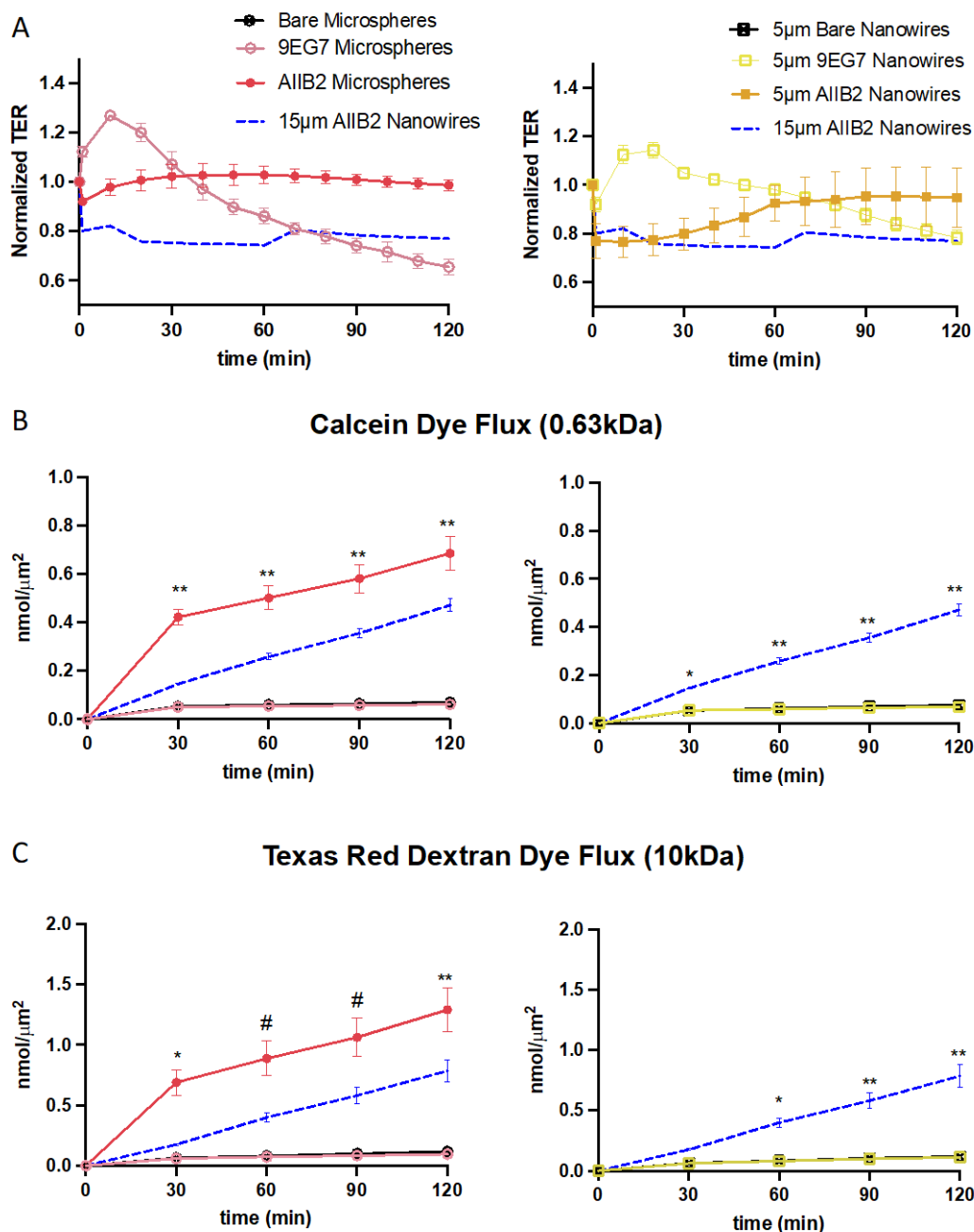


Figure 5.5. Anti-integrin nanoparticle geometry and the effect on barrier function.

(A) Transepithelial electrical resistance (TER) measurements on Caco-2 cells for 2hr following treatment. Measurements taken with a cellZscope impedance system every 10 minutes, and each reading was normalized to baseline TER readings. Each point is the average TER for that treatment \pm SEM (n=2-6 wells per treatment). (B) Dye flux permeability for calcein (0.63kDa) in Caco-2

cells. Each point is the average permeability for each treatment \pm SEM (n=4-8 wells/treatment). *The 15 μ m AIIB2 nanowire data that appears in this figure is replicated from Chapter 4 (Fig. 4.4C) and was reproduced here for comparison purposes.* (C) Dye flux permeability for Texas red dextran (10kDa) in Caco-2 cells. Each point is the average permeability for each treatment \pm SEM (n=4-8 wells/treatment). **(B and C)** Significance was determined by two-way ANOVA with Bonferroni correction for multiple comparisons of simple row effects. *p=0.0004, #p=0.0005, **p<0.0001.

	Surface area (μm^2)	Aspect ratio
2 μm microsphere	12.6	1
5 μm nanowire	3.2	25
15 μm nanowire	9.5	75

Table 5.1. Nanoparticle surface area and aspect ratio.

References

1. Kam KR, Walsh LA, Bock SM, Koval M, Fischer KE, Ross RF, Desai TA. Nanostructure-mediated transport of biologics across epithelial tissue: Enhancing permeability via nanotopography. *Nano Letters* 13, 164-171. (2013).
2. Walsh L, Ryu J, Bock S, Koval M, Mauro T, Ross R, Desai T. Nanotopography facilitates *in vivo* transdermal delivery of high molecular weight therapeutics through and integrin-dependent mechanism. *Nano Letters* 15, 2434-2441. (2015).
3. Stewart T, Koval WT, Molina SA, Bock SM, Lillard JW, Ross RF, Desai TA, Koval M. Calibrated flux measurements reveal a nanostructure-stimulated transcytotic pathway. *Experimental Cell Research* 2, 153-161. (2017).
4. Garbi C, Negri R, Cali G, Nitsch L. Collagen interaction with apically expressed $\beta 1$ integrins: Loss of transepithelial resistance and reorganization of cultured thyroid cell monolayer. *European Journal of Cell Biology* 69, 64-75. (1996).
5. Leve F, Bonfim DP, Fontes G, Morgado-Díaz JA. Gold nanoparticles regulate tight junctions and improve cetuximab effect in colon cancer cells. *Nanomedicine* 14, 1565-1578. (2019).
6. Lamson NG, Berger A, Fein KC, Whitehead KA. Anionic nanoparticles enable the oral delivery of proteins by enhancing intestinal permeability. *Nature Biomedical Engineering* 4, 84-96. (2020).
7. Coyuco JC, Liu Y, Tan BJ, Chiu GNC. Functionalized carbon nanomaterials: exploring the interactions with Caco-2 cells for potential oral drug delivery. *International Journal of Nanomedicine* 6, 2253-2263. (2011).

8. Stephansen K, García-Díaz M, Jessen F, Chronakis IS, Mørck Nielsen H. Bioactive protein-based nanofibers interact with intestinal biological components resulting in transepithelial permeation of a therapeutic protein. *International Journal of Pharmaceutics* 495, 58-66. (2015).
9. Barua S, Yoo JW, Kolhar P, Wakankar A, Gokarn YR, Mitragotri S. Particle shape enhances specificity of antibody-displaying nanoparticles. *Proceedings of the National Academies of Science of the United States of America* 110, 3270-3275 (2013).
10. Jiang W, Kim BYS, Rutka JT, Chan WCW. Nanoparticle-mediated cellular response is size dependent. *Nature Nanotechnology* 3, 145-150. (2008).
11. Gratton SEA, Ropp PA, Pohlhaus PD, Luft JC, Madden VJ, Napier ME, DeSimone JM. The effect of particle design on cellular internalization pathways. *Proceedings of the National Academy of Sciences of the United States of America* 105, 11613-11618. (2008).
12. Zamecnik CR, Lowe MM, Patterson DM, Rosenblum MD, Desai TA. Injectable polymeric cytokine-binding nanowires are effective tissue-specific immunomodulators. *ACS Nano* 11, 11433-11440. (2017).
13. Zamecnik CR, Levy ES, Lowe MM, Zirak B, Rosenblum MD, Desai TA. An injectable cytokine trap for local treatment of autoimmune disease. *Biomaterials* 230, 119626. (2020).
14. McCall RL, Sirianni RW. PLGA nanoparticles formed by single- or double-emulsion with vitamin E-TPGS. *Journal of Visualized Experiments* 82, e51015. (2013).

15. Huang X, Shi X, Hansen ME, Setiady I, Nemeth CL, Celli A, Huang B, Mauro T, Koval M, Desai TA. Nanotopography enhances dynamic remodeling of tight junction proteins through cytosolic liquid complexes. *ACS Nano* 14, 13192-13202. (2020).

Chapter 6: Practical issues related to applications of anti-integrin nanowires

Abstract

In Chapters 4 and 5 we examined how particles of different shapes targeting apical integrins in different conformations were able to regulate the epithelial barrier. We determined that targeting integrins in the closed conformation with low aspect ratio particles is a requirement for stimulating increased paracellular ion permeability and ruffled tight junctions. Alternatively, using high aspect ratio particles were able to increase ionic permeability and induce ruffling when targeting integrins in the open conformation. In order to investigate some of the practical concerns related to future applications of the anti-integrin nanoparticle platform we tested the effects of longer treatment times with AIIB2 nanowires and found that AIIB2 induced ZO-1 ruffling persists for at least 4 hours, and at longer treatment times can promote a new spike-like ZO-1 morphology. We began to test the reversibility of the nanowire system by using glutathione to compete AIIB2 half antibody fragments off nanowires and saw ZO-1 linearity return. We tested a hypothesis that matrix metalloproteases (MMPs) played a role in AIIB2 nanowire mediated junction remodeling and ion permeability and found that inhibiting MMP-2 in AIIB2 nanowire treated cells prevented ZO-1 ruffling and decreases in TER. We also began to show evidence that the changes in cell response to AIIB2 nanowires is conserved in airway cells.

6.1 Introduction

Though the focus of this dissertation was ultimately centered on elucidating some the basic biology that linked the ways in which pools of apical integrins regulate tight junction structure and function, the larger project that the dissertation work is ultimately a part of was initially intended to be more translational work rooted in furthering our understanding of novel drug delivery targets. Because previous work with nanostructured films (NSFs) implicated integrin regulation in the movement of macromolecules [1-3], a motivation for understanding the basic biology that allows apical integrins to regulate the epithelial barrier was to use the findings to provide a better understanding of the pathways that target the delivery of biologics and identify limitation to certain modes of drug delivery. Some of the findings made during this project can be leveraged as a starting point for studies that further examine potential therapeutic applications for examining potential therapeutic uses for anti-integrin nanoparticles, or other antibody conjugated nanoparticles.

A strength of the NSF platform as a permeation enhancer for biologics is that it doesn't rely on chemical enhancers that increase drug absorption but can cause problems ensuring that permeation is transient and controlled with minimal cell toxicity [4-7]. Despite this strength, the nature of the NSF platform limits the types of therapeutic applications that it can be used in [5,8]. One of the key strengths of the nanowire platform we have been using to target apical integrins is that the material has been used in a variety of clinical applications [9-11] and because they are discrete particles and not a plastic film can be used in a wider variety of therapeutics than NSFs. However, unlike the anti-integrin nanoparticles, NSFs are easy to remove and are thus a more reversible permeation enhancer. It is not known how long the effects of anti-integrin nanoparticle mediated permeability is maintained or if it is easily reversible.

While anti-integrin nanoparticles have the capability of increasing permeability via actin cytoskeleton reorganization and tight junction remodeling, they do not appear to trigger local junction remodeling, rather they stimulate action at a distance (Chapters 4 and 5). Understanding the mechanism that allows our anti-integrin nanoparticle platform to promote permeability at a distance could clarify uses for an apical integrin targeting platform. Interesting candidates for this are matrix metalloproteases (MMPs), a family of zinc dependent enzymes that selectively degrade different components of the ECM [12] and have been demonstrated to degrade tight junctions resulting in increased permeability [13]. Additionally, in certain disease states like cancer, integrin $\beta 1$ signaling upregulates the activity of specific classes of MMPs to promote cell migration [14].

Outside of these more mechanistic issues, another barrier to translational applications of this work requires addressing the system we did experiments in. Though the Caco-2 cell line is a well validated model for use in drug delivery studies [15-17], experiments in a single cell type don't demonstrate whether the results we have observed are universally conserved for other epithelial tissues, which is an important consideration for therapeutic applications. Though it has been established that apical integrins have been identified in a variety of cell and tissue types (Table 3.1), the work in Chapters 4 and 5 of this dissertation only included data collected using the Caco-2 intestinal cell line. Examining how targeting apical integrins with nanoparticles effects the regulation of tight junction structure and barrier function in different cell types is crucial for understanding how translationally relevant these findings are.

In this chapter we demonstrate how anti-integrin nanowires effect cell response up to 24hr after treatment, establish a method to reverse anti-integrin nanowire/cell interactions, investigate anti-integrin nanoparticle induced MMP-2 secretion, and examine how targeting apical integrins

in airway cells compares to our results in intestinal cell lines. This provides preliminary evidence to support future work examining therapeutic applications of integrin targeting nanowires.

6.2 Materials and Methods

6.2.1 Fabrication and conjugation of nanoparticles

Derivatizable PCL nanoparticles were fabricated from a mix of 45kDa PCL (Sigma Aldrich, 704105), maleimidophenyl-PCL (MP-PCL), and Nile Red dye (Sigma Aldrich, 19123) in 2,2,2-trifluoroethanol (Sigma Aldrich, T63002), as described in Chapter 4.

Nanoparticles were conjugated as described in Chapter 4 with either the AIIB2 blocking anti-integrin antibody (Millipore, MAB409T) or the 9EG7 activating antibody (BD Pharmingen, 553715). Antibody conjugated nanoparticles were always used within 4 hours of conjugation.

6.2.2 Caco-2 cell culture

Caco-2 cells were maintained and seeded for immunofluorescence experiments and barrier function assays as described in Chapter 4.

6.2.3 NhBE cell culture

NhBE cells were collected with donor consent under an IRB approved protocol (protocol #00005792), expanded using F+Y medium and seeded at 150,000 cells per well on Transwells (Costar, 3470). Cells were maintained at liquid/liquid interface for 2 days and were incubated in a CO₂ incubator at 37°C before being switched to air/liquid interface (ALI) conditions for 18 days until cells were fully differentiated, and high resistance monolayers were achieved. E-ALI media

was changed 3 times per week while cells were at ALI conditions, as previously used for other studies [18].

6.2.4 Glutathione competition

A 20mM solution of L-Glutathione reduced (Sigma Aldrich, G6013) solubilized in deionized water was diluted to 1mM in fresh Caco-2 media before being added to anti-integrin nanowire treated coverslips and incubated for 8hr. After incubation, cells were then prepared for immunofluorescence.

6.2.5 Immunofluorescence

Treated cells were prepared for immunofluorescence as described in Chapter 4. Caco-2 cell preparations were fixed with only 4% PFA, while NhBE cell preparations were fixed with 4% PFA followed by a methanol:acetone fixation step. Primary mouse anti-ZO-1 antibody (Thermo Fisher Scientific, 33-9100) was diluted in 3% Bovine Serum Albumin (BSA) (Gemini Bio-Products, 700-102P) and incubated on cells overnight at 4C. Cells were washed with 3% BSA before secondary Cy2 goat anti-mouse antibody (Jackson ImmunoResearch Laboratories, 115-225-166) was diluted in 3% BSA and incubated for 1h at room temperature before washing with PBS with calcium and magnesium before mounting the coverslip to a slide with Prolong antifade with DAPI (Thermo Fisher Scientific, P36962). Images were obtained and processed as described in Chapter 4

6.2.6 Barrier function

Transepithelial Electrical Resistance (TER) time courses were measured over a time course of 2-hours or 24-hours using the cellZscope 2 and its accompanying software for data acquisition as described in Chapter 4.

6.3 Results

6.3.1 Duration of nanowire mediated changes of epithelial barriers

Understanding the timescale by which anti-integrin nanowires can trigger integrin mediated regulation of the epithelial barrier is an important step in determining the application(s) this platform could be relevant in. Though the ruffled tight junction morphology is robust at the 2hr time point, we do not have immunofluorescence data before that time point that would indicate when tight junction ruffling is initiated. Furthermore, though the cell/anti-integrin nanowire interaction seems to be fairly stable, as we are able to observe cell associated nanoparticles in immunofluorescence experiments that undergo 15 or more washing steps depending on what protein is being imaged (see Chapters 4 and 5), we do not have immunofluorescence or functional data that demonstrates how long the effects of the anti-integrin nanowires might last.

To address this, we conducted experiments where we treated Caco-2 cells with AIIB2 15 μ m nanowires and fixed the samples at different time points after treatment before staining for ZO-1 (Fig. 6.1A). We observed that significant changes in junctional morphology did not appear until 1hr after treatment with AIIB2 nanowires and persisted until at least 4hr after treatment (Fig. 6.1B). Interestingly, ZO-1 morphology began to change in appearance at the 4hr time point, where in addition to ruffled junctions (Fig. 6.1A, arrow) linear almost spike-like projections began to appear (Fig. 6.1A, arrowhead). Though the appearance of the traditional ZO-1 ruffles disappeared

by the 12hr time point and junctions returned to being fairly linear, this new non-linear ZO-1 morphology persisted, and by 24hr after treatment with blocking AIIB2 nanowires the spike-like projections appeared to have condensed. This data suggests that apical integrin mediated regulation of tight junction proteins persists for at least 4hr after treatment, and changes in junctional structure can last for up to 24hr after treatment.

To test whether anti-integrin nanowires were able to regulate barrier function beyond the 2hr time courses conducted in other experiments, we conducted a TER time course for the 24hr treatment period (Fig. 6.1C). The cells treated with the AIIB2 nanowires showed a significant decrease in TER as compared to untreated cells. Interestingly, TER for cells treated with AIIB2 nanowires increases back to baseline at the 4hr mark before continuing to decrease for the rest of the time course. This correlates with the appearance of ZO-1 ruffles and the new linear projections of ZO-1 from the membrane suggesting that perhaps these structures reflect intermediates involved in a cycle of tight junction remodeling. Over the course of the 24hr treatment, the TER of cells treated with AIIB2 nanowires decreases to about 35% of the baseline barrier function. Surprisingly, the TER of the untreated cells decreases to about 60% of the baseline barrier function. This can likely be attributed to collecting data while taking continuous impedance measurements over such a long period of time, and this loss in TER is a response by the cells after being exposed to alternating current for such a long time. While this creates challenges with regard to interpreting the magnitude of TER loss, the general trends from the functional experiments and IF experiments together suggest that AIIB2 nanowires are fairly stable and can trigger changes in epithelial barrier structure and function beyond the initial treatment.

6.3.2 Reversibility of anti-integrin nanowire/cell interactions

Work by Kam et al., determined that the decrease in TER and ruffled ZO-1 morphology were reversed 24 hours after the removal of the NSFs [1]. A challenge with assessing the reversibility of the anti-integrin nanowires is that it appears that effects of AIIB2 nanowires can persist for many hours after treatment and that the cell/anti-integrin nanowire interaction is fairly stable. Though this is interesting for studying the basic biological mechanisms at play, it meant that removing anti-integrin nanowires from cells could not be accomplished simply by washing them. To assess whether the anti-integrin nanowire induced changes to the epithelial barrier are reversible, we can exploit the fact that the thiol group on the tripeptide glutathione (GSH) can compete the half antibody fragments off the maleimide handle on the nanowires [19,20]. In the anti-integrin nanowire platform, this results in GSH bound nanowires and half antibody fragments that remain bound to apical integrins (Fig. 6.2A).

For the GSH competition assay, we first treated cells with AIIB2 nanowires for two hours before aspirating off treatment medium and incubating with fresh media (control condition) or medium with 1mM GSH before incubating for 8hr. With this assay, we observed that there were significantly fewer cell-associated AIIB2 nanowires in each field of view as compared to AIIB2 nanowire treated cells that were not further treated with GSH (Fig. 6.2B). Additionally, when we stained for ZO-1, we saw that cells treated with both AIIB2 nanowires and GSH had much more linear junctions and the junction/length ratio of those cells was comparable to that of untreated cells or cells treated with bare nanowires (Fig. 6.2C). Interestingly, we observed (but did not quantify) that GSH competition may have changed the orientation of the remaining cell-associated nanowires. In cells only treated with AIIB2 nanowires, the large majority appeared to be positioned perpendicular to the tight junction while cells treated with both AIIB2 nanowires and GSH as well

as bare nanowires tended to be oriented parallel with tight junctions (Fig. 6.2D,E). This lends further support for the hypothesis that anti-integrin nanowire orientation relative to junctions is controlled by engaging integrins underscoring the need to test how anti-integrin nanowires targeting closed vs open integrins orient in real time with respect to tight junctions.

6.3.3 The effects of AIIB2 nanowires are abrogated by MMP-2 inhibitors

Preliminary data from previous work suggests that permeability resulting from direct contact between NSFs and cells may be regulated by MMPs, specifically the gelatinases MMP-2 and MMP-9 [21]. In these experiments, Stewart observed that cells treated with NSFs appear to increase apical secretion of active MMP-2 and MMP-9 as compared to untreated cells [21]. Other research has demonstrated that the activation of integrin $\alpha 5\beta 1$ with monoclonal antibodies is known modulate MMP-2 activity [22]. However, in several cases multivalent ligand/receptor interaction rather than simple ligand binding was a requirement for $\alpha 5\beta 1$ integrin mediated regulation of MMP-2 [14]. Together these findings and consideration of the multivalent nature of the anti-integrin nanoparticle platform made MMP-2 secretion an ideal candidate to examine as a possible mechanism by which our anti-integrin nanoparticles are able to regulate barrier function.

To test whether MMP-2 secretion might be responsible for AIIB2 nanoparticle stimulated increases in permeability, we treated cells with an MMP-2 inhibitor and stained for ZO-1 and ran barrier function tests (Fig. 6.3A,B). Treating cells with both 15 μ m AIIB2 nanowires and MMP-2 inhibitor abrogated the ruffled ZO-1 morphology we observe when cells are treated with AIIB2 nanowires alone (Fig. 6.3A). Cells treated with 2 μ m AIIB2 microspheres alone or 2 μ m AIIB2 microspheres and MMP-2 inhibitor showed no difference in ZO-1 morphology which was linear (data not shown). In barrier function experiments where cells were treated with AIIB2

nanoparticles in the presence or absence of MMP-2 inhibitor, we saw that the combination of MMP-2 inhibitor and AIIB2 nanoparticles of either shape increased barrier function compared to the AIIB2 nanoparticles alone (Fig. 6.3B). That inhibiting MMP-2 prevented changes in junction morphology and barrier function when cells were treated with AIIB2 nanoparticles suggests that MMP-2 secretion may play a role how anti-integrin nanowires mediate integrin regulation of the epithelial barrier. Further work needs to be done to confirm that cells treated with AIIB2 nanowires are secreting active MMP-2 and test whether it is preferentially secreted apically.

6.3.4 Targeting apical integrins in upper airway epithelial cells

Though previous work has identified pools of apical integrins in airway cells [23,24], no work with collagen overlays or NSFs has been done to examine whether integrins can be stimulated to impact barrier integrity in airway cells. In order to examine the potential for using anti-integrin nanoparticles therapeutically in the airway, we measured the effects of anti-integrin nanowires in cultured primary normal human bronchial epithelial (NhBE) cells.

In immunofluorescence experiments where NhBE cells were treated with AIIB2 nanowires for 2hr before staining for ZO-1, we see that the AIIB2 nanowires caused a change in ZO-1 morphology and localization compared to untreated NhBE cells (Fig. 6.4A). The observed changes in ZO-1 suggest that tight junction architecture in NhBE cells, like Caco-2 cells, can be regulated by apical integrins. Though treatment with AIIB2 nanowires triggers non-linear junctions in NhBE cells, they look more jagged than the sinuous ruffling morphology we observed in Caco-2 cells. In addition to the appearance of a non-linear ZO-1 morphology, the AIIB2 nanowires also appeared to increase the number of non-junctional ZO-1 puncta observed, similar to structures observed in Caco-2 cells treated with NSFs (V). ZO-1 staining is dimmer for NhBEs treated with AIIB2

nanowires compared to untreated NhBE cells. Together these observations suggest that apical integrins in NhBE cells can regulate tight junction structure when targeted with AIIB2 nanowires.

We also conducted functional assays to examine how targeting apical integrins in NhBE cells impacts TER for the duration of a 2hr time course (Fig. 6.4B). The results of this time course are fairly consistent with results from experiments with Caco-2 cells (see Figs. 4.4 and 5.5). In NhBEs we see a decrease in TER when cells are treated with AIIB2 nanowires which opposes the response when cells are treated with soluble AIIB2 antibodies, while both the soluble and nanowire bound activating 9EG7 antibody have similar trends, as do our control conditions. However, while the increase in ionic permeability for NhBE cells treated with AIIB2 nanowires is similar in magnitude to what is observed with Caco-2 cells, the trend for the 9EG7 conditions is different in NhBE cells as compared to Caco-2 cells. 9EG7 nanowire treatments cause NhBE cells to maintain a fairly steady baseline TER for the duration of the time course while in Caco-2 cells they cause a significant increase in TER. This still supports a model where anti-integrin nanowires have differential effects, depending on whether they target closed or open integrin conformations, however this also underscores that there are cell-specific differences as well.

6.4 Discussion

These experiments have provided preliminary data that suggests AIIB2 nanowire mediated integrin regulation of tight junctions lasts at least 4hr after treatment, that there is a method for reversing anti-integrin nanowire treatment, that MMP-2 secretion may be a candidate for AIIB2 nanowire action at a distance, and that apical integrin regulation of the epithelial barrier also occurs in airway cells. Together these data suggest that there is merit in conducting future experiments to evaluate the ways in which anti-integrin nanowires can be used as a therapeutic platform.

Future experiments that examine the timescale in which anti-integrin nanowires have an effect on barrier function will provide insight into applications that are most suitable for using anti-integrin nanowires while having the added benefit of helping elucidate the relationship between the appearance of ruffled and other non-linear ZO-1 morphologies and changes in both ionic and large molecule permeability. One possibility is that these structures are precursors to junctional rearrangements that eventually lead to endocytosed cytosolic ZO-1 complexes when cells are treated with NSF s [25].

We found that GSH provided a method to remove anti-integrins that were bound to the cell surface. While effective, this approach requires several considerations. First, we need to determine 8hr is required for GSH to fully cleave half antibody fragments from nanowires. The 8hr incubation was a starting point that was initially determined in a cell-free *in vitro* competition assay, but it is possible that the competition could occur at a different rate in cells. Though data suggests that soluble AIB2 half antibody fragments don't impact permeability or morphology (see Figs. 4.1 and 4.4), this would pose a challenge in understanding reversibility for 9EG7 mAb conjugated nanowires as soluble 9EG7 half antibody fragments are able to regulate tight junction structure and function.

We also need to consider what other consequences adding 1mM of GSH to cells could have. GSH increases the reductive state of the cell, it has also been demonstrated that changes in cytosolic GSH levels can lead to changes in gene expression, cell signaling pathways, proliferation [26], and in some cases impair barrier function [27]. In order to better understand the consequences of adding GSH to the cells themselves, control experiments are needed to measure the impact of GSH on cell viability, proliferation and gene expression. Additionally, reducing agents have been demonstrated to activate integrins (see Chapter 3, section 2.3). While GSH alone has not been

shown to activate integrins, at much lower concentrations, GSH has been shown to prime integrins for activation [28]. Though GSH is competing the half antibody fragments off the nanowires, there is undoubtedly free GSH that could activate integrins or prime integrins for activation and could result effects that confound the use of this approach to simply reverse targeting by anti-integrin nanowires.

Our findings that inhibition of MMP-2 prevents changes in ZO-1 morphology and decreases in TER in cells treated with AIIB2 nanowires serve as an intriguing starting point for future studies. Crude experiments with conditioned media suggest that MMP is apically secreted in cells treated with AIIB2 nanowires (data not shown), and further experiments that test secretion and activity of MMP-2 in cells treated AIIB2 nanoparticles is necessary. Testing how cells treated with 9EG7 nanoparticles respond to MMP-2 inhibition will also be informative. Preliminary data for cells treated with NSFs and MMP-9 inhibitor also exhibit a more linear ZO-1 morphology and barrier function recovery (R. Peterson and C. Lancaster, data not shown) point to MMP-9 being of interest for future anti-integrin nanoparticle experiments.

Given that our anti-integrin nanoparticle platform gives us the ability to target specific integrin conformation states, we might be able to elucidate the link between integrins and the gelatinase family of MMPs and the claudin family of MMPs and claudins. This is of interest because our data suggests that AIIB2 nanowires cause claudin-1 depletion at junctions (Supplemental Fig. 4.2B) but is sensitive to MMP-2 inhibition. However, in colon cancer, increases in claudin-1 expression resulted in increased activity of MMP-2 and MMP-9 [29]. This prompts the question is there crosstalk in the integrin mediation of claudin localization and integrin mediation of MMP secretion? which is worth further investigation.

We have primarily focused on using Caco-2 cells as a model system to study the effects of anti-integrin particles on cell behavior. Whether their effect on Caco-2 cells is universal or cell-specific remains an open question, although studies using NSFs have recapitulated their effect in skin cells [2]. Here we tested NhBE cells as a starting point for future work to examine apical integrin regulation of epithelial barriers in other cell and tissue types. Our data suggests that AIIB2 nanowires act similarly in airway cells as they do in epithelial cells. The appearance of non-junctional puncta of ZO-1 are similar in appearance to the endocytosed structures observed after Caco-2 cells are treated with NSFs [25]. Pointing to similarities in apical integrin regulation between different types of cells.

While experiments presented here used normal airway cells, experiments in cells effected by certain disease states are of interest, as certain diseases increase apical localization of integrin subunits [23,24,30,31]. Published reports of increased apical localization of integrin $\beta 1$ in upper airway cells in a murine model of cystic fibrosis (CF) [23,24] are consistent with findings in our lab using CF patient derived primary nasal epithelial cells. We used immunofluorescence microscopy and found that nasal cells from patients with G551D and F508del CF genotypes have more apically localized integrin $\beta 1$ than nasal cells from non-CF patients (A. Moonwiriyaakit, data unpublished). Interestingly, Grassmé, et al., and Badaoui, et al., both identified large apical populations of integrin $\beta 1$ in the open conformation state using the 9EG7 antibody [23,24], while work in our lab identified populations of apical integrin $\beta 1$ in G551D and F508del primary cells in the closed conformation using the AIIB2 antibody. Whether pools of active and inactive apical integrins have different functions, are distinct versus colocalized, are tissue dependent, or dependent on the type of CFTR defect remains to be seen and could be an interesting avenue to study to better understand the implications of differential apical localization of integrins in disease

states, but not necessarily for therapeutic purposes in the lung. However, work with nanoparticles and airway cells could lay the groundwork for more realistic applications such as treating chronic rhinosinusitis and nasal polyposis.

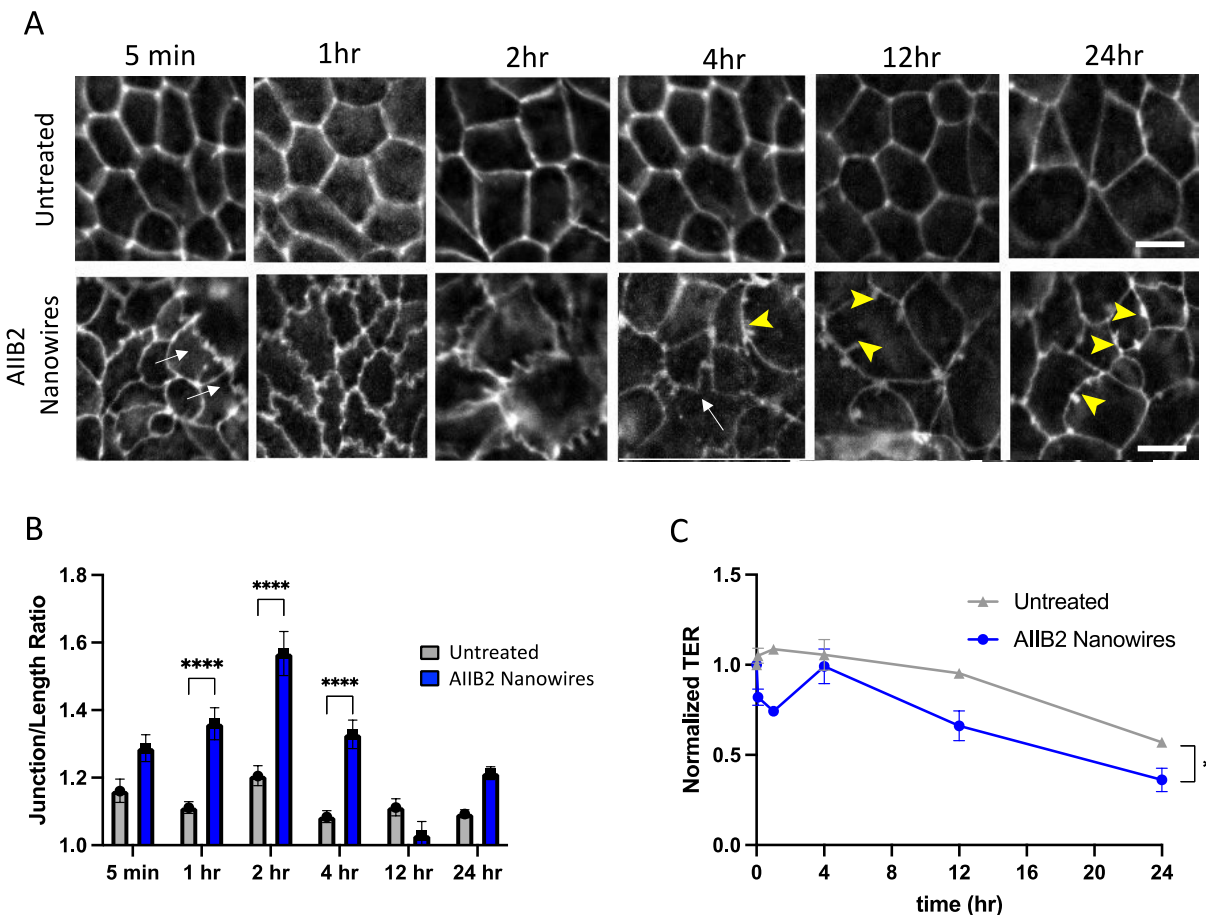


Figure 6.1. Effects of AIIB2 nanowires influence cells for at least 24hr.

(A) Representative immunofluorescence images of Caco-2 cells labeled with ZO-1 (grey) fixed at multiple time points after treatment with AIIB2 nanowires, bar=10 μ m. Minor ZO-1 ruffling indicated by arrows (white), ZO-1 projects indicated with arrowheads (yellow). (B) Quantifications of junction/length ratios for both treatments at each time point, data displayed as mean junction length ratio \pm SEM (n=50 measurements from 1 field of view per treatment per time point), treatment key on right. ****p<0.0001, Significance was determined by two-way ANOVA with Bonferroni's correction for multiple comparisons. (C) TER measurements of Caco-2 cells for 24hr following treatment. Continuous measurements taken with a cellZscope impedance system and normalized to baseline TER measurement before treatment. Each point displayed as

average TER \pm SEM (n=6 wells/treatment), *p=0.0174. Significance was determined by one-tailed paired T-test.

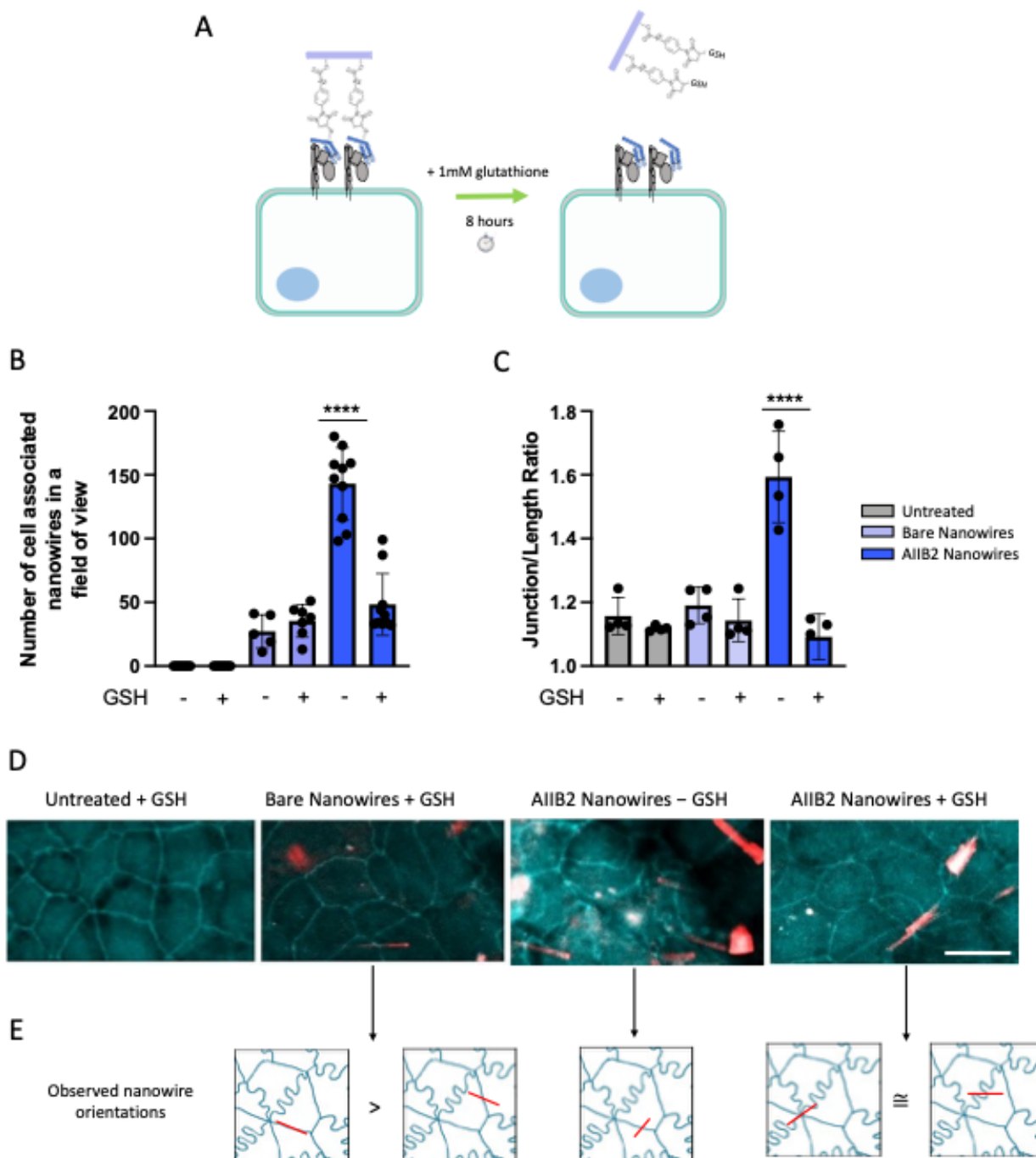


Figure 6.2. Glutathione competition can reverse AIIB2 nanowire effects on tight junction morphology.

(A) Schematic depicts glutathione (GSH) competition assay where cells are incubated with AIIB2 nanowires for 2hr, and 1mM GSH is added for 8hr where it is allowed to compete the AIIB2 half-

antibody fragments off the nanowires. **(B)** Quantification of the number of cell associated nanowires in a field of view for each treatment, each data point represents a count for a single field of view \pm SD (n=5-10 fields of view, n=1 biological replicate). **(C)** Quantification of junction/length ratios for each treatment, each data point represents the average of a single field of view \pm SD (n=50 measurements each for 3-4 fields of view, n=1 biological replicate). **(D)** Representative immunofluorescence images of Caco-2 cells fixed following GSH competition assay and stained for ZO-1 (cyan), direct visualization of Nile Red nanowires (red), bar=10 μ m. **(E)** Schematic depicting observation that GSH competition changes the orientation of cell associated AIIB2 nanowires. **(B and C)** Significance determined by two-way repeated measures ANOVA with Bonferroni's correction for multiple comparisons. ****p<0.0001.

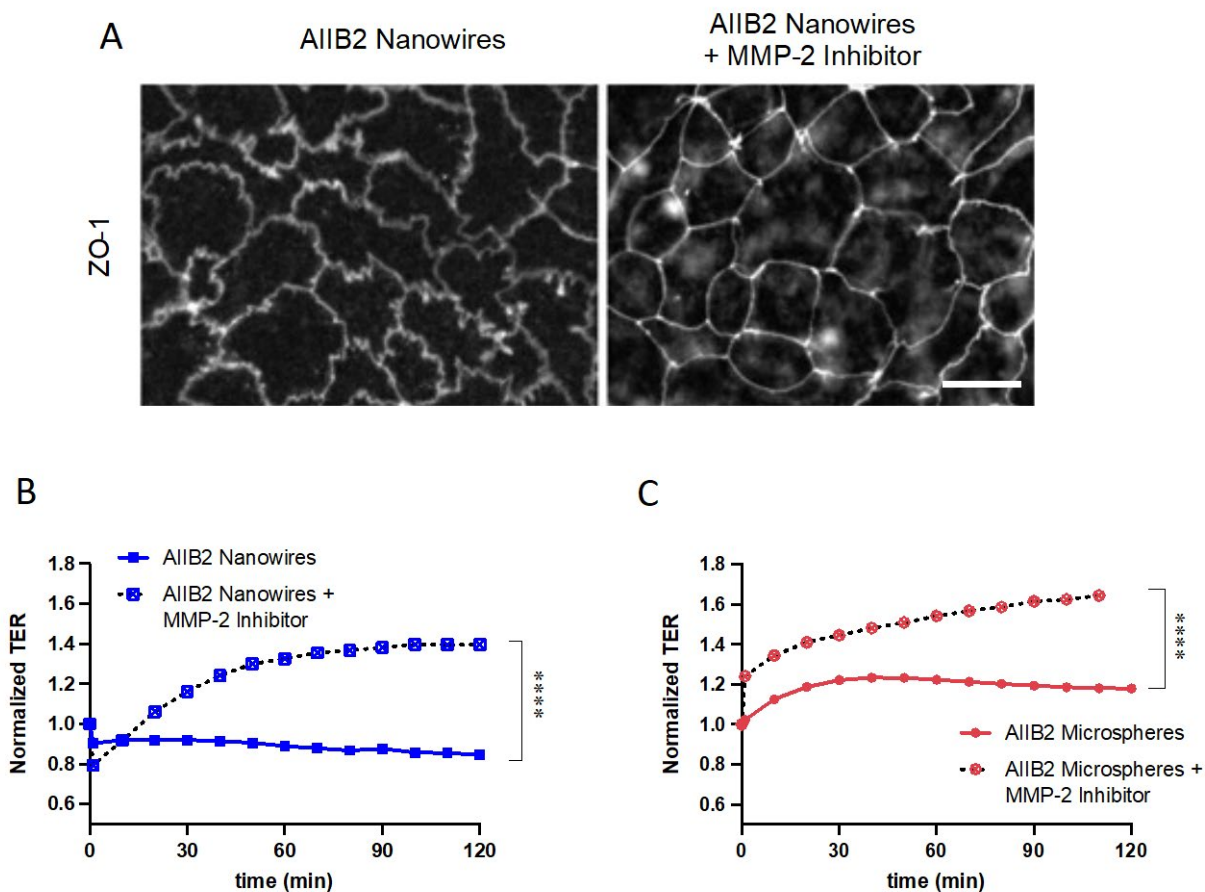


Figure 6.3. Inhibiting MMP-2 in AIIB2 nanowire treated cells prevents changes in barrier morphology and function.

(A) Representative immunofluorescence images of Caco-2 cells labeled with ZO-1 (grey) fixed 2hr after treatment with AIIB2 nanowires or AIIB2 nanowires + MMP-2 inhibitor, bar=10 μ m. (B) TER measurements of Caco-2 cells for 2hr following treatment. Each point is the average TER for that treatment \pm SEM (n=2 wells per treatment), ****p<0.0001. Significance was determined by one-way repeated measures ANOVA with Bonferroni correction.

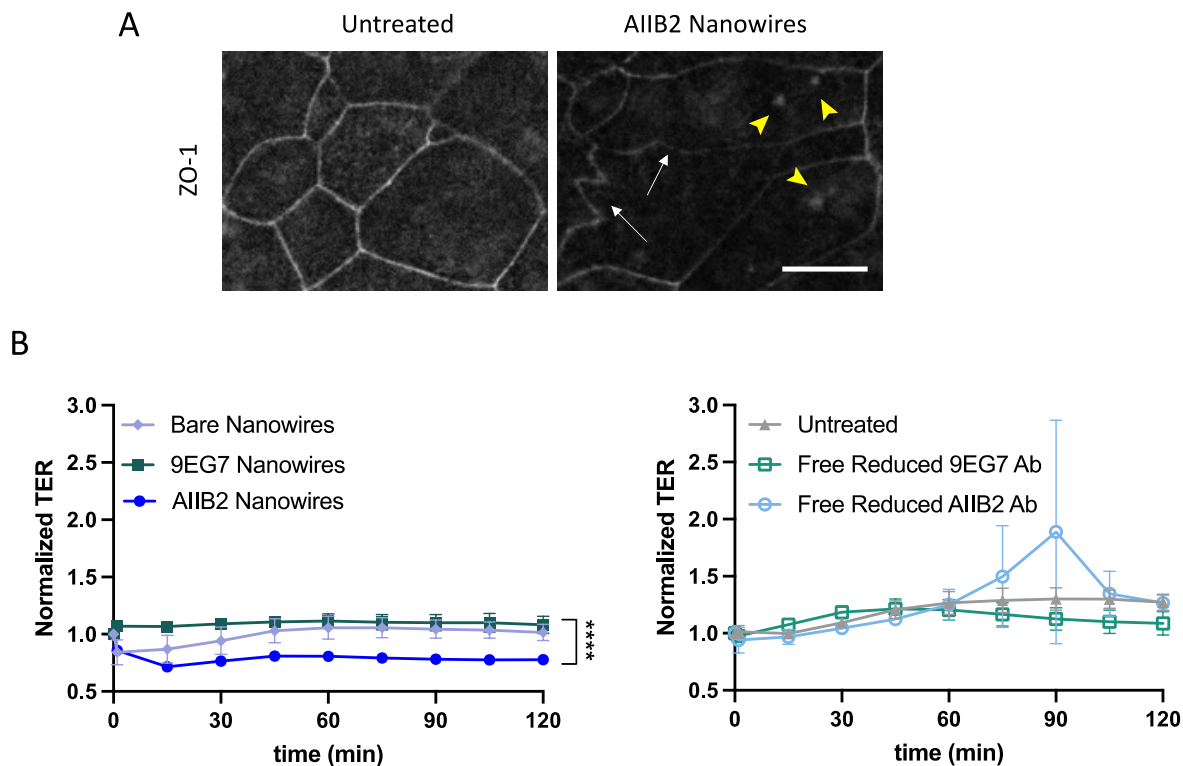


Figure 6.4. Apical integrin targeting in NhBE cells causes changes in barrier structure and function.

(A) Representative immunofluorescence images of NhBE cells labeled with ZO-1 (grey) fixed 2hr after treatment with AIB2 nanowires, bar=10 μ m. ZO-1 ruffling identified by arrow (white), puncta of endocytosed ZO-1 indicated by arrowheads (yellow). **(B)** TER measurements of NhBE cells for 2hr following treatment. Measurements taken every 15 minutes with a cellZscope impedance system, and all points were normalized to baseline TER readings before treatment. Each point is the average TER for that treatment \pm SEM (n=2 wells per treatment). Comparison between AIB2 nanowires and 9EG7 nanowires ****p<0.0001. Bare nanowires vs 9EG7 nanowires p=0.0075, bare nanowires vs AIB2 nanowires p=0.0013. Significance was determined by one-way repeated measures ANOVA with Bonferroni correction.

References

1. Kam KR, Walsh LA, Bock SM, Koval M, Fischer KE, Ross RF, Desai TA. Nanostructure-mediated transport of biologics across epithelial tissue: Enhancing permeability via nanotopography. *Nano Letters* 13, 164-171. (2013).
2. Walsh L, Ryu J, Bock S, Koval M, Mauro T, Ross R, Desai T. Nanotopography facilitates *in vivo* transdermal delivery of high molecular weight therapeutics through and integrin-dependent mechanism. *Nano Letters* 15, 2434-2441. (2015).
3. Stewart T, Koval WT, Molina SA, Bock SM, Lillard JW, Ross RF, Desai TA, Koval M. Calibrated flux measurements reveal a nanostructure-stimulated transcytotic pathway. *Experimental Cell Research* 2, 153-161. (2017).
4. Whitehead K, Karr N, Mitragotri S. Safe and effective permeation enhancers for oral drug delivery. *Pharmaceutical Research* 25, 1782-1788. (2008).
5. Mitragotri S, Burke PA, Langer R. Overcoming the challenges in administering biopharmaceuticals: formulation and delivery strategies. *Nature reviews Drug Discovery* 13, 655-672. (2014).
6. Karande P, Mitragotri S. Enhancement of transdermal drug delivery via synergistic action of chemicals. *Biochimica et Biophysica Acta* 1788, 2362-2373. (2009).
7. Aungst BJ. Absorption enhancers: applications and advances. *The AAPS Journal* 14, 10-18. (2012).
8. Singh R, Singh S, Lillard JW, Jr. Past, present, and future technologies for oral delivery of therapeutic proteins. *Journal of Pharmaceutical Sciences* 97, 2497-2523. (2008).

9. Williams JM, Adewunmi A, Schek RM, Flanagan CL, Krebsbach PH, Feinberg SE, Hollister SJ, Das S. Bone tissue engineering using polycaprolactone scaffolds fabricated via selective laser sintering. *Biomaterials*. 26, 4817-4827 (2005).
10. Naito Y, Imai Y, Sin'oka T, Kashiwagi J, Aoki M, Watanabe M, Matsumura G, Kosaka Y, Konuma, Hibino H, Marata A, Miyake T, Kurosawa H. Successful clinical application of tissue-engineered graft for extracardiac Fontan operation. *Journal of Thoracic Cardiovascular Surgery* 125, 419-420. (2003).
11. Li Z, Tan BH. Towards the development of polycaprolactone based amphiphilic block copolymers: molecular design, self-assembly and biomedical applications. *Materials Science Engineering: C Materials for Biological Applications* 45, 620-634. (2014).
12. Sternlicht MD, and Werb Z. How matrix metalloproteinases regulate cell behavior. *Annual Review of Cell and Developmental Biology* 17, 463-516. (2001).
13. Yang Y, Estrada EY, Thompson JF, Liu W, and Rosenberg GA. Matrix metalloproteinase-mediated disruption of tight junction proteins in cerebral vessels is reversed by synthetic matrix metalloproteinase inhibitor in focal ischemia in rat. *Journal of Cerebral Blood Flow and Metabolism* 27, 697-709. (2007).
14. Pal S, Ganguly KK, Moulik S, Chatterjee A. Modulation of MMPs by cell surface integrin receptor $\alpha 5\beta 1$. *Anti-Cancer Agents in Medicinal Chemistry* 12, 726-732. (2012).
15. Hidalgo IJ, Raub TJ, Borchardt RT. Characterization of the human colon carcinoma cell line (Caco-2) as a model system for intestinal epithelial permeability. *Gastroenterology*. 96, 736-749. (1989).

16. Sambuy Y, De Angelis I, Ranaldi G, Scarino ML, Stammati A, Zucco F. The Caco-2 cell line as a model of the intestinal barrier: influence of cell and cell culture-related factors on Caco-2 cell functional characteristics. *Cell Biology and Toxicology* 21, 1-26. (2005).
17. Shah P, Jogani V, Bagchi T, Misra A. Role of Caco-2 cell monolayers in prediction of intestinal drug absorption. *Biotechnology Progress* 22, 186-198. (2006).
18. Molina SA, Moriarty HK, Infield DT, Imhoff BR, Vance RJ, Kim AH, Hansen JM, Hunt WR, Koval M, McCarty NA. Insulin signaling via the PI3-kinase/Akt pathway regulates airway glucose uptake and barrier function in a CFTR-dependent manner. *American Journal of Physiology Lung Cell and Molecular Physiology* 312, L688-L702. (2017).
19. Baldwin AD, Kiick KL. Tunable degradation of maleimide-thiol adducts in reducing environments. *Bioconjugate Chemistry* 22, 1946-1953. (2011).
20. Shen BQ, Xu K, Liu L, Raab H, Bhakta S, Kenrick M, Parsons-Reponte KL, Tien J, Yu SF, Mai E, Li D, Tibbitts J, Baudys J, Saad OM, Scales SJ, McDonald PJ, Hass PE, Eigenbrot C, Nguyen T, Solis WA, Fuji RN, Flagella KM, Patel D, Spencer SD, Khawli LA, Ebens A, Wong WL, Vandlen R, Kaur S, Sliwkowski MX, Scheller RH, Polakis P, Junutula JR. Conjugation site modulates the *in vivo* stability and therapeutic activity of antibody-drug conjugates. *Nature Biotechnology* 30, 184-189. (2012).
21. Stewart TV. Regulation of epithelial cell permeability by nanostructured thin films. Morehouse School of Medicine, PhD Dissertation. (2017).

22. Mitra A, Chakrabarti J, Chatterjee A. Binding of $\alpha 5$ monoclonal antibody to cell surface $\alpha 5 \beta 1$ integrin modulates MMP-2 and MMP-7 activity in B16F10 melanoma cells. *Journal of Environmental Pathology Toxicology Oncology* 22, 167-178. (2003).
23. Grassme H, Henry B, Ziobro R, Becker KA, Riethmuller J, Gardner A, et al. Beta1-Integrin Accumulates in Cystic Fibrosis Luminal Airway Epithelial Membranes and Decreases Sphingosine, Promoting Bacterial Infections. *Cell Host Microbe* 21(6), 707-718 e708. (2017).
24. Badaoui M, Zoso A, Idris T, Bacchetta M, Simonin J, Lemeille S, et al. Vav3 Mediates Pseudomonas aeruginosa Adhesion to the Cystic Fibrosis Airway Epithelium. *Cell Rep* 32(1), 107842. (2020).
25. Huang X, Shi X, Hansen ME, Setiady I, Nemeth CL, Celli A, Huang B, Mauro T, Koval M, Desai TA. Nanotopography enhances dynamic remodeling of tight junction proteins through cytosolic liquid complexes. *ACS Nano* 14, 13192-13202. (2020).
26. Wu G, Fang YZ, Yang S, Lupton JR, Turner ND. Glutathione metabolism and its implications for health. *The Journal of Nutrition* 134, 489-492. (2004).
27. Overgaard CE, Daugherty BL, Mitchell LA, Koval M. Claudins: Control of barrier function and regulation in response to oxidant stress. *Antioxidants and Redox Signaling* 15, 1179-1193. (2011).
28. Mor-Cohen R. Disulfide bonds as regulators of integrin function in thrombosis and hemostasis. *Antioxidants & Redox Signaling* 24, 16-31. (2016).
29. Dhawan P, Singh AB, Deane NG, No Y, Shiou SR, Schmidt C, Neff J, Washington MK, Beauchamp RD. Claudin-1 regulates cellular transformation and metastatic behavior in colon cancer. *J Clin Invest* 115, 1765-1776. (2005).

30. Zuk A, and Hay ED. Expression of beta 1 integrins changes during transformation of avian lens epithelium to mesenchyme in collagen gels. *Dev Dyn* 201(4), 378-393. (1994).
31. Schoenenberger CA, Zuk A, Zinkl GM, Kendall D, Matlin KS. Integrin expression and localization in normal MDCK cells and transformed MDCK cells lacking apical polarity. *J Cell Sci* 107 (Pt 2), 527-541. (1994).

Chapter 7. Conclusions and future directions

7.1 Overview of findings and significance

Understanding the biology that underpins the regulation of junctions and other components that maintain the epithelial barrier has implications for both basic science and translational research. Though apically localized integrins have been observed in a variety of cell and tissue types and have been identified as mediators of a variety of functions including regulation of the epithelial barrier (Chapter 3), to date, there has been little work done to demonstrate that apical integrins alone are capable of regulating epithelial barrier. We leveraged a novel approach using functional monoclonal anti-integrin antibodies conjugated with polymeric nanoparticles to understand if apical integrins were able to regulate barrier structure and function. In this dissertation, we set out to understand the specific role apical integrins play in regulating the epithelial barrier and tested this by manipulating both the functionality of antibodies conjugated to the nanoparticles we used to target integrins and the geometry of the nanoparticle themselves. Though we observed changes in actin cytoskeleton organization as a result of nanoparticle treatment, the mechanism that links apically localized $\beta 1$ integrin with tight junctions is still not well understood.

In Chapter 4, we discovered that the regulation of the epithelial barrier by apical integrins was largely dependent on integrin conformation that our activity specific antibodies targeted. We demonstrated that nanowires conjugated with AIIB2 antibodies that target the closed conformation promoted ruffled barrier structure and increased permeability. AIIB2 nanowires triggered cortical recruitment of actin and talin enrichment at cell/cell borders. Meanwhile treatment with both soluble and nanowire bound 9EG7 antibody, which targets integrins in the open conformation, had

similar effects on barrier structure and function. Targeting of apical integrins in the open conformation linearized tight junctions and decreased ionic permeability.

The results of Chapter 4 show for the first time that apical integrin stimulation alone is sufficient for regulating the epithelial barrier as previously seen with substrates that contact apical integrins as well as the entire apical membrane [1-4]. Furthermore, this is the first evidence that apical integrin conformation and activity plays a role in the ability of integrins to regulate the epithelial barrier. Despite the fact that tight junction ruffling has been broadly observed [reviewed in 5], our findings are the first that demonstrate that ruffled junctions have two distinct pools of claudins that are participants in ruffling or not involved in ruffling. Our results also indicated that apical integrin stimulation in combination with contact between other parts of the apical plasma membrane are responsible for the magnitude of the decreases in barrier function that NSFs can facilitate [1-3]. To get a better understanding of how these anti-integrin nanowires facilitated permeability to IgG probes, the expression of FcRn receptors should be examined.

In Chapter 5 we demonstrated that the geometry of the nanoparticle platform plays a role in how integrins are able to regulate the epithelial barrier. For AIIB2 labeled particles, a smaller aspect ratio particle was better able to regulate ZO-1 ruffling and increased ionic permeability. However, for 9EG7 labeled particles, larger aspect ratio particles were able to induce ZO-1 ruffling and increased ionic permeability. Some of our data suggested that a possible reason for the difference between AIIB2 nanowires and AIIB2 microspheres could be due to internalization of spherical particles.

In Chapter 6, we tested how our findings from Chapters 4 and 5 could be used more practically. We demonstrated that AIIB2 nanowires influence ionic permeability and junction morphology for at least 24hr, but interestingly that the ruffled ZO-1 morphology does not persist

through 12hr after treatment. We demonstrated that competing AIIB2 half antibody fragments off nanowires with glutathione for 8hr was sufficient to re-linearize tight junctions. We observed that inhibiting MMP-2 activity in cells treated with AIIB2 nanowires prevents changes in tight junction morphology and barrier function. We also observed that there is conservation of cell response between intestinal and airway cells treated with anti-integrin nanowires.

7.2 Future directions

Though the findings from this work push the field of junctional biology forward, the results also serve as a starting point for other studies. The following is a discussion of hypotheses and future experiments that if completed will add to our understanding of apical integrins and the epithelial barrier but were simply outside the scope of this dissertation.

7.2.1 Integrins

A major focus of this work has been testing to see if targeting apical integrins with functionalized antibodies conjugated to a nanoparticle platform was sufficient to induce integrin mediated regulation of tight junctions. These experiments generated data that suggests both the functionality of the antibody used (activating or blocking) and the geometry of the nanoparticle used are important considerations. Our data also provided insight for the first time into what junctional proteins participate in ruffling and that their localization might be regulated by apical integrins. While Chapters 4 and 5 suggest that these changes at the junction might be linked to apical integrins through the actin cytoskeleton, there isn't a lot of data how integrins manage this.

To get a more complete picture of the mechanism of action, an important consideration for the future of this project is for it to shift from being tight junction focused to focusing more on the

integrins themselves. We assume that anti-integrin nanoparticles, namely the nanowires, produce the changes in barrier structure and function by clustering apical $\beta 1$ integrin subunits despite not having evidence for that. In order to move forward, it will be important to examine how the integrins are organized as a result of treatment with anti-integrin nanoparticles.

It could be particularly informative to use super resolution microscopy to test how anti-integrin nanoparticle treatment effects integrin organization on cells expressing fluorescently labeled $\beta 1$ integrins. The caveat to an experiment like this, is that there is no guarantee that a significant amount of fluorescently labeled $\beta 1$ integrins are localized apically. That being said, even if the experiment didn't start with enough apically localized fluorescent $\beta 1$ integrins, it could be interesting to see if treatment with anti-integrin nanoparticles actively change the recruitment of apically localized $\beta 1$ integrins, which could be informative in its own way.

Another option would be to molecularly manipulate integrin $\beta 1$ subunits and examine the effect this has on anti-integrin nanoparticle induced cell responses. A good candidate for this would be to conduct tail swap experiments [6] or knockout experiments, which would allow us to test the hypothesis that integrin regulation of barrier function is mediated through scaffold proteins like talin. Though tail-swap and knockout experiment still do not allow us to directly examine the integrins themselves, it will shed light on if and how integrins are coordinating certain scaffold proteins differently as a result of nanoparticle targeting of apical integrins. This is a particularly interesting consideration because in endothelial cells, it has been demonstrated that knocking out talin causes ZO-1 to become disorganized [7].

In order to better understand integrin specific determinants of observations from this work, we could expand the antibodies that we conjugate with nanowires. This could include using non-functional polyclonal antibodies that have epitopes that are recognized in both conformation states.

Depending on results from those experiments, we might be better positioned to understand why targeting integrins in their closed, inactive state is able to elicit changes in the epithelial barrier. We could also conjugate different concentrations of mixed populations of anti-integrin mAbs to the nanoparticles. In light of the discovery in Chapter 4 that integrin conformation state plays a role in how tight junction structure and function is impacted by anti-integrin nanowires, this could help us elucidate what happens if we have mixed populations of integrins with different conformation states in the same general regions. It could also be of interest to gain a better understanding of what other α and β integrin subunits localize apically in the various cells we study.

7.2.2 The nanoparticle platform itself

One of the challenges we have faced using our maleimide linker-based nanowire platform to study integrin regulation of the epithelial barrier is removing the anti-integrin nanowires. In Chapter 6 we discussed using a GSH competition assay to promote antibody release from the nanowires. However, there are other approaches that we could consider that would make reversibility experiments more feasible. One such approach is incorporating a photocleavable linker into the nanowires. The benefit of using a photocleavable linker to attach the antibodies to the nanoparticles is that we could cleave the antibody/linker bond by irradiating the treated cells with a certain wavelength of light. If this was done in parallel with live cell imaging, we would have the ability to observe the effects in the exact region where the cleavage occurred and better understand how the cells respond to removal of the anti-integrin nanowires and the timescale on which this occurs. However, using a photocleavable linker could complicate the nanowire

synthesis process as well as the make the conjugation reactions more difficult than the current one step process.

There are other reasons aside from reversibility that merit consideration for changing linker composition, one of which is so that we may better test how external tension from the nanowire impacts cell response. As discussed in Chapters 4 and 5, treating cells with anti-integrin nanoparticles appears to cause a change in tension as denoted by changes in actin cytoskeleton reorganization. However, what isn't readily apparent is how important the tension between apical integrins and the antibody bound nanowires is. Using longer linkers to conjugate nanowires with anti-integrin antibodies would allow us to test what happens to cell response when the linker is floppier where the antibody is further away from the wire structure and thus puts the cell under less tension.

The most apparent solution might be adding a polyethylene glycol (PEG) linker between the MP-PCL polymer we use. However, in a PEG/MP-PCL polymer there would be too much solvent accessibility during the nanowire etching step that would completely hydrolyze the maleimide group. This means that we could likely use this linker making spherical micro- and nanoparticles, but to use this linker for nanowires, it would necessitate changing the current nanowire synthesis scheme. We could get around this issue and continue using the current synthesis scheme by using a PCL-PEG-amine polymer with an NHS ester linked maleimide. The main thing this would change is that the conjugation reaction would occur in two steps: 1) functional amine + NHS ester, 2) antibody conjugation.

Aside from simply considering changing the linker composition for experimental purposes, there are also considerations for changing the linker composition so that conjugation is more controlled. One of the strategies we considered was antibody conjugation with amine groups is

quite common, but it would create challenges in our nanowire platform because antibodies have many lysine groups that could react during conjugation leading to antibodies conjugating in random orientations resulting in heterogeneous antibody layers [8]. Furthermore, binding on the nanowire itself would likely be decreased due to steric hindrance from the protein itself [8]. Other strategies we could consider would include using particles functionalized with DNA scaffolds, such as those developed by Huang, et al., that act as crosslinkers for antibodies to ensure more control over protein density on the surface of the particles [9]. There is even an argument for generating bifunctionalized particles that would allow for controlled addition of different antibodies to examine how changing the ratios of two distinct antibodies added to these particles would affect barrier structure and function. The significant challenge with many of these strategies is that not all of the strategies are easily integrated into the existing nanowire synthesis scheme and would require extensive modification of these protocols.

7.2.3 Tension

As discussed in the previous sections, a crucial part of the future direction of this project will be understanding how tension changes as a result of interactions with anti-integrin nanoparticles. Chapter 4 hypothesizes that blocking anti-integrin nanowires might cause a decrease in tension in areas surrounding the location of cell associated nanowires as suggested by increases in cell size that might be due to cell flattening. Though visualizing the actin cytoskeleton and its reorganization is a useful technique, it doesn't directly address how force is changing in the cell. One way that this could be addressed is by using a live cell membrane tension probe called FliptR. The probe is a membrane dye with a propeller that rotates to accommodate changes in the order of the lipid bilayer it can report areas with differences in tension because when the membrane is at

high tension the lifetime fluorescence of the probe is higher than in areas with lower tension and data can be collected with fluorescence lifetime microscopy (FLIM) [10]. In addition to collecting data on how anti-integrin nanoparticles effect membrane tension, we can take this a step further by overlaying FLIM images of tension with fluorescent images of the nanoparticles to assess where tension changes are occurring relative to the localization of the particles. Though the probe is a membrane dye, not a marker for tight junctions, preliminary data collected while trying to optimize the treatment conditions (data not shown) suggest that it is possible to visualize membrane ruffling with the dye. While it is not known whether this membrane ruffling exactly correlates with ZO-1 or claudin ruffles, that can be examined.

Throughout this project we have continually kept in mind that cell responses resulting from anti-integrin nanoparticles could be a result of tension changing within the cell, or at the nanowire itself. However, future experiments should also test how tension from the ECM affects anti-integrin nanoparticle mediated changes in barrier structure and function. To test this, we could seed cells on coverslips coated with materials of different stiffnesses and conduct experiments assessing barrier structure upon anti-integrin nanoparticle treatment. While it would also be useful to conduct barrier function assays, this would be more challenging as commercially available ECM coatings of varying stiffnesses do not yet exist. These experiments would help us determine how important tension at the basolateral surface of the cell is with regard to the changes in cell response that we have observed. Furthermore, this would give us a more physiologically relevant environment to do experiments in, as traditional glass coverslips are much stiffer than the matrices that cells grow on *in vivo*.

Using these various tools to study how anti-integrin nanowire treatment impacts cellular tension, and how ECM stiffness impacts cell response could be very useful in trying to better

understand the mechanism by which the clustering of apical integrins regulates tight junction barrier structure and function.

References

1. Kam KR, Walsh LA, Bock SM, Koval M, Fischer KE, Ross RF, Desai TA. Nanostructure-mediated transport of biologics across epithelial tissue: Enhancing permeability via nanotopography. *Nano Letters* 13, 164-171. (2013).
2. Walsh L, Ryu J, Bock S, Koval M, Mauro T, Ross R, Desai T. Nanotopography facilitates *in vivo* transdermal delivery of high molecular weight therapeutics through and integrin-dependent mechanism. *Nano Letters* 15, 2434-2441. (2015).
3. Stewart T, Koval WT, Molina SA, Bock SM, Lillard JW, Ross RF, Desai TA, Koval M. Calibrated flux measurements reveal a nanostructure-stimulated transcytotic pathway. *Experimental Cell Research* 2, 153-161. (2017).
4. Garbi C, Negri R, Cali G, Nitsch L. Collagen interaction with apically expressed beta 1 integrins: loss of transepithelial resistance and reorganization of cultured thyroid cell monolayer. *European Journal of Cell Biology* 69, 64-75. (1996).
5. Lynn KS, Peterson RJ, Koval M. Ruffles and spikes: Control of tight junction morphology and permeability by claudins. *Biochimica et Biophysica Acta-Biomembranes* 1862, 183339. (2020).
6. Pfaff M, Liu S, Erle DJ, Ginsberg MH. Integrin β cytoplasmic domains differentially bind to cytoskeletal proteins. *Journal of Biological Chemistry*. 273, 6104-6109. (1998).
7. Pulous FE, Grimsley-Myers CM, Kansal S, Kowalczyk AP, Petrich BG. Talin-dependent integrin activation regulates VE-cadherin localization and endothelial cell barrier function. *Circulation Research* 124, 891-903. (2019).

8. Makaraviciute A, Jackson CD, Miller PA, Ramanaviciene A. Considerations in producing preferentially reduced half-antibody fragments. *Journal of Immunology Methods* 429, 50-56. (2016).
9. Huang X, Williams JZ, Chang R, Li Z, Burnett CE, Hernandez-Lopez R, Setiady I, Gai E, Patterson DM, Yu W, Roybal KT, Lim WA, Desai TA. DNA scaffolds enable efficient and tunable functionalization of biomaterials for immune cell modulation. *Nature Nanotechnology* 16, 214-223. (2021).
10. Colom A, Derivery E, Soleimanpour S, Tomba C, Dal Molin M, Sakai N, González-Gaitán M, Matile S, Roux A. A fluorescent membrane tension probe. *Nature Chemistry* 10, 1118-1125. (2018).